UNIVERSITY OF CAPE TOWN
IYUNIVESITHI YASEKAPA • UNIVERSITEIT VAN KAAPSTAD

Medical Biotechnology & Immunotherapy Research Unit
Institute for Infectious Disease & Molecular Medicine
South African Research Chair in Cancer Biotechnology
Department of Integrative Biomedical Sciences
Faculty of Health Sciences
University of Cape Town

Next-Generation version of Pseudomonas Exotoxin A based immunotoxins with reduced immunogenicity for Triple Negative Breast Cancer (TNBC) treatment

Dissertation submitted for the degree of Master of Science (MSc) in Medicine

Jabulisile Mthethwa (MTHJAB013)

January 2025

Supervisor:

Prof. Dr. Dr. Stefan Barth

Declaration

1. I know plagiarism is wrong. Plagiarism is to use another person's work and pretend that it is one's own. Each contribution to, and quotation in this research study from the work(s) of other people has been attributed, cited, and referenced.

2. This research study is my own work. I have not allowed and will not allow anyone to copy with the intension of passing it off as his or her own work.

3. This dissertation has been submitted to the Turnitin module (or equivalent similarity and originality checking software), and I confirm that my supervisor has seen my report and that any concerns revealed by such have been resolved with my supervisor.

4. I grant the University of Cape Town free licence to reproduce the content of this dissertation, in whole or in part, for the purpose of research.

Name: Jabulisile Mthethwa

Signature: Signed by candidate

Date: 21 January 2025

Acknowledgements

Firstly, I would like to express my deepest gratitude to my supervisor, Prof. Dr. Dr. Stefan Barth, for his guidance, encouragement, and unwavering support throughout my Master's journey.

To Sizalobuhle Masuku, Jesmika Sigh and Marc Henry, your support throughout my MSc journey is greatly appreciated. I am also deeply thankful to my colleagues from MB&I research group and academic staff, each individual really played so much role in my master's journey, I am grateful for their assistance by providing a conducive environment for learning, insightful discussions, and enriching my experience throughought my MSc journey.

I would also like to thank Prof. Dirk Lang for his assistance and training at the UCT Confocal Microscopy.

I would like to acknowledge the all the funders from University of Cape Financial Aid for their financial support, which made this research possible.

My heartfelt thanks go to my family and friends, whose unconditional love and encouragement have been a constant source of strength throughout this process. Last but not least, I would like to extend my heartfelt gratitude to my partner for his unwavering love, patience, and support throughout this journey.

This thesis reflects the collective support and contributions of all these individuals, to whom I am sincerely thankful.

Dedication

This work is lovingly dedicated to God almighty who made everything possible and to the memory of my late parents, **Mr. S.H. Mthethwa** and **Mrs. Q.R. Mthethwa**. Your unwavering love, sacrifices, and encouragement continue to inspire me every day. Though you are no longer with me, your values and dreams have been the guiding light on this journey. I hope this accomplishment makes you proud, as it reflects your boundless support and belief in me.

May your souls rest in eternal peace!

Table of Contents

Index of figures

Index of tables

List of Abbreviations

Acronym	Definition
‘x’(scFv)	Collective term for all scFv
ADC	Antibody-drug conjugate
AGE	Agarose gel electrophoresis
BC	Breast cancer
BL	Basal-like
BRCA	Breast cancer gene
BSA	Bovine serum albumin
C	Constant domain
CDR	Complementarity-determining region
CFU	Colony forming units
CO	Control
CSC	Cancer stem cell
CTC	Circulating tumor cells
CV	Column volume
DD	Double digest
ddH_2O	Deionised distilled water

Deta	Deimmunized version of *Pseudomonas Exotoxin* A (RG7787)
DMEM	Dulbecco's Modified Eagle Medium
DNA	Deoxyribonucleic acid
DTT	DL-Dithiothreitol
EGFR	Epidermal growth factor receptor
EKS	Enterokinase cleavage site
EMT	Epithelial-mesenchymal transition
ER	Oestrogen receptor
ETA	Pseudomonas Exotoxin A
Fab	Antigen-binding fragment
FBS	Foetal bovine serum albumin
Fc	Crystallizable fragment
FDA	U.S. Food and Drug Administration
FR	Framework regions
HC	Heavy chains
HER	Human epidermal growth factor receptor
His-Tag	10x Histidine affinity tag

hLIV22(scFv)	Humanized scFv targeting LIV-1
HRP	Horseradish peroxidase
IC50	50% inhibitory concentration
Ig	Human immunoglobulin
IM	Immunomodulatory
IMAC	Immobilized metal affinity chromatography
IPTG	Isopropyl-ß-d-1-thiogalactopyranoside
KanR	Kanamycin resistance gene
LAR	Luminal androgen receptor
LB	Luria-Bertani
LC	Light chains
LIV-1	Zinc Transporter LIV-1
M	Mesenchymal-like
Mab	Monoclonal antibody
MB&I	Medical Biotechnology and Immunotherapy
MMAE	Monomethyl auristatin E
MSL	Mesenchymal stem-like
MW	Molecular weight

NEB	New England Biolabs
OD	Optical density
ORF	Open reading frame
PBS	Phosphate-buffered saline
PD-L	Programmed death ligand
PE	Anti-His-Tag phycoerythrin
PelB	Pectate lyase of Erwinia carotovora
PFA	Paraformaldehyde
PR	Progesterone receptor
PVDF	Polyvinylidene difluoride
RBS	Ribosome binding site
Rit	Recombinant immunotoxin
RNA	Ribonucleic acid
RPMI	Roswell Park Memorial Institute (Medium)
ScFv	Single-chain variable fragment
SD	Single digestion
SDS-PAGE	Sodium dodecyl sulphate polyacrylamide gel electrophoresis

SG	Sacituzumab govitecan
SiRNA	Small interfering RNA
SOC	Super Optimal Broth with Catabolite repression
TAA	Tumour-associated antigen
TAE	Tris-acetate-EDTA
TB	Terrific broth
TBS-T	Tris-buffered saline-Tween®
TNBC	Triple-negative breast cancer
Trop-2	Human trophoblast cell-surface antigen 2
UD	Undigested
UV	Ultraviolet
v/v	Volume per volume
VH	Variable heavy chain
VL	Variable light chain
w/v	Weight per volume
WB	Western blot
XTT	2,3-bis(2-methoxy-4-nitro-5-sulphophenyl)- 5-carboxanilide-2H-tetrazolium

Abstract

Breast cancer continues to have the highest mortality rate in comparison to other cancer types, with approximately 19.4 million women aged 15 years and older living at risk of being diagnosed with breast cancer in South Africa. Triple-negative breast cancer (TNBC) subtype, which is mainly characterized by a lack of expression of the oestrogen receptor (ER), progesterone receptor (PR) and human epidermal growth factor receptor 2 (HER2), patients do not benefit from current standard treatments since they are based on these absent biomarkers leading to off-targets which results to an adverse side effects in TNBC patients. TNBC subtypes tend to be more common in women younger than age 40, who are Black, or who have a Breast Cancer gene 1 (*BRCA1)* mutation. The five-year survival rate for TNBC in South Africa is approximately 19.26% and the major causes of this include the late diagnosis of disease, highly aggressive tumor growth, and the early formation of metastases. Therefore, it is crucial than ever to use a multi-targeted precision medicine approach exploiting the differential overexpression of TNBC-specific cell surface receptors. As part of this effort, tumors should be screened and evaluated for therapeutic and prognostic biomarkers that can precisely show the clinicians which treatment plan will work best for their patients. Combining novel immunotherapies with conventional treatment approaches has demonstrated significant promise for improving cancer quality of the patient's life and survival. Although, when it comes to TNBC, these immunotherapies are frequently used as a last option after more traditional treatments have failed such as chemotherapy.

Overexpression of zinc transporter (LIV-1) and trophoblast cell surface antigen-2 (trop2) has been implicated in the oncogenesis of TNBC and associated with an unfavorable

prognosis. Consequently, the LIV-1 and TROP-2 biomarkers represent a specific target antigen suitable for immunotherapy.

In this study, we successfully developed recombinant immunotoxins by fusing an anti-hliv22 and anti-trop2 single chain variable fragment (scFv) antibody to a truncated mutant of Pseudomonas Exotoxin A (ETA') and deimmunized version of (ETA') RG7787, herewith termed (dETA') introducing a cysteine in position R456.

Using the bacterial expression vector pMT, functional (scFv)-ETA' and scFv-dETA' were periplasmically expressed under osmotic stress conditions in the presence of compatible solutes. The 72 kDa, His10-tagged fusion proteins were purified using a two-step Immobilised Metal-ion Affinity Chromatography (IMAC). Specific binding of these recombinant immunotoxins to LIV-1- and TROP2-positive breast cancer cell line MCF-7 were confirmed by confocal microscopy in comparison to an antigen-negative control.

The introduction of the new mutation in the RG7787 rIT indicates a partial recovery of enzymatic activity with trop2-targeting rITs showing a 1.4-fold reduction in cytotoxic activity, which is a significant improvement when compared with the 4 to13-fold reductions in IC_{50} values reported for RG7787 in the Alewine study.

This is the first report documenting the specific cytotoxicity of a RG7787 recombinant immunotoxins with cysteine (C) mutation in position R456 introduced towards triple-negative breast carcinoma cells, suggesting that liv-1 and trop-2 specific antibody toxins may become valuable therapeutic reagents for the treatment of triple-negative breast cancer in the future.

Chapter 1: Literature Review

1.1. Defining Breast Cancers (BCs)

Breast cancer (BC) is defined as a heterogeneous disease with microarray profiling studies having identified many biologically distinct subtypes of breast tumors, each associated with different clinical outcomes [1]. It is one of the common cancers that affects women globally, however studies have also documented some men can also get breast cancer and people assigned female at birth. BC can initiate from different parts of the breast in a human body, either left or right breast, and each one is made up of ducts, glands, and fatty tissues [2].

Breast cancer (BC) occurs when cells in the breast tissue mutate and begin to multiply uncontrollably, resulting in the formation of a tumor as shown in **figure 1**. BC incidence rates may be elevated due to increased risk factor prevalence, opportunistic or organized mammography screening detections, aging, and population growth. Approximately 80% of breast cancer cases are invasive, meaning a tumor may spread beyond the breast to other areas of the body. In past decades, there has been a significant expansion in understanding of this disease at the cellular, molecular, and genomic levels due to the rapid advancements in molecular biology, systems biology, and genome sciences [1], [3].

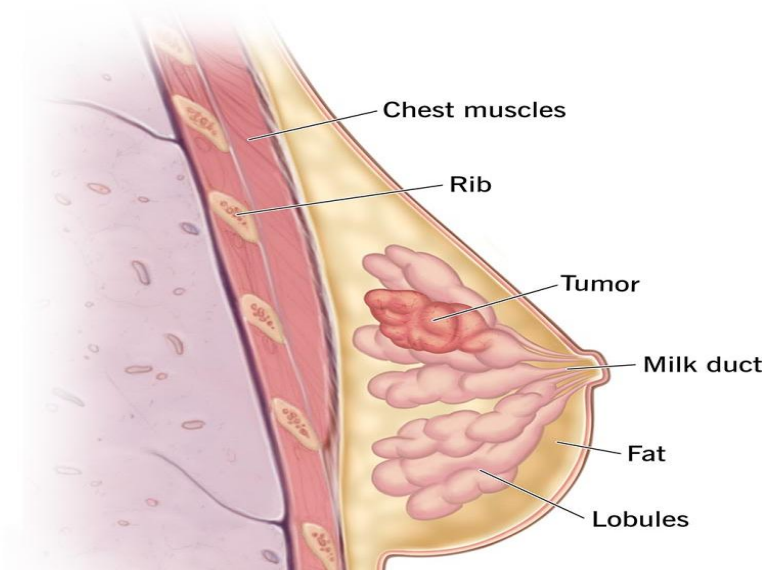

Figure 1: ***Tumor formation in breast due to the mutation and uncontrollably growth of the breast.*** *Image obtained from: https://my.clevelandclinic.org/-/scassets/Images/org/health/articles/3986-breast-cancer*

1.2. Breast Cancer Prognosis

Over the past years, an understanding of the prognosis of breast cancer has significantly progressed based on various prospective and retrospective studies that have been performed. The young age at diagnosis has been generally accepted to correlate with a worse clinical outcome compared to their older counterparts. Studies have showed that breast cancer survival rates are usually lower for women under 40 compared to older women across all histological subtypes and stages. However, there is ongoing debate about whether age itself is an independent risk factor for poorer prognosis. Many studies challenge this idea, suggesting that the impact of young age on outcomes reflects the higher prevalence of other known prognostic pathological factors. These include poorer differentiation grades, lymph vascular invasion, higher mitotic rates, reduced expression of oestrogen receptor (ER) or progesterone receptor (PR), and increased expression of human epidermal growth factor receptor 2 (HER2) [4]. Some studies have associated the poorer outcomes in younger women to more advanced disease at the time of diagnosis,

characterized by higher rates of axillary lymph node positivity and larger tumor sizes. Others have suggested that differences in gene expression between age groups could also be a factor but regardless of this, understanding the true impact of age on prognosis is crucial, as it could influence breast cancer management. If age is proven to be an independent factor, younger women may need more aggressive treatment compared to older women with similar clinical and pathological profiles [5].

1.3. Breast Cancer Classification

A breast cancer type is determined by the specific cells in the breast that become cancer [6]. BC's can be broadly classified as either sarcomas or carcinomas, depending on which cell origin is involved. Breast carcinomas are malignancies that originate from the epithelial tissue of the breast, made up of the cells that form the lining of the lobules and terminal ducts involved in milk production. Cancers in the breast often manifest as adenocarcinoma, a more specialized type of cancer that originates in cells of the milk ducts or lobules. Sarcomas, on the other hand, is a less common form of breast cancer, accounting for less than 1% of primary breast cancer cases. They usually initiate from the stromal components of the breast, including myofibroblasts and blood vessel cells. However, these groups may not always be adequate classifications as, in certain instances, a single breast tumor can consist of several cell types. Most breast cancers are carcinomas. Among the extensive category of carcinomas, certain breast cancer types are distinguished according to their level of invasiveness concerning the original tumor locations. Accurately distinguishing between the many subtypes is critical since each has a different prognosis and therapeutic consequences. Common breast cancers are classified into three types based on pathological characteristics and invasiveness:

non-invasive (or in situ), invasive, and metastatic [6], [7]. The breast consists of different parts shown in (**Table 1**).

Table 1: Shows the different parts of a breast, their function, and the type of cancer that initiates in each part.

Breast Part	Function	Cancer Type	References
Lobules glands	produce breast milk	lobular cancers	[8]
Ducts	transport milk to the nipple.	ductal malignancies	[8]
Nipple	milk expulsion	Paget's disease of the breast	[8]
Stroma	help ducts and lobules by holding them in place	phyllodes tumor	[8]
Blood arteries and lymphatic vessels	supply nutrients to the breast tissue, filter out substances that are harmful, and regulate fluid balance in the breast.	Angiosarcoma	[8]

1.4. Breast Cancer Diagnosis

BC is one of the most common causes of cancer-related illness and mortality for women globally, therefore, prognosis improvement depends on early detection and treatment. Research indicates that patients with smaller tumours have a far higher chance of surviving from cancer. To improve the efficacy of breast cancer treatment, different

technologies are being developed to assist in the early detection of primary tumours, as illustrated in (**Figure 2**), as well as distant metastases and recurring disease [9], [10].

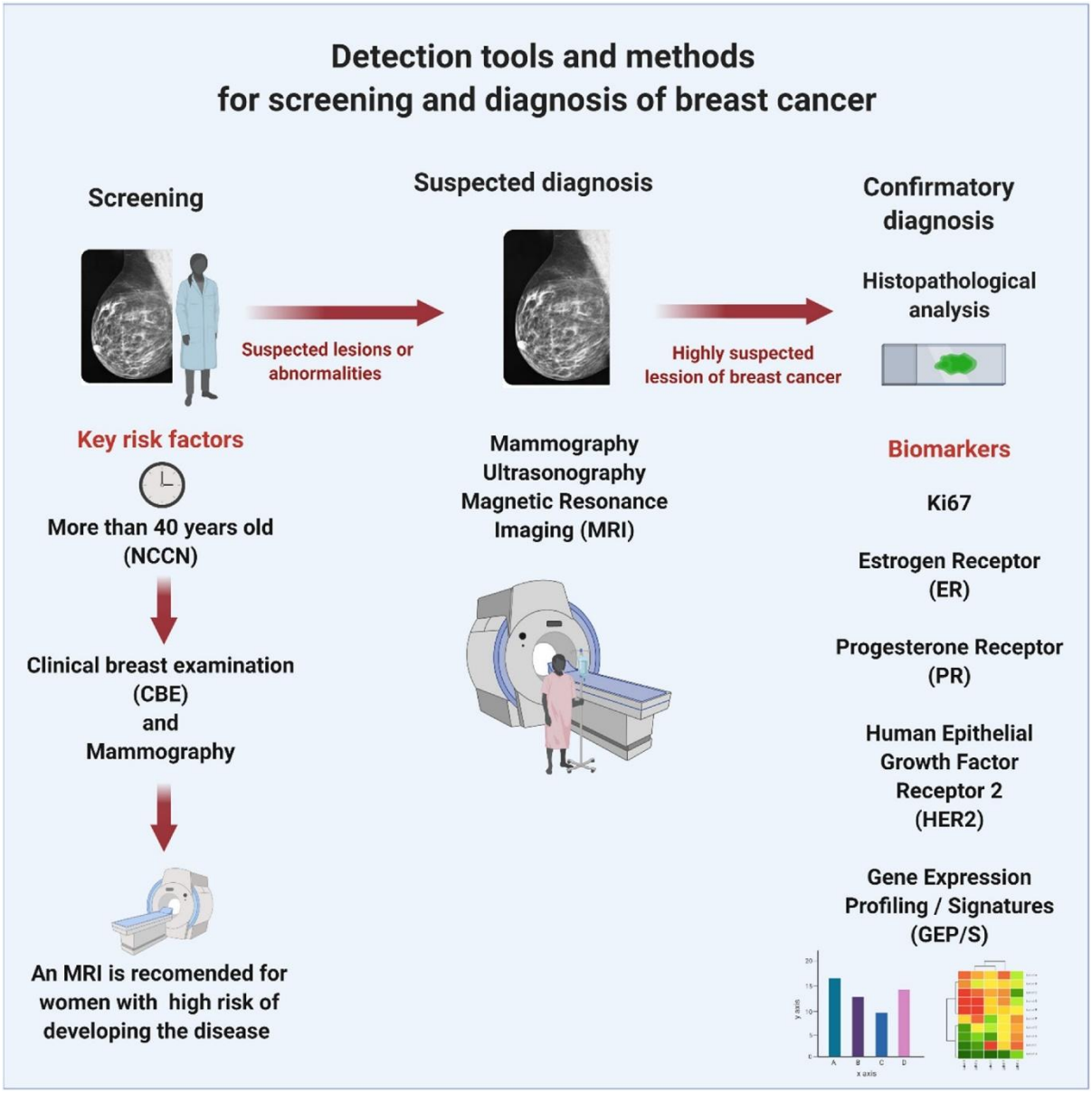

Figure 2: ***Tools and procedures for detecting and diagnosing breast cancer****. Image obtained from the article: Breast cancer, screening and diagnostic tools [11].*

1.5. Breast Cancer Statistics Worldwide

In 2021, Lei *et al.*, has shown that breast cancer statistics has exceeded lung cancer as the most diagnosed cancer with an estimated 2.3 million cases and 685,000 deaths in 2020 worldwide, and with cases expected to reach 4.4 million in 2070. Also, the World

Health Organization, in 2022, showed that there were 2.3 million women diagnosed with breast cancer and 670,000 deaths globally. Global estimations demonstrate remarkable disparities in the breast cancer burden based on human development [12], [13].

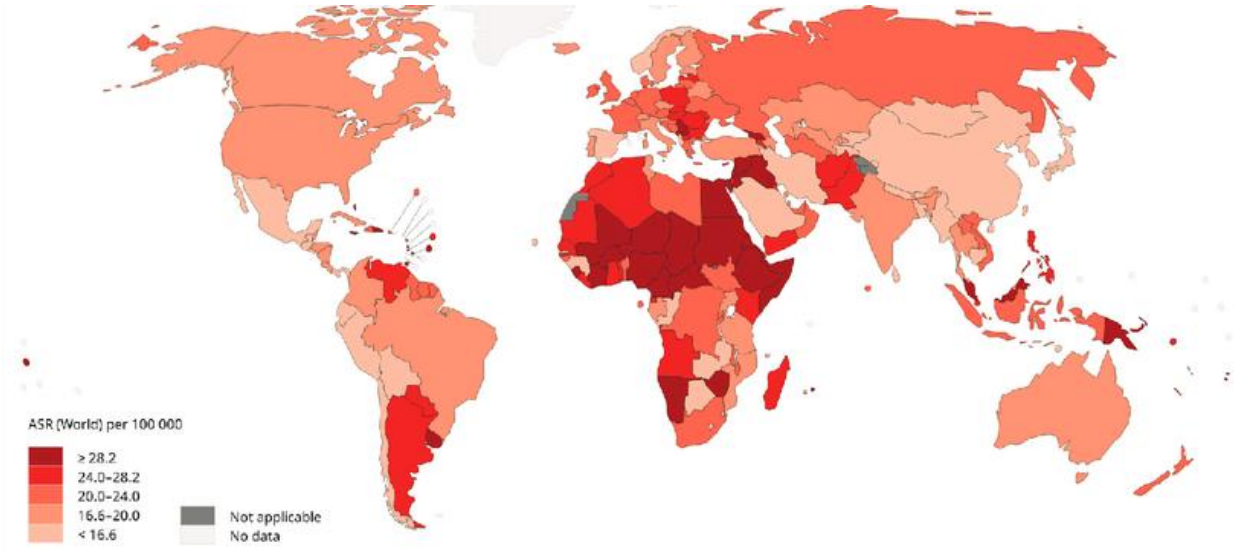

*Figure 3**: World maps for breast cancer age-standardized mortality rates.** Estimated age-standardised mortality rates for breast cancer globally, in 2020. Image Data obtained from GLOBOCAN 2020, International Agency for Research on Cancer 2023 [14].*

1.5.1. Breast cancer in Sub-Saharan Africa

In sub-Saharan Africa, breast cancer is the most common malignancy among women with approximately 129,000 new cases reported in 2020. In high-income countries, BC typically has a good prognosis while in sub-Saharan Africa, the survival rate is significantly lower. The 5-year survival rate in this region is estimated to be around or below 50%, meaning that one in two women diagnosed with the disease dies within five years. In comparison, the corresponding rates in the United States are one in five for Black women and one in ten for White women. Due to ageing and population increase, it is predicted that the yearly incidence of breast cancer in sub-Saharan Africa would almost double by 2040. In 2020, the African Breast Cancer - Disparities in Outcomes

Study (ABC-DO) was set up to examine determinants of breast cancer survival across five African countries at different stages of economic and epidemiological transitions. The study discovered varying BC incidence rates across five African countries, with Zambia at 20.0 per 100,000 women and Namibia at 57.6 per 100,000. Survival rates were relatively lower in Black African women: 90% in White Namibian women at 3 years post-diagnosis, compared to 58% in Black Namibian and South African women, 46% in Ugandan and Zambian women, and 36% in Nigerian women. The study also highlighted that the primary factors contributing to lower survival in women from lower socioeconomic backgrounds were late-stage diagnoses and limited access to surgery and systemic therapy. While higher rates of young-onset breast cancer, HIV positivity, and more aggressive tumor subtypes also contributed, they had a smaller impact on overall survival [15].

In South Africa, approximately 19.4 million women aged 15 years and older live at risk of being diagnosed with breast cancer [15], [16]. In 2013, deaths from breast cancer and cancers of the female genital tract accounted for 0.7% and 1% of all deaths in South Africa respectively [17]. In 2022, Nel C *et al.,* conducted a retrospective review of 151 treatment naïve TNBC patients that were presented to the Charlotte Maxeke Johannesburg Academic Hospital Breast Unit (CMJAH BU) from 1 July 2017 to 31 October 2020, and from this study most patients were postmenopausal and presented with an advanced disease which emphasizes the lack of diagnostic tools for breast cancer in South Africa. At 18 months, 26.5% of these patients had died [18]. Therefore, there is an urgent need to address the advanced stage of diagnosis and improve access to high-quality treatment in South Africa.

1.6. Risk Factors of BCs

Breast cancer can be caused by a combination of genetic mutations, environmental factors, and lifestyle. Age and breast density are naturally occurring characteristics that may raise the risk of acquiring the condition. Circadian rhythm, alcohol, and tobacco intake have been associated and linked to an increased risk of breast cancer. These factors can lead to cellular stress, increase the generation of reactive oxygen species (ROS), and alter oestrogen and progesterone hormone concentrations, exacerbating the tumor's aggressiveness. Poor eating habits have also been linked to an increased chance of developing breast cancer [19]. Breast cancer incidence rates may also be elevated due to increased risk factor prevalence, opportunistic or organized mammography screening detections, ageing, and population growth. However, it has been known since 1896 that hormone ablation through oophorectomy causes a subset of breast cancers to regress, and in the late 1950s, Elwood Jensen first described the oestrogen receptor (ER), which was then used to identify patients who responded to endocrine-based therapies. Progesterone, the other major ovarian hormone, has also been explored in breast cancer. Disparities in the burden of breast cancer resulted from differences in main risk factors, screening procedures, and population size or structures among areas [13].

1.7. Triple Negative Breast Cancer (TNBC)

Although the effect of progesterone on cancer growth has been variable, early studies suggested that progesterone receptor (PR) positive may better select individuals for endocrine therapy, as PR expression was a detectable outcome of oestrogen action, indicating intact downstream signalling. Shortly after, it was discovered that amplification of human epidermal growth factor 2 (HER2) was associated with a particularly dismal prognosis, resulting in a spate of HER2-directed medicines that have

eliminated the negative risk of HER2 expression. TNBC is defined as tumors that lack ER and PR expression as detected by immunohistochemistry, as well as HER2 expression as detected by immunohistochemistry and/or in situ hybridization [20]. From 2012 to 2016, triple-negative breast cancer accounted for 12% of all cases diagnosed in the United States, with 5-year survival rates 8% to 16% lower than the best prognosis subtype. These cancers tend to be more common in women younger than age 40, who are Black, or who have a Breast Cancer gene 1 (*BRCA1*) mutation. Despite the mortality of this subtype, preventative medications such as tamoxifen and mammographic screening procedures, which begin around age 40 to 50, are tailored to the biology and demographics of more frequent and less fatal luminal malignancies. To develop effective screening and prevention measures and address societal concerns, physicians must recognize linked ethnic, genetic, and modifiable risk factors associated with TNBC [21], [22].

1.7.1. TNBC Subtypes

By analysing the gene expression of 386 tumours, researchers have discovered six different subtypes of triple-negative breast cancer (TNBC), each with its own biological characteristics. Luminal androgen receptor (LAR), mesenchymal (M), mesenchymal stem-like (MSL), immunomodulatory (IM), and two basal-like (BL1 and BL2) subtypes are among them. Genes linked to the cell cycle and DNA damage response are highly expressed in the BL1 subtype, whereas growth factor signalling and myoepithelial markers are more frequently expressed in the BL2 subtype. While the MSL subtype contains lower levels of genes linked to cell proliferation, both the M and MSL subtypes show increased gene expression linked to growth factor signalling and the epithelial-mesenchymal transition (EMT). Consistent with the de-differentiated mesenchymal gene

expression pattern is the recent analysis of metaplastic breast cancers showing the majority of chondroid and spindle cell carcinomas to be of the MSL subtype. The IM subtype is composed of immune antigens and genes involved in cytokine and core immune signal transduction pathways. The AR drives the LAR subtype, which is distinguished by luminal gene expression. In contrast to MSL, which includes a significant proportion of normal-like subtypes, LAR is primarily composed of luminal and HER2 subtypes, and BL1, BL2, IM, and M are primarily composed of basal-like subtypes, according to comparison with the intrinsic subtypes. Apart from the intrinsic subtypes, a claudin-low subtype that is enriched for immune response, cancer stem cell-like genes, and EMT markers has just been identified. M and MSL TNBC subtypes make up the majority of this claudin-low subtype [23], [24], [25], [26], [27].

1.7.2. TNBC current treatments

Currently, treatment of TNBC involves chemotherapy, which is mostly used to shrink the tumor, making it less aggressive. Surgery is also used usually after chemotherapy to remove more of the tumor. Radiation therapy which uses beams of radiation is also used to destroy cancer cells using different techniques to avoid harming healthy tissues surrounding the breast. When it comes to targeted therapy, patients with TNBC are unlikely to benefit from currently available targeted therapies such as endocrine or anti-HER2 drugs, because there are no typical molecular targets. As a result, the only systemic treatment option for these patients is chemotherapy using typical cytotoxic drugs. Fortunately, multiple trials have demonstrated considerable chemosensitivity for these tumors, particularly in the neoadjuvant setting. In multiple trials, TNBCs have

exhibited high response rates (RR) to neoadjuvant chemotherapy, which includes anthracyclines and taxanes [28].

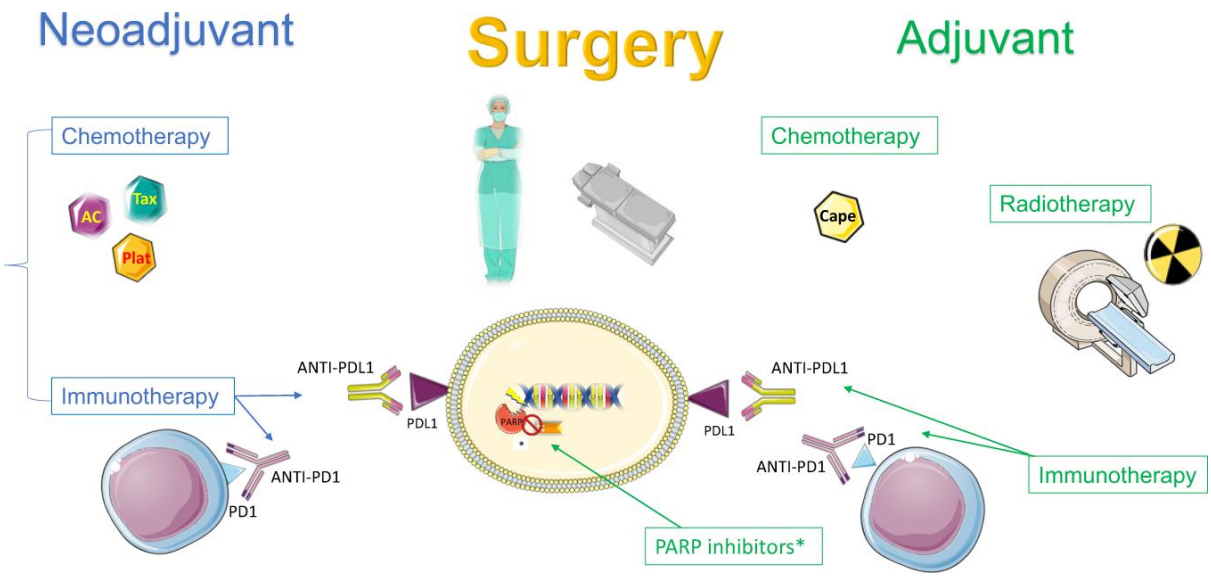

Figure 4: ***TNBC is currently being treated interdisciplinary, with neoadjuvant chemotherapy plus immunotherapy, surgery and radiation, and adjuvant treatment with continuous immunotherapy***. *Figure obtained from an article:* ***Triple-negative breast cancer: Pitfalls and progress*** *[29]*

1.7.3. Challenges in treating TNBC

Triple-negative breast cancer (TNBC) poses a significant clinical challenge due to its aggressive nature and lack of targeted treatment options. Several factors contribute to the difficulties in managing TNBC, emphasizing the need for innovative therapeutic approaches.

TNBC exhibits substantial molecular heterogeneity, making it challenging to identify uniform treatment strategies. The absence of ER, PR, and HER2 expression in TNBC leads to diverse subtypes with distinct genetic profiles, necessitating personalized and targeted therapies. TNBC also often exhibits poor response to conventional chemotherapy, leading to challenges in achieving durable remissions. Chemoresistance

is a significant hurdle, necessitating the exploration of alternative treatment modalities and combination therapies. Another challenge in treating TNBC is led by the tumor microenvironment in TNBC, which is characterized by immunosuppressive features, limiting the efficacy of immunotherapy therefore strategies to overcome immune evasion and enhance the anti-tumor immune response are critical for improving treatment outcomes [30], [31], [32].

TNBC also often presents with early relapse and a higher propensity for distant metastasis. The aggressive nature of the disease necessitates the development of targeted therapies that can prevent recurrence and effectively manage metastatic disease. Therefore, addressing these challenges requires ongoing research efforts, innovative clinical trial designs, and a comprehensive understanding of the molecular mechanisms underlying TNBC [31].

1.8. Impact of Biomarker Testing on Cancer Treatment Decisions

Biomarker testing has a substantial impact on cancer treatment decisions, particularly in TNBC. Biomarker testing aids in the identification of the most appropriate targeted medicines for individuals, hence improving patient outcomes through more effective and personalized treatment regimens. Biomarker testing is crucial for guiding treatment decisions and connecting patients to the most relevant medications based on their unique biological characteristics. Biomarker testing is critical in pre-operative cancer therapy because it helps guide optimal treatment decisions before surgery. Recognizing the relevance of biomarker testing and its impact on treatment allows healthcare providers to advance cancer care and provide patients with personalized, effective treatments [33].

The expression of tumor-associated calcium signal transducer 2 (Trop2) and Zinc transporter (LIV-1) in a variety of solid tumours has led to their utilisation in antibody–drug combination designs as a transport gate for cytotoxic drugs entering cells.

1.8.1. Trophoblast cell-surface antigen 2 (TROP2) role in TNBC

Precision medicine has created new opportunities in the field of targeted therapy development. Trophoblast cell-surface antigen 2 (trop2) is a promising therapy option for TNBC, as it is expressed in approximately 85% of tumors. Trop2 is one of many targetable gene mutations or marker proteins being explored in cancer therapy. Trop2 was initially found in trophoblast cells as a surface marker. Tumor-associated calcium signal transducer 2 (TACSTD2), found on chromosome 1p32, encodes Trop2. Trop2 consists of extracellular and transmembrane domains, as well as a cytoplasmic tail. Trop2 involvement in breast cancer progression spans various facets, from promoting cell proliferation to resisting therapies. Crucially, it activates several tumorigenic signaling pathways, like the Wingless-related integration site beta (Wnt/b-catenin) and epidermal growth factor receptor (EGFR)-linked to the mitogen-activated protein kinase/Extracellular signal-regulated kinases (MAPK/ERK) and phosphatidylinositol-3 kinase/ protein kinase B (PI3K/Akt) pathways as shown in **(Figure 5**). Additionally, it has an impact on matrix metalloproteinases, which promote the invasion of cancer cells, and it also contributes to the maintenance of cancer stem cells (CSCs), which are linked to tumour recurrence and resistance to treatment. These pathways highlight trop2's potential as a therapeutic target by illuminating its diverse functions [25],[37],[38].

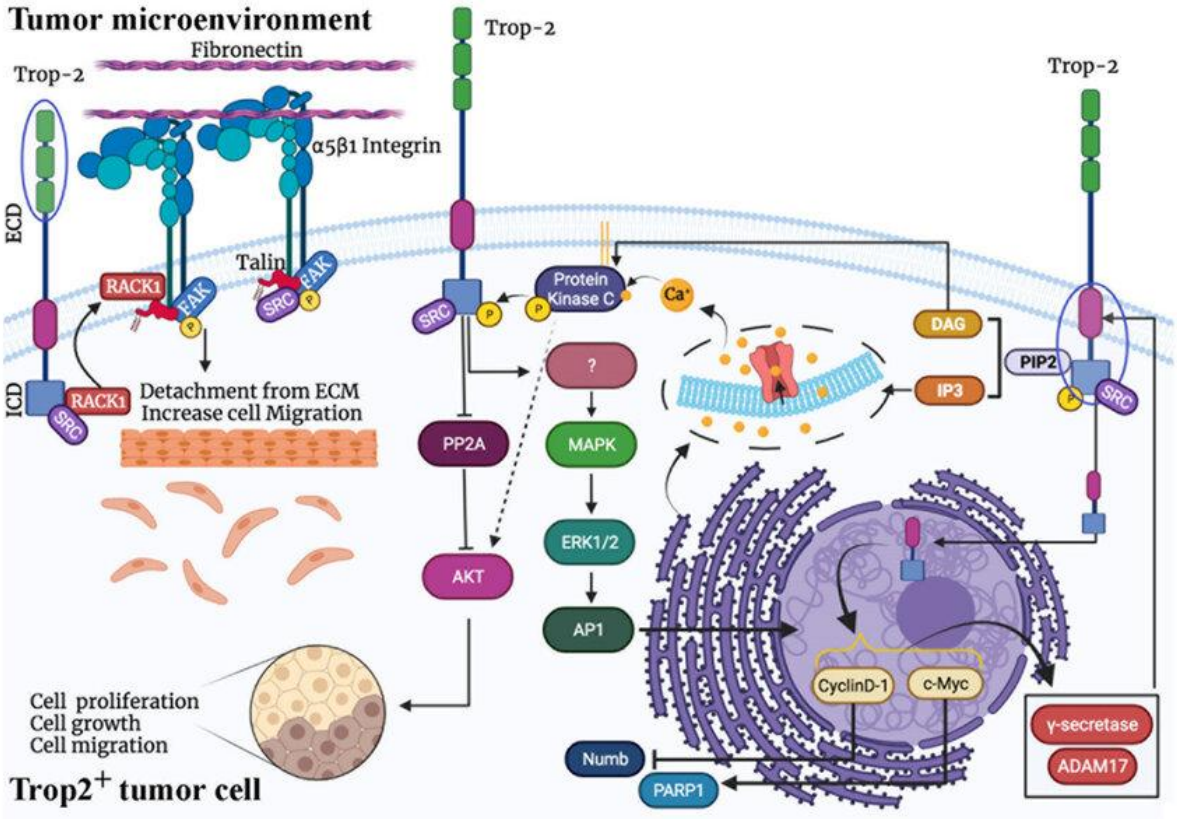

Figure 5: ***Diagram illustrating the involvement of TROP2 in various oncogenic signaling cascades****. Trop2 activation is reliant on or independent of growth factors. Trop2 then raises internal Ca2+ levels, enhancing protein kinase C (PKC) signaling. Trop2 phosphorylation, on the other hand, engages the RACK1 scaffold protein, which allows Trop2 to connect with other signaling pathways such as the PI3K/Akt, MAPK, and FAK pathways. Trop2's transmembrane and intracellular portions are separated by γ-secretase and ADAM-17, and its movement into nuclease interacts with other genes involved in cancer growth. Overall, Trop2 can stimulate cell proliferation, growth, and migration in a variety of ways. [34].*

1.8.2. Zinc Transporter (LIV-1) role in TNBC

Solute Carrier Family 39 Member 6 (SLC39A6), commonly known as LIV-1, is a zinc transporter controlled by oestrogen and more prevalent in oestrogen receptor-positive breast cancer and lymph node metastases. The LIV-1 subfamily of Zinc transporters (Zrt)- and Iron transporters (Irt)-like protein (ZIP) zinc transporters is made up of nine human sequences that are highly homologous across transmembrane domains. Several of these sequences can transport zinc and other ions across cell membranes. Recent research

has linked the LIV-1 transporter subfamily to many diseases. It is a multi-span, histidine-rich transmembrane cell adhesion protein with metalloproteinase activity, and is classified as a zinc transporter since it mediates intracellular signaling pathways and zinc influx into the cytoplasm, controlling zinc levels alongside Cation Diffusion Facilitators (CDFs) and zinc-binding proteins. Zinc's participation in tumor surveillance and apoptosis is the result of an interplay between zinc transporter expression, zinc levels, and immunological signaling pathways [35],[36], [37].

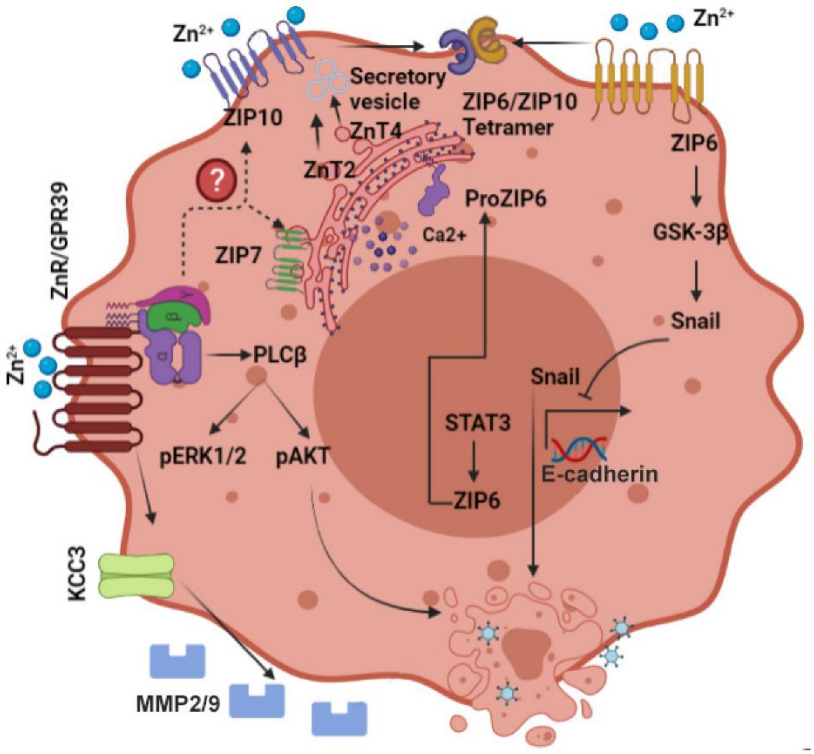

Figure 6: ***A schematic illustrating the activation of signaling pathways involved in breast cancer growth and metastasis****. Zn2+ dyshomeostasis activates several pathways that influence cell shape, migration, and proliferation. ZIP10 and ZIP6 cooperate to govern epithelial to mesenchymal transition, while ZnR/GPR39 stimulates membrane protrusions and MMP2/9 release. Arrows represent established channels, whereas dotted lines and question marks represent possible pathways for regulation and interaction [38]*

1.9. Immunotherapy approaches in TNBC

Immunotherapy has emerged as a potentially effective therapeutic strategy that stimulates the immune system to specifically target and eliminate cancer cells. Immune editing is the basis of this tactic, which increases tumour cells' antigenicity and immune cells' capacity to kill tumours. It also helps to boost anti-tumor immune responses, activate or restore immune system function, neutralise immunosuppressive chemicals, and stop tumour cell development. It so offers a chance to lower the death rate from triple-negative breast cancer (TNBC) [39], [40]. Due to the absence of three biomarkers, TNBC patients do not currently treatment endocrine or anti-HER-2 therapy as it targets the absent biomarkers. For a long time, chemotherapy was the only systemic treatment for TNBC. Due to the lack of effective treatment options. TNBC has the worst prognosis of any breast cancer subtype and is more likely to react to immunotherapy due to increased programmed death-ligand 1 (PD-L1) expression and a higher proportion of tumor-infiltrating lymphocytes. Immunotherapy has transformed TNBC treatment, particularly with the Food and Drug Administration’s (FDA's) approval of pembrolizumab (Keytruda) in combination with chemotherapy for advanced cases, opening up new paths for treating this fatal disease. While immunotherapy can greatly improve outcomes for some patients, achieving the desired response in all patients remains a challenge. Strategies aimed at improving the effectiveness of immune checkpoint blockade such as combining immunotherapy with chemotherapy, targeted molecular therapies, or radiotherapy may help improve response rates and overall clinical outcomes [41], [42].

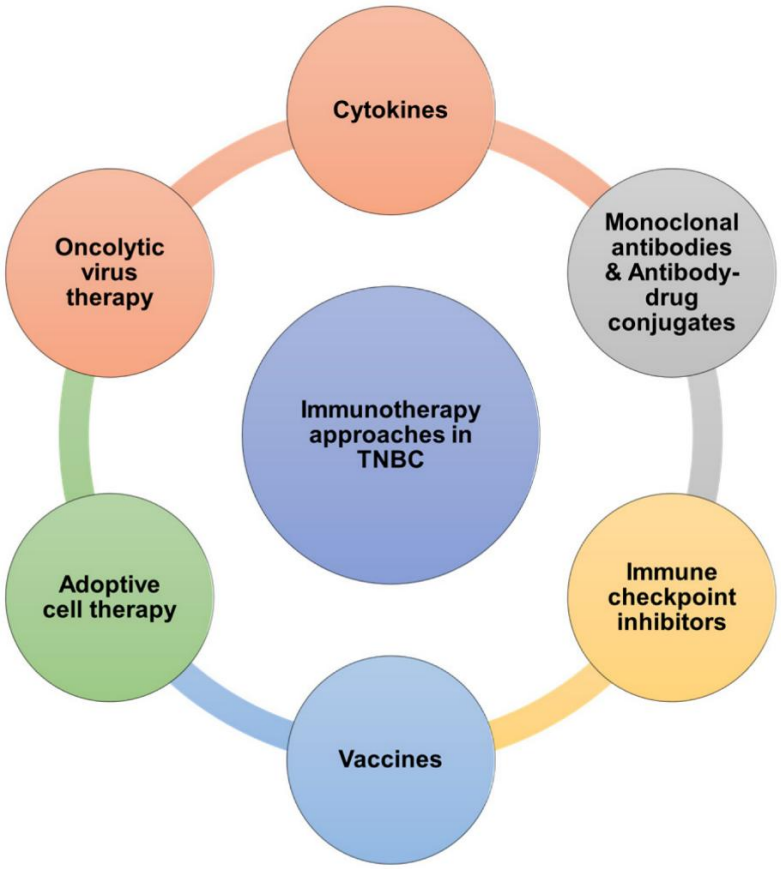

*Figure 7**: Current clinical approaches in TNBC Clinical immunotherapy approaches for TNBC**. Figure obtained from the article: Present and Fure of Immunotherapy for Triple-Negative Breast Cancer [41].*

1.9.1. Rationale of Combining Immunotherapy with Other Therapies

TNBC is an aggressive disease that frequently develops resistance to standard-of-care (SOC) treatments. Thus, immunotherapy combined with SOC is predicted to enhance outcomes for various reasons. Firstly, different medicines use distinct strategies to target cancer cells. Combining immunotherapy with chemotherapy, targeted therapy, or radiation therapy allows cancer cells to be attacked through many channels at the same time, resulting in a robust response [43]. Secondly, some medicines can improve the immune system's ability to recognize and target cancer cells. Chemotherapy, for example, can cause immunogenic cell death, releasing tumor antigens that trigger the immune response, hence enhancing immunotherapy effectiveness [44]. Also, TNBC

frequently develops resistance to single-agent treatments. Combination therapy can target many pathways involved in carcinogenesis and immune evasion, lowering the risk of acquiring resistance [45] and not every patient responds to immunotherapy alone. Furthermore, combining immunotherapy with additional medicines may extend the range of individuals who benefit from treatment, leading to better overall outcomes [46] as well as combining lower doses of several medications can lessen individual treatment-related toxicities while preserving efficacy, thereby enhancing patients' quality of life [45]. Lastly, by eliminating any remaining cancer cells that can spread to other tissues or organs, treating TNBC with a combination of medicines may reduce the chance of metastasis or recurrence [47]. Immunotherapy combined with combination methods offers a thorough strategy for treating TNBC, addressing its resistance mechanisms and heterogeneity while optimizing treatment efficacy and reducing toxicity.

1.9.2. Discovery of toxin-delivering Immunotherapeutics

In 1877, Paul Ehrlich reported on the distinct staining of tissues and proposed a reasonable approach to developing cancer-specific agents. The discovery of monoclonal antibodies (mAbs) and the capacity to generate vast quantities of mAbs that respond with specific antigens on cancer cells rekindled interest in utilizing toxins to kill cancer cells. Novel Immunotherapeutics for tumor cell killing were developed by connecting such toxins to mAbs: antibody-drug conjugates employ chemical conjugation to synthetic small molecule toxins, whereas in immunotoxins catalytically active protein toxins are used [43].

1.9.3. Antibody Drug Conjugates (ADC's) generation

Antibody-drug conjugates (ADCs) are developed to deliver potent small molecules of toxins usually to cancer cells. This approach involves the specificity of a monoclonal antibody (mAb) with the high potency of synthetic molecules and has the potential to improve cancer treatment. ADCs are made up of three components. An antibody which is directed to a tumor antigen, a highly potent cytotoxic payload, and a linker between the former two components [48].

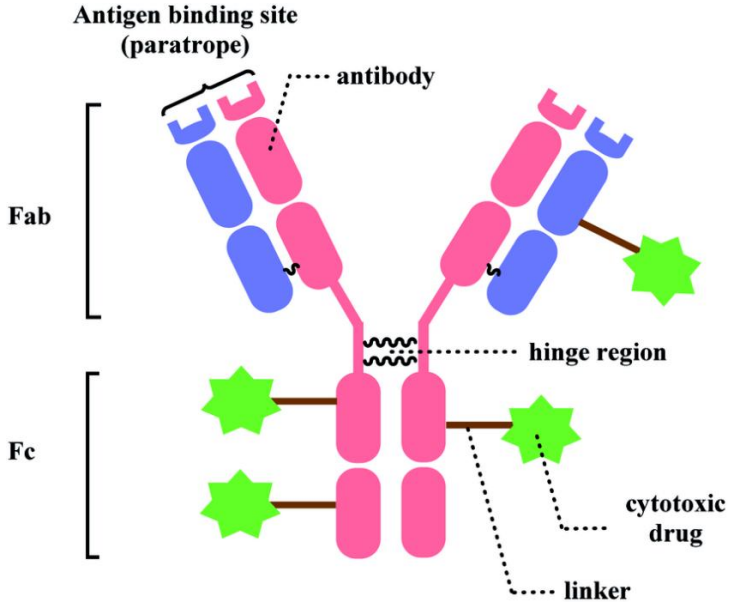

Figure 8: ***Schematic representation of an antibody-drug conjugate (ADC)****; each component (the antibody, payload, linker, and conjugation chemistries) can all have important implications for the properties of the ADC. Diagram obtained from a review article: Recent developments in chemical conjugation strategies [49].*

Among different types of antibodies, humanized and fully human immunoglobulin G (IgGs) are commonly used as the backbone for antibody-drug conjugates (ADCs) due to their stability in the bloodstream (with an elimination half-life of 14–21 days) and their strong ability to activate innate immune cells, like natural killer (NK) cells and macrophages, through Fcγ receptor interactions [48], [50]. The use of human IgGs,

particularly IgG1, assists in reducing the overall immunogenicity of the ADC, minimising the risk of hypersensitivity reactions and the formation of anti-drug antibodies (ADAs) [48], [50].

The payloads used in antibody-drug conjugates (ADCs) are usually more toxic than chemotherapies, showing sub-nanomolar or even picomolar levels of cytotoxicity *in vitro,* compared to the micromolar levels seen with many standard chemotherapies. Most payloads are moderately to highly hydrophobic, which plays a key role in both their efficacy and toxicity. While this hydrophobicity is beneficial, it can also be a challenge for ADC effectiveness. For example, hydrophobic payloads can be substrates for multidrug resistance proteins, potentially reducing the effectiveness of ADCs in tumors that express these transporters [51], [52].

Chemical linkers play a crucial role in ensuring that cytotoxic payloads stay attached to the antibody until they reach their target. Two main types of linkers involve non-cleavable and cleavable. Non-cleavable linkers are made of stable bonds that resist degradation, offering strong stability in the bloodstream. However, to release the cytotoxic payloads attached to these linkers, complete endocytosis and antibody digestion are required. This process is carried out by cytosolic and lysosomal proteases, releasing the payloads while leaving behind a residual amino acid (typically cysteine or lysine) from the degraded antibody. On the other hand, cleavable linkers, commonly used in current ADCs, are designed to break down in response to tumor-specific conditions, such as acidic or reducing environments, or through intracellular proteases. These linkers allow for the efficient release of active payloads once inside cancer cells, leading to cytotoxicity and enhancing ADC potency, while also promoting the bystander effect [51], [53].

1.9.3.1. Antibody Drug Conjugates Mechanism of Action

The most appealing feature of antibody-drug conjugates (ADCs) is their ability to selectively deliver the drug directly to cancer cells. To prevent degradation by stomach acid, the drug is given intravenously. It then locates and binds to specific target antigens, after which the drug-antigen complex is internalized by the cell through receptor-mediated endocytosis. As illustrated in **figure 9**, this process leads to the formation of an early endosome, where the influx of proton ions creates an acidic environment [20]. The late endosome fuses with the cell lysosome containing proteases resulting in lysosomal degradation. The cleavage of the linker due to acidic pH or the presence of protease in the lysosome allows the release of payloads into the cytoplasm and the payloads to take effect [21],[54], [55], [56], [57].

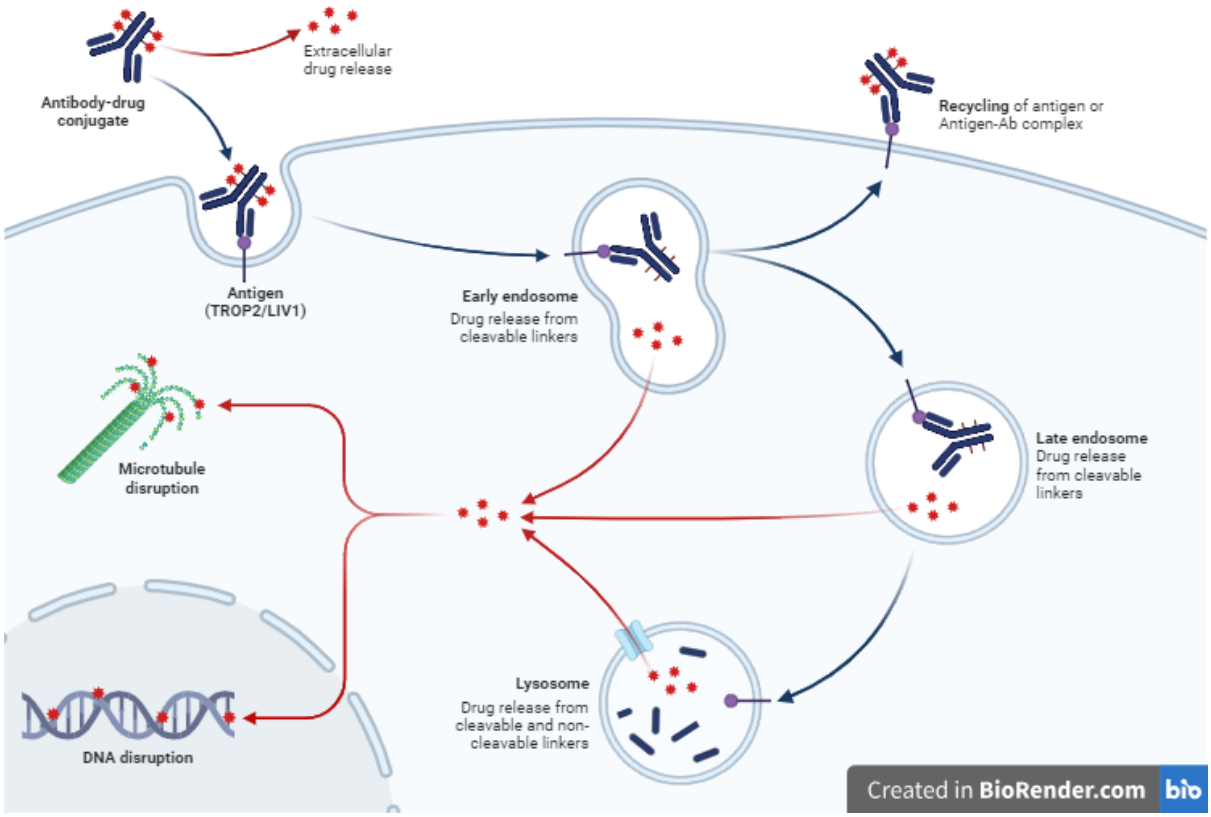

Figure 9: ***Antibody drug-conjugate mechanism of action****. The binding of the antibody to the cell surface receptor triggers the signal for receptor-mediated internalization. Multivalent antibodies can engage with several antigens, resulting in clusters or homodimers of antibody-antigen complexes (1). The development of these homodimers improves the signal for clathrin-mediated endocytosis, resulting in more effective uptake of the complex by cells. Alternatively, a monovalent antibody can engage with only one antigen at a time, resulting in fewer clusters (2). This type of antigen-antibody complex exhibits weaker receptor-mediated endocytosis. Once endocytosed, the complex is transported to early endosomes, where it can be recycled back to the cell surface or mature into late endosomes, where its intracellular pathway is defined. Recycling can start from the late endosomal stages. Monovalent ligand-mediated endocytosis is thought to often undergo receptor recycling. The cytotoxic chemical coupled to the antibody can cause cell death by disrupting microtubules or DNA once released in the cytoplasm. The figure was created using Biorender.com.*

1.9.4. General Features of Immunotoxin

Immunotoxins are defined as chimeric proteins made up of either an antibody or antibody fragment derived from the immune system that confer target specificity fused or conjugated to a toxic protein. Immunotoxins have evolved with time and technology

and can be categorised into three generations [58]. As research progressed, toxin autonomic cell-binding domains were identified and eliminated, resulting in a toxin fragment that could no longer bind normal cells, which was coupled to an antibody. While full-length immunoglobulin G (IgG) has good *in vivo* half-life and effector functions, its large size limits antibody tissue penetration, especially in solid tumours, and complicates the manufacturing process. The first generation of immunotoxins was created by chemically coupling native toxins to antibodies using crosslinking reagents that create disulphide bonds between the toxin and the antibody. Furthermore, most of monoclonal antibodies (mAbs) used in the first two generations were derived from murine sources. The use of non-human mAbs presents several therapeutic limitations [24]. Third-generation immunotoxins are engineered using recombinant DNA technology, combining the variable fragments of an antibody (Fv) with toxins that do not have their cell-binding domains, all within the same protein. Since the initial report of Fv production in 1988, where the variable regions of the antibody's heavy and light chains were linked by a peptide, over 1,000 third-generation immunotoxins have been developed. These immunotoxins primarily target antigens specifically expressed on cancer cells. It was anticipated that these agents could induce regression of malignant diseases in patients. However, because the toxins and toxin domains originate from bacteria or plants, they are highly immunogenic in humans, limiting treatment to only a few doses per patient. Current research focuses on reducing the immunogenicity of these toxins by removing immunogenic epitopes from their surfaces [58], [59], [60].

1.9.4.1. Advantages of Immunotoxins over Antibody Drug Conjugates (ADCs)

Immunotoxins possess several advantages properties that differentiates them from ADCs. Firstly, their unique mechanism of action results in a specific toxicity profile,

making them highly compatible with standard-of-care treatments. Secondly, unlike conventional chemotherapeutics and those used in ADCs, immunotoxins can effectively target quiescent, non-dividing cells. Additionally, immunotoxins show minimal cross-resistance with other therapeutic agents and have shown efficacy in patients resistant to chemotherapy. Lastly, while ADCs may cause off-target toxicity due to premature dissociation of the payload from the chemical linker, modern recombinant immunotoxins avoid this issue. Their recombinant peptide linkers, which connect the toxin to the antibody, require specific intracellular proteases for activation, ensuring greater precision [54], [56], [61].

1.9.4.2. Disadvantages of Immunotoxins

Unlike chemotherapy, immunotoxins are composed of proteins that the human immune system recognizes and responds to due to their non-human origin. The immune system reacts to both the murine antibody fragment and the non-human protein toxin by producing human anti-mouse antibodies (HAMA) and human anti-toxin antibodies (HATA). Once antibody levels in the bloodstream become too high, the patient can no longer continue the treatment. To address this issue, newer generations of immunotoxins are being developed using humanized or fully human antibody fragments, and efforts are underway, as discussed in subsequent chapters, to reduce the immunogenicity of the toxin component. However, a significant drawback of immunotoxins is their potential to cause Vascular Leak Syndrome (VLS). Administered intravenously, immunotoxins can interact with epithelial cells lining blood vessels, leading to VLS, which can range from severe to fatal. Other serious side effects, such as hepatotoxicity, have also been observed, leading to the discontinuation of some clinical trials [62], [63], [64].

1.9.5. *Pseudomonas Exotoxin* A (ETA) Recombinant Immunotoxins (rIT)

Recombinant immunotoxins (rITs), a unique class of anticancer drugs, are made of a bacterial toxin that has been modified and fused to an antibody fragment to target cancer cells. Using antisera for species-specific extracellular antigens, Liu *et al*. isolated pathogenic *Pseudomonas* species and found the PE toxin. Because the extracellular antigens were heat-liable and caused necrotic lesions in rabbit skin, they demonstrated exotoxin properties. In several animal species, including rats, rabbits, dogs, and rhesus monkeys, purified PE toxin proved fatal. Four hours after exposure to the toxin, the animals developed disseminated hepatic necrosis. The increased levels of fibrin splits in the blood samples demonstrated that infected mice and dogs frequently had hypofibrinogenemia (either alone or in conjunction with thrombocytopenia). In laboratory guinea pigs, sublethal intradermal injections of PE toxin caused non-haemorrhagic skin necrosis, whereas in rabbits, intracorneal injections caused stromal, endothelial, and epithelial necrosis [65], [66]. P*seudomonas* exotoxin A (PE) (ETA') is a strong bacterial toxin produced by *Pseudomonas aeruginosa* that quickly stops all protein synthesis in cells and causes cell death by altering and inactivating the vital Elongation Factor-2 (eEF-2). By substituting an antibody against a cell surface protein that expresses differently in normal and cancer cells for the natural binding domain, PE can be targeted selectively to the target malignant cell. After binding, the full RIT molecule is ingested with the target and processed within the cell to release PE into the cytosol. Many cells can undergo apoptosis when just a few PE catalytic units are introduced into the cytoplasm [67]. In early-stage clinical studies for leukaemia patients, immunotoxins containing the PE38 fragment of the PE catalytic domain showed significant effectiveness, including inducing complete remissions in individuals who had

previously failed to respond to treatment [68]. These immunotoxins target antigens involved in B-cell differentiation, which are not present in essential organs. This provides a big enough therapeutic window for clinical application [69].

1.9.5.1. Pseudomonas aeruginosa exotoxin A structure & domain functions

Pathogenic *Pseudomonas aeruginosa* species often produce PE toxin, a virulence component encoded on their chromosomes. This proenzyme, comprising 638 amino acids, possesses mono-Adenosine diphosphate (ADP) ribosyl transferase activity. Its carboxyl-terminal features a specific 5-amino acid sequence (REDL residue). The crystalline structure of the toxin, determined at 3.0 Å resolution, reveals three main domains: domain I is subdivided into Ia (amino acid residues 1-252) and Ib (amino acid residues 365-404), while domain I comprises of residues 253-364 and domain III covers residues 405-613. Domain I exhibit a structure similar to the β-rolls found in influenza hemagglutinin and consists of 17 antiparallel β strands that form an elongated β-barrel shape. Domain Ia was removed during the process of rIT formation [70].

Domain II, is necessary for the catalytic domain to go intracellularly into the cytosol of cells. It is made up of a disulfide bond joining six successive helices [71]. Histidine 275 and glutamic acid 80, arginine 274 and aspartic acid 139, and glutamic acid and lysine 114 form salt bridges that connect these helixes to domain Ia. Hydrogen bonds and cysteine (265–287) disulfide linkage reinforce the α-helices' surface loop between arginine 279 and glycine 280, which contains protease and furin cleavage sites. The tryptophan 281 (Trp281) is located at the P20 position, closer to the furin cleavage site. Regardless of the furin cleavage site being exposed, any mutation in Trp281 results in the loss of PE toxin effectiveness. Furthermore, a decrease in toxin activity was linked to the

substitution of glutamic acid or glycine for the amino acids His246, Arg247, and His249. Nevertheless, PE cytotoxicity was unaffected by the substitution of lysine for the three residues [72]. The shortened PE moiety indicates less immunogenicity, and the protease cleavage sites can be removed without impairing toxin function. On the other hand, as furin cleavage sites are essential for toxin detachment from antibodies in the endosomal compartment and the start of cellular poisoning, their loss decreased the effectiveness of the IT [73].

Lastly, the catalytic domain III starts at amino acid 405 and finishes at amino acid 613. The flexible loops (L1, L3, and L4) in domains I and II are structurally distinct from this one, which is interesting. It indicates that the flexible loop L1, which is controlled by Alanine 457 (Ala 457) and Ala 464, is inhibitory in its closed conformation. By forming a salt bridge with the domain II helix at Glu348 the side chain Arg467 stabilises the L3 loop. The side chains of Leu462, glutamine 460 (Gln460), and arg458 prevent Nicotinamide adenine dinucleotide (NAD+) from attaching to the active site. The binding of PE toxin to the ADP ribose sugar of NAD+ is made possible by conformational alterations in the L2 (517–522) and L3 (546–551) loops [72], [74]. Additionally, domain III gains a carboxyl terminal that contains the REDL, a sequence of five amino acids: Arg-Glu-Asp-Leu-Lys. The KDEL motif is similar to the REDL sequence [74]. According to a study by Chaudhary *et al.*, toxin activity was unaffected by mutations in the amino acids 602–608. However, the elimination of PE cytotoxicity was linked to deletions of Arg 609 and 612–613. Additionally, the amount of cytotoxicity was reduced by a factor of 6–10 when glycine, glutamic acid, or leucine were substituted for Arg 609. Nevertheless, the cytotoxic profile of the PE toxin remained unchanged when Arg 609 was substituted with lysine. Because of this, basic amino acids must be present at this location [74].

To elucidate the connection between the carboxyl-terminal of PE toxin and ADP-ribosyl transferase activity, Arg-609 and Asp-611 were removed from the mutant PE molecule using RPHMPGDILK. The endocytic vesicle did not internalize this chemical, and it did not have any harmful consequences. The molecule's cytotoxic activity was restored when RPHMPGDPDYASQPGKPPREDLK was added to the carboxyl terminus. The five amino acids of REDLK can be retained while attaching a binding ligand (such as TGF-α) to the PE toxin inside the carboxyl terminus of PE. PE domain III was shown to share significant similarities with dehydrogenases and nicotinamide adenine dinucleotide (NAD+/NADH) binding enzymes that were isolated from different animals. However, NAD+ is used as a substrate rather than a cofactor by PE domain III. Without creating a hybrid ion, it can break the C-N bond that connects the nicotinamide and ADP ribose moiety [70], [72], [74], [75].

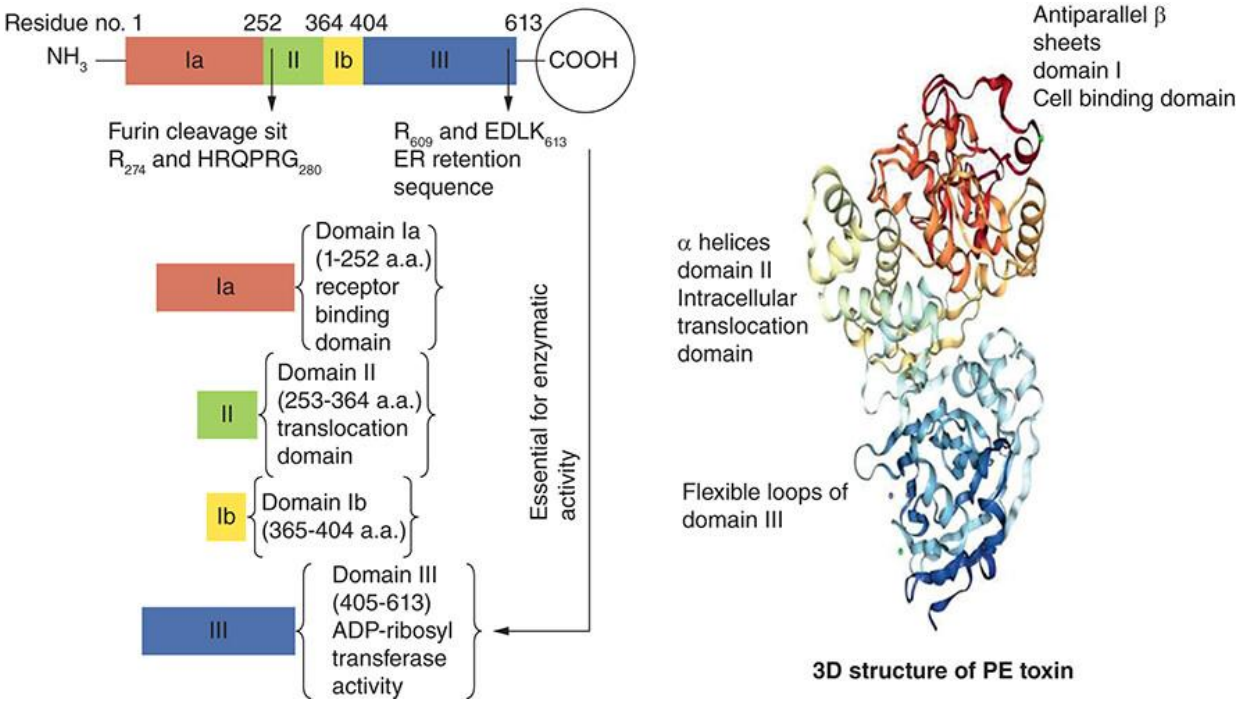

Figure 10: PE (A) toxin showing amino acid sequences of three domains (I, II, and III) and their intracellular function [66].

1.9.5.2. Mechanism action of rITs

The plant and bacterial toxins used in immunotoxins kill cells by disrupting protein synthesis. For the toxin to be effective against tumors, it must be delivered to the cytosol. This process initiates when the immunotoxin's targeting component binds to specific receptors on the surface of cancer cells, such as CD91. For instance, *Pseudomonas Exotoxin A* targets CD91 within the mammalian cell as shown in **figure 11**. Initially, domain I of the toxin binds to the α2-macroglobulin CD91 receptor, also known as low-density lipoprotein receptor-related protein 1 (LRP1), which leads to internalization into the endocytic cell compartment. The processing and movement of these molecules are specific to both the target and the toxin, but they eventually result in the transfer of the active enzymatic fragment of the toxin to the cytosol. Immunotoxins are internalized through receptor-mediated endocytosis and travel through the endolysosomal system to the Golgi apparatus, where they are transported to the endoplasmic reticulum (ER). After that the toxin is activated through the reduction of a disulfide bond and cleavage by the protease furin, which separates the Fv fragment from the catalytic part of the toxin. Once activated, the toxin translocates into the cytosol, where its ADP-ribosylates and inactivates elongation factor 2, a crucial component of the protein synthesis machinery. This blockage of protein synthesis eventually results into cell death [64], [79], [80].

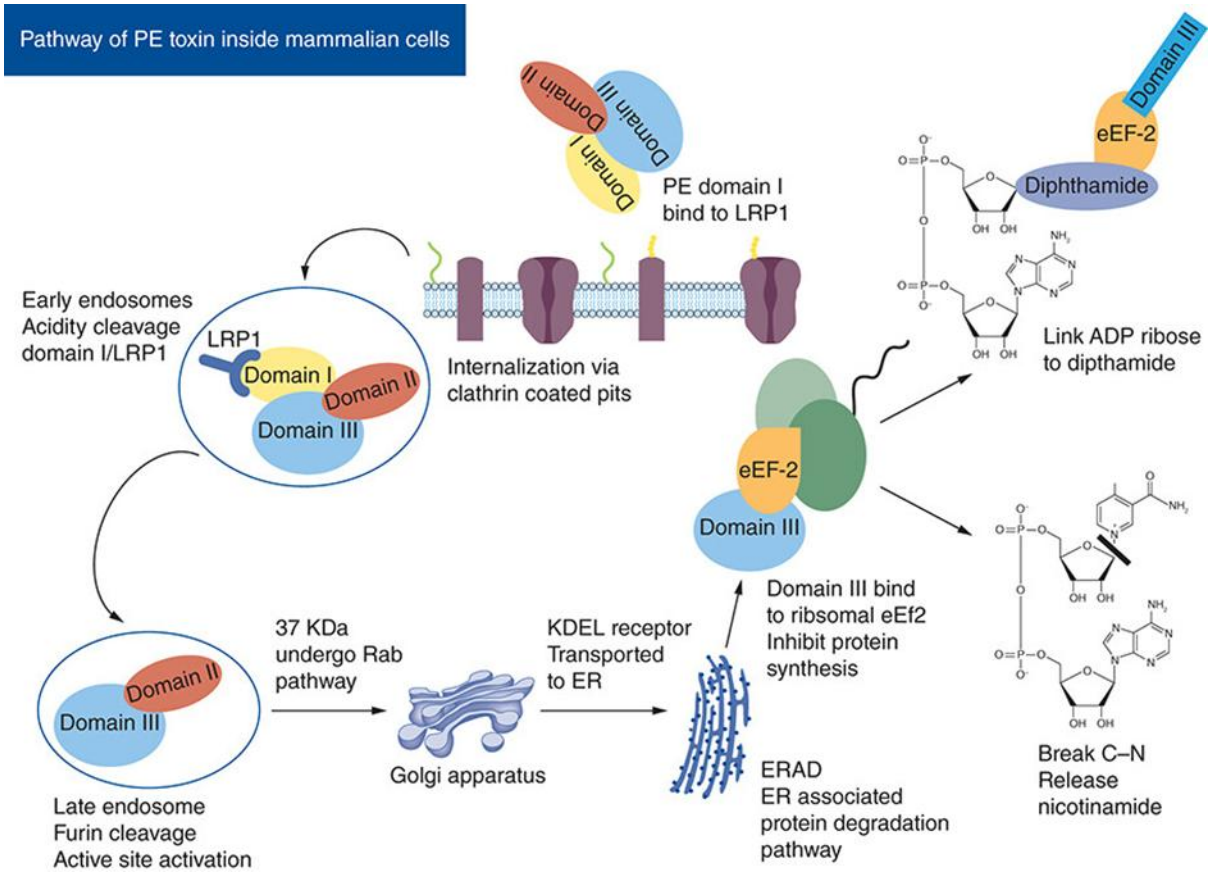

Figure 11: ***Pathway of Pseudomonas aeruginosa exotoxin A (ETA') toxin inside the affected cell and ADP-ribosylation of ribosomal elongation factor 2****. An immunotoxin is genetically fused to a scFv antibody that binds to an antigen on a target cell. Once the immunotoxin binds to the target cell, the antigen-immunotoxin complex enters the target cell through endocytosis. The immunotoxin is either localized to an acidified endosome or endoplasmic reticulum (ER) and Golgi apparatus in the cell. Once inside these organelles the linker connecting the toxin and scFv is cleaved. The free toxin catalytically inactivates the protein synthesis machinery of the cell. This is achieved by catalyzing ADP ribosylation and inactivating elongation factor 2. This results in the arrest of protein translation and leading to cell death. The figure was obtained from the article: Advances in Anticancer Immunotoxin Therapy [66].*

1.9.6. Recombinant Immunotoxins (RITs) for solid tumors

1.9.6.1. SS1P Recombinant Immunotoxin

Alewine *et al.,* in 2015 identified SSIP immunotoxin and it is one of the immunotoxins currently being clinically tested as a systemic agent in solid tumor patients. SS1P contains the same PE38 fragment found in moxetumomab pasudotox and LMB-2 (an

immunotoxin targeting the interleukin 2 receptor), but it uses the SS1 antibody, which targets mesothelin (MSLN). Two phase I trials of single-agent SS1P were conducted, each with a different administration schedule. The efficacy and toxicity profiles were compared, and they found that most patients developed antidrug antibodies by the end of the first treatment cycle, leading to subtherapeutic drug levels if additional cycles were administered. Dose-limiting toxicities included self-limiting pleuritis, likely caused by the targeting of MSLN, which affected the normal pleura. Subsequent experiences showed that this toxicity could be effectively managed with steroids and prompt narcotic pain medication at the first signs as well as vascular leak syndrome and fatigue were also observed. These findings highlighted the need for strategies to manage the immune response against this therapeutic. In their study they further tested SS1P in combination with standard chemotherapeutics (cisplatin and pemetrexed) in patients with newly diagnosed malignant mesothelioma and they observed the toxicity in this phase I study similar to that seen with the individual drugs. No reduction in the established SS1P dose was required for the combination to be safe. Fatigue was identified as the dose-limiting toxicity. In this study, 12 out of 20 patients achieved a partial response, although the chemotherapy-induced hematologic suppression did not prevent the development of neutralizing antidrug antibodies [61].

1.9.7. Immunogenicity of the therapeutic rITs

The compounds known as recombinant immunotoxins are immunogenic. Humanising this part of the molecule can prevent host anti-mouse antibodies from attacking the antibody portion of the immunotoxin. The toxin domain, predictably, is even more immunogenic. Due to their tumour, patients with haematologic malignancies typically have compromised immune responses and either produce antidrug antibodies later in

their treatment or not at all [76]. Conversely, nearly all patients with solid tumours quickly produce anti-immunotoxin antibodies following the administration of therapy. There have been several immunosuppressive regimens evaluated on this population. Immunotoxin treatment was found to be ineffective when cyclophosphamide was administered as a single intravenous dosage. Pretreatment with oral cyclosporine A also did not decrease the production of anti-immunotoxin antibodies. Additionally, rituximab's suppression of the antibody response was investigated. Even though none of the patients had detectable peripheral B cells when immunotoxin was given, they all generated antibodies against immunotoxins [77],[78].

A recent study demonstrated that a new lymphocyte-depleting treatment, combining pentostatin and cyclophosphamide, effectively delays the formation of neutralizing anti-antibodies in patients with solid tumors. Originally developed to address host-versus-graft reactions in patients receiving allogeneic bone marrow transplants with major histocompatibility complex mismatches, this regimen depletes T and B cells while sparing myeloid cells. Additionally, it leads to a significant and prolonged suppression of T-cell effector function, which is more pronounced than would be expected based solely on the depletion of cell numbers [79], [80], [81]. The combination was evaluated as a preparatory regimen prior to immunotoxin treatment in preclinical mouse studies and subsequently in patients with malignant mesothelioma. In the clinical pilot study, 8 out of 10 patients were able to receive multiple cycles of immunotoxin treatment before developing neutralizing antibodies against the immunotoxin. This advancement makes it possible to administer immunotoxins repeatedly to solid tumor patients for the first time [82].

1.9.7.1. Structural optimization in PE38 to reduce immunogenicity and enhance its efficacy

Framework humanization, chimerization, and the use of humanized germlines in mice have all been proposed as approaches for managing the immunogenicity of therapeutic monoclonal antibodies. These approaches greatly reduce the prevalence of anti-mouse and anti-chimera antibodies. Immunogenicity to the variable complementarity-determining region domains may continue. Other ways to minimize immunogenicity of RITs include masking immunogenic epitopes through PEGylation, however, combined therapy with immune suppressive drugs might be harmful and limit treatment options [83], [84], [85].

1.9.7.1.1. Deletion of Domain II of PE38

Protease evasion can interfere with protein processing in the endosome and late endosome, leading to a decrease in peptide presentation by MHC II molecules and reduced T-cell activation. Weldon *et al.*, found that domain II of PE38 was highly susceptible to digestion by lysosomal proteases, and that up to 102 out of 113 amino acids in this domain could be deleted without compromising function, as long as the furin cleavage site (amino acids 274-284) was preserved. Deleting most of domain II also eliminated the immunogenic B and T cell epitopes within it. The resulting mutant toxins, referred to as (LR) for lysosome protease resistance or PE24, were tested in three different strains of mice, showing a significant reduction in antibody response [86].

1.9.7.1.2. Identification of B-Cell Epitopes

Regions on the surface of a protein known as B-cell epitopes are where antibodies and B-cell receptors attach. The majority of immune responses can be regulated by these epitopes, which frequently cluster together on the surface of the antigen. The B cell

epitopes in blood samples from humans and monkeys treated with immunotoxins were mapped by Roscoe *et al*., using synthesised peptides from PE38 [83], [87]. The linear epitopes of the toxin were detected using this method, but discontinuous conformational B cell epitopes were not. Using a capture assay, Onda and Nagata isolated monoclonal antibodies that reacted with native PE38 in solution while studying rIT-immunized animals. In PE38, they found seven murine conformational epitopes, and they found single-point alanine alterations that prevented those antibodies from binding. They created the new de-immunized mouse rIT and named it **8M**. Significantly, this rIT exhibited a low immunogenicity response upon injection into mice while maintaining outstanding cytotoxic and anti-tumor effectiveness. By eliminating B cell epitopes, these research provided the first evidence that immunogenicity might be significantly reduced [87], [88].

Human B-cell epitopes in domain III were identified using phage display techniques. The focus on domain III of PE was due to the discovery that most of domain II is not essential for the activity of immunotoxins and can be removed. B cells were isolated from seven patients undergoing immunotoxin therapy, and phage Fv libraries were created from these B cells, specifically those with Fvs that reacted with domain III of PE. This selected library represented the antibody repertoire capable of binding and neutralizing rITs containing domain III. Next, an immunotoxin library was generated, containing 36 mutant PE immunotoxin constructs, each with a single point mutation replacing large amino acids such as arginine, glutamine, and glutamic acid with alanine. The phage library was then panned against each mutant rIT, identifying point mutations that disrupted binding [89], [90], [91]. Seven primary B-cell epitopes were discovered and silenced by changing key residues in these epitopes to **alanine (A)**. The modified toxin, named **LO10** (after the

initials of the two scientists who developed it), has since been used to create immunotoxins targeting both CD22 and mesothelin [89].

1.9.7.1.3. Identification of T-Cell Epitopes

Eliminating B-cell epitopes, as discussed in **subsection 1.9.7.1.2**, assisted in avoiding recognition by pre-existing antibodies. However, the removal of immunodominant B-cell epitopes does not stop B cells with low-affinity receptors from undergoing affinity maturation and class switching, processes that are supported by professional antigen-presenting cells and helper T cells [96]. In contrast to B cells, the specificity of T-cell receptors remains constant when encountering an antigen. Once T-cell epitopes are removed, the formation of new specificities is unlikely [97]. In a proof-of-concept experiment, murine T-cell epitopes in PE38 were mapped using a peptide library and IL2 ELISpot analysis of spleen samples from immunized mice. By performing alanine scanning on each amino acid within 15-mer epitopes, specific point mutations were identified that could block the T-cell response. A new recombinant immunotoxin (rIT) with multiple point mutations in PE38 was developed, which effectively prevented the formation of anti-PE antibodies. Further experiments with BALB/c mice confirmed the identification of a subdominant T-cell epitope in domain III. The study also revealed that a slightly altered version of the de-immunized PE (A505H), when delivered with a different method and adjuvant, demonstrated significantly reduced immunogenicity compared to PE24. To map the human T-cell epitopes in PE38, PBMCs from 50 donors with HLA profiles similar to those of typical Western patients were utilized. These PBMCs were expanded using PE38 to enhance antigen processing and presentation, thereby enriching the T cells that recognized PE38 epitopes [92].

The enriched T cells were re-stimulated with overlapping peptides that span the sequence of PE38. T cell activation was monitored using IL-2 ELISpot [93], [94]. Twenty-three peptides whose sequence overlap had positive responses and made up eight T cell epitopes [79]. One of these epitopes, located in domain II, was present in 21 out of 50 donors [92]. The eight T-cell epitopes found in PBMCs from naïve donors were also present in samples from 16 cancer patients who had been treated with PE38-based RITs and had generated an immune response to the protein. This indicates that PE38 includes these eight T-cell epitopes, while other areas of the protein are less likely to trigger an immune reaction. It was also observed that when similar assays were performed with PBMCs from immunized Hairy Cell Leukemia (HCL) patients, several epitopes were not detected [79]. A promising immunodominant epitope that can be removed without significantly reducing activity or stability was among the T-cell epitopes in PE38 that were identified. Since nearly all of the amino acids in domain II of immunotoxin HA22-LR have been deleted, 34% of donors were not immunogenic, and another 42% were less immunogenic. Point mutations that eliminate domain III epitopes will be combined with the deletion of domain II in this study. For patients with healthy immune systems, it is expected that immunotoxins with mutations that destroy T-cell epitopes can be administered for multiple cycles, improving antitumor responses [95] .

1.9.7.1.4. SS1-LR Recombinant Immunotoxin

SS1P is comprised of an anti-mesothelin antibody Fv linked to a cytotoxic fragment of *Pseudomonas* exotoxin A ETA' (PE) that includes domains II and III of native PE. The clinical effectiveness of SS1P was found to be limited by its tendency to trigger neutralizing antibodies and to cause a dose-limiting capillary leak syndrome (CLS) in patients. To address this issue, the knowledge of the PE intoxication pathway was used

to re-engineer SS1P with improved properties. This “lysosomal degradation resistant” (LR) variant rIT was developed by removing protease-sensitive regions of PE38 and targeting it to the B-cell specific CD22 receptor with the HA22 high-affinity anti-CD22 Fv. The modified immunotoxin showed cytotoxic activity similar to SS1P in various mesothelin-expressing cell lines and demonstrated significantly enhanced activity in primary cells from mesothelioma patients [108], [109]. The modifications involved removing the majority of PE domain II (residues 251-273 and 284-394 of the native PE), retaining only an 11-residue furin cleavage site, inserting a Gly-Gly-Ser peptide linker after the cleavage site, and substituting eight solvent-exposed residues in the catalytic domain of PE. In a mouse xenograft tumor model, high doses of SS1-LR/GGS/8M exhibited better antitumor effects compared to SS1P at its highest tolerated dose. Additionally, SS1-LR/GGS/8M caused significantly less CLS in a rat model and exhibited reduced antigenicity, showing decreased reactivity with antibodies from patients previously treated with SS1P [110], [111], [112].

1.9.7.2. RG7787 Recombinant Immunotoxin

The efficacy of SSIP immunotoxin was limited because 90% of patients developed neutralizing antibodies against the bacterial toxin after just one cycle of treatment, which hindered effective and continuous use of the rIT. To address this challenge, Alewine *et al.,* explored a strategy to reduce neutralizing antibody formation by using protein engineering to design a less immunogenic version of PE38. This involved introducing seven-point mutations into the catalytic domain of PE to eliminate human B-cell epitopes. Removing most of domain II also eliminated additional epitopes and protease cleavage sites that hindered intracellular processing efficiency. The resulting modified

PE, known as PE24, showed similar in vitro activity to PE38 but with reduced reactivity to human anti-sera and lower nonspecific toxicity in rodent models. This allowed for the safe administration of 5- to 10-fold higher doses. The PE24 platform was subsequently used to create a new mesothelin-targeted RIT called RG7787, developed by Ira Pastan's group in collaboration with Roche. RG7787 combines PE24, a variant of ETA' with seven human B-cell epitopes deleted using alanine scanning mutagenesis, and a humanized anti-MSLN antibody Fab fragment. The mutated human B-cell epitopes in RG7787, including R490A & R467A (common to both mouse and human B cell epitopes), as well as R427A, R505A, and D463A (shared B and T cell epitopes), retained full cytotoxic activity. RG7787 demonstrated the same stability and binding properties as previous mesothelin-targeted RITs, but with reduced immunogenicity and a longer half-life compared to smaller dsFv-based PE24 molecules [59], [62], [63], [64], [96].

1.9.7.3. New version RG7787 rIT (dETA')

One of the advantages of RG7787 rIT is its ability to have a longer half-life and is less immunogenic than smaller dsFv-based PE24 molecules, but drawbacks such as reduced enzymatic activity and cytotoxicity in comparison to its wild-type control when evaluated in gastric cancer cell lines raise concerns for future use and application in clinical studies. Therefore, to try and restore the enzymatic activity of this recombinant immunotoxin, our group (Medical Biotechnology & Immunotherapy Research Unit) in collaboration with the group of Prof. Paolo Carloni (Institute for Advanced Simulation, Forschungszentrum Julich, German), identified and is currently studying point mutations identified by dynamic protein interaction modelling that might at least recover the cytotoxic/enzymatic activities of proteins bearing the RG7787 mutations as shown in (**Table 2**). The newly identified point of mutations with the mutations that were already

existing in RG7787 RIT were introduced into a proDer p-1 backbone bearing the wild-type PE38 variant of ETA' by one of the PhD candidates from our lab to evaluate improvement in enzymatic activity [62], [82].

Table 2: Mutations identified by Prof. Paolo Carloni group to improve the cytotoxic activity of proteins bearing RG7787 mutations, red highlighted being the focus of this study. (Table Duplicated from Daramola Adebukola PhD thesis**)**

No	Point mutations identified by MDS to restore enzymatic activity	Point mutations from MDS added to mutations present on RG7787 (Herewith termed dETA')
1	R456T	R427A, R456T, D463A, R467A, R490A, R505A, R538A
2	R456C	R427A, R456C, D463A, R467A, R490A, R505A, R538A
3	R456T, R490A^{deletion}	R427A, R456T, D463A, R467A, R505A, R538A
4	R456C, R490A^{deletion}	R427A, R456C, D463A, R467A, R505A, R538A

Chapter 2: Aims & Objectives

2. Aims & Objectives

This section focuses on explaining the overall aim of the study and the objectives that were followed to accomplish the results of the study.

2.1.1. Study Aim

TNBC is a highly aggressive and rapidly progressing type of breast cancer that mainly affects women of African descent. It is difficult to treat because it does not express hormone receptors or overexpress human epidermal growth factor receptor 2 (HER2). While chemotherapy may initially be effective, recurrence is common, resulting in a low survival rate [97]. RITs are currently researched as an appealing alternative to conventional therapeutics for TNBC and other diseases. Immunotoxins can currently be made using a variety of recombinant antibody forms. Although design improvements have enhanced immunotoxin efficacy *in vitro* and preclinical *in vivo*, increasing potency does not address the two main issues for these drugs: immunogenicity and toxicity [98]. Therefore, this research study aims to generate a next version of *Pseudomonas Exotoxins* A (ETA') based recombinant immunotoxins with reduced immunogenicity and potentially recover excellent enzymatic activity targeting differentially overexpressed antigens in triple-negative breast cancer cells, LIV-1 and TROP2 cell surface antigens.

2.1.2. Main objectives

To achieve our study aim, the following study objectives had to be followed:

1. In-silico design and molecular cloning of trop2(scFv) and LIV-1(scFv) with R456C mutation recombinant plasmids.
2. Expression of recombinant proteins in the periplasmic space of BL21 *E. coli* bacteria, using compatible solutes supported stress expression and purification of full-length fusion proteins using the established protocols.
3. Structural validation of a full-length his-tag fusion proteins using Sodium Dodecyl Sulphate Polyacrylamide Gel Electrophoresis (SDS PAGE) and Western Blot techniques.
4. Confirming the in vitro binding activity to LIV-1/TROP2-positive cell lines.
5. Followed by establishing an enzyme assay as per PhD of Adebukola Daramola and compare relative activities of anti-TROP2 and anti-LIV-1 fused to:
   i) ETA' Wild-Type (WT)
   ii) dETA' (RG7787(R456T))
   iii) dETA' (RG7787(R456C))
   iv) dETA' (RG7787-R490A(R456T))
   v) dETA' (RG7787-R490A(R456C))
   vi) dETA' (RG7787-R490A)
   vii) dETA' (RG7787)
6. Finishing up by confirming a dose-dependent toxicity of the constructs with highest enzymatic activities to determine molar IC50 values.

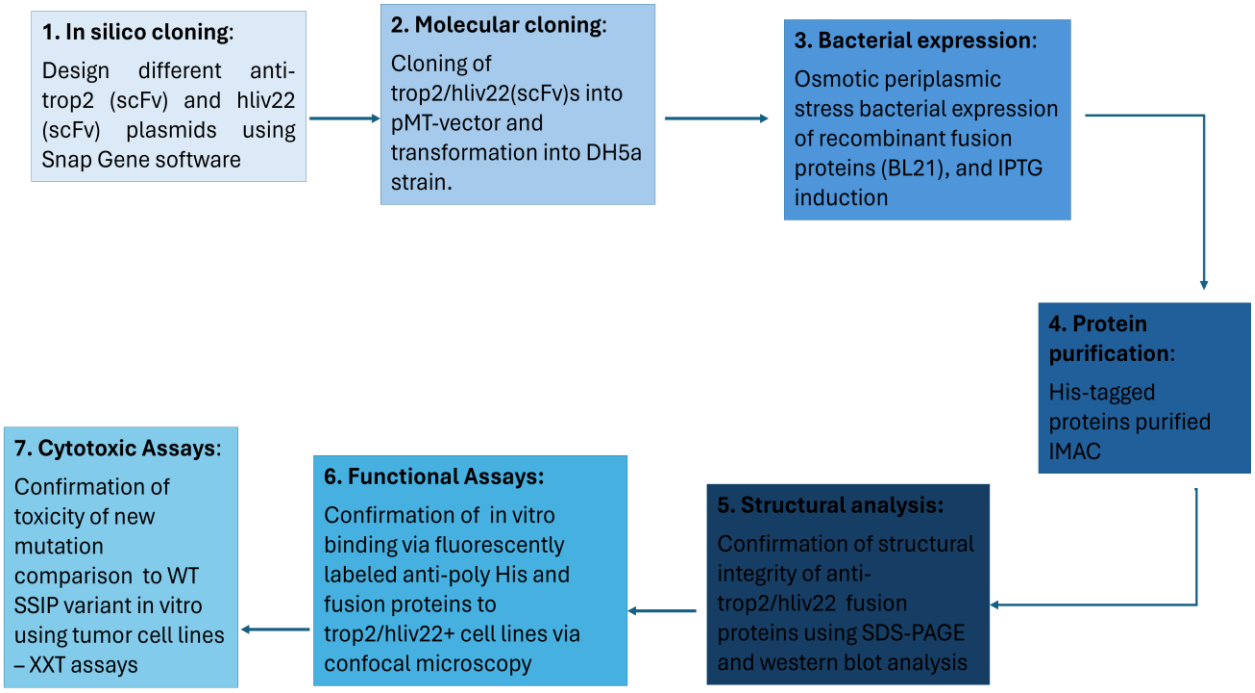

Figure 12: Shows the study workflow. Showing a step-by-step summary of the work done to achieve the stated objectives.

Chapter 3: Materials and Methodology

This chapter explains the materials and equipment's used to develop methodologies, protocols, and standard operating procedures at the Medical Biotechnology and Immunotherapy Research Unit (MB&I). The methodology described is used by members of the MB&I and is therefore representative.

3.1. Materials & Methodology

For all the objectives to be successful, the following experiments had to be conducted. Therefore, in this section, the experimental methods using materials found in **(Appendix section)** are explained.

3.1.1. In silico Plasmid Design

In silico plasmid design refers to scientific work or findings that are carried out using computer simulation instead of biological studies. With readily available information such as antibody sequences, species of origin such as human or mouse, epitope identification within an antigen, and with the application of recombinant DNA (rDNA) technology, mAb against target antigen was created in a short period. Understanding the antibody sequences that identify the target antigen was critical for the creation of scFv. Two students from our lab (Jesmika Sigh and Sizalobuhle Masuku) had already identified the antibody sequences of interest using "Google Patents" and DEPATISnet online public libraries, and they developed pMT recombinant plasmids, which I utilized to source the scFv DNA sequences of interest. SnapGene® software (v.5.0.8, GSL Biotech LLC, USA) was used to create the ORF encoding the RITs for expression in the pMT vector.

To generate the pMT-dETA' vector, the readily available pMT-ETA' which is flanked with *Not*I and *Blp*I restriction sites was used, which allowed us to do the excision of the ETA' portion and compatible insertion of the different dETA' versions, to generate pMT-dETA' recombinant plasmid versions. The resultant constructs are expressed within the periplasm of (*E. coli*, BL21 cells) using an osmotic stress induction protocol, in the presence of compatible solutes. The pMT-dETA' plasmids have been engineered to have a pelB leader sequence that allows the exportation of the produced recombinant proteins periplasm. The bacterial expression vector also comprises the scFv and upstream of the scFv is the N-terminal pelB peptide signal/leader sequence that directs the fusion protein to the bacterial periplasm, where the sequence is removed by signal peptidase, followed by (in order, N → C) the two recommended alanine (AA) residues, a poly(10x)-histidine tag, or His-tag233 and an enterokinase cleavage site (DDDDK), which allows digestive cleavage of the fusion protein for optional removal of the N-terminal elements.

Table 3: Elements of the pMT bacterial expression vector and their functions.

FEATURE	**FUNCTION**
pelB leader sequence	signal sequence for transportation of the recombinant protein to the periplasmic space
N-terminal poly-histidine tag (10X His-tag)	Essential for protein enrichment with the IMAC for protein purification and to detect the protein by western blot analysis.

Enterokinase cleavage (EKS)	Responsible for the separation of the recombinant protein from the 10X His-tag
C-terminus (dETA')	Is a deletion mutant of *Pseudomonas* Exotoxin A' and its deimmunized version responsible for tumor cell killing

3.1.2. Molecular Cloning

The molecular cloning technique is used for isolating a DNA sequence from any species (usually a gene) and inserting it into a vector for propagation without altering the original DNA sequence. Once isolated, molecular clones can be utilized to make multiple copies of the DNA for gene sequence analysis and/or to express the resulting protein for study or application of its function. Clones can also be altered and changed in vitro to change the protein's expression and function.

New England Biolabs (USA) supplied the restriction enzymes (SfiI, NotI, BlpI, MauBI, PstI, and PvuII), CutSmart® buffer, T4 DNA ligase, and T4 ligase buffer. All specified reagents were utilized according to the manufacturer's guide instructions.

3.1.2.1. Transformation of plasmid DNA using competent bacterial cells

Commercially available NEB® 5-alpha *E. coli* calcium-competent cells (Catalogue number: C2987I, New England Biolabs, USA), were thawed on ice. The 50µL of competent cells were incubated with 1µg of plasmid DNA for 30 minutes on ice. The cells were heat-shocked for 60 seconds at 42 °C. The heat shock disrupts the bacterial membrane, resulting in the formation of pores that allow DNA entry. The cells were treated with 950µL of room temperature Super Optimal Broth with Catabolite Repression (SOC). Each tube

was mixed thoroughly and incubated at 37 °C for 60 minutes. All tubes were spun down to pellet the cells, 900µL of the supernatant was discarded and the cells were resuspended in the remaining 100µL and streaked on a kanamycin-supplemented LB agar plate. The streaked plates were incubated overnight at 37 °C. The next day, single colonies were selected from each plate and inoculated in 50mL of LB Broth, supplemented with kanamycin (100ng/µL). The cultures were incubated overnight on a shaking incubator at 37 °C.

3.1.2.2. Growth and maintenance of E. coli

On the following day, a single recombinant colony of *E. coli* obtained from the above procedure was used to inoculate an LB medium containing the kanamycin antibiotic and grown overnight at 37°C with vigorous shaking (225 rpm). Glycerol stocks were prepared by mixing 500 µl of overnight culture with 500 µl of 50 % (v/v) sterile glycerol. Glycerol stocks were immediately stored at -80°C for long-term storage.

Plasmid DNA from 50 ml liquid cultures of recombinant *E. coli* was isolated/purified using the NucleoSpin Plasmid Kit (Macherey-Nagel) according to the manufacturer´s instructions and stored at 4°C in nuclease-free water. The concentration of DNA in plasmid preps was determined by measuring the absorbance at 260 nm and the purity of the nucleic acid was determined by measuring the 260 nm / 280 nm absorbance ratio, which is 1.8 or higher for pure DNA.

3.1.2.3. Restriction Digest of DNA

Restriction digest of plasmid DNA was carried out by incubating 2 µg of plasmid DNA reaction with corresponding restriction enzyme and buffer in a heating block following recommended temperature and time points by the manufacturer. To analyse the size and

concentration of isolated plasmid DNA an analytical agarose gel electrophoresis was performed. Briefly, 1.2 % (w/v) agarose gels were prepared in TAE buffer containing a 10:1 ratio of SYBRTM Safe DNA gel stain. After casting the gel, DNA-containing samples were gently loaded into the pre-cast wells and a 2-log DNA ladder (New England Biolabs) was used as a standard to evaluate DNA size and fragment integrity. DNA bands were visualized on a UV transilluminator at a wavelength of 509 nm and an agarose block containing the DNA fragments of interest was excised with a sterile blade. DNA extraction and purification were performed using a QIAquick gel extraction kit (Qiagen) according to the manufacturer´s guidelines and stored at 4°C.

3.1.2.4. Ligation of DNA

The ligation of DNA fragments was performed using the T4 DNA ligase kit according to the manufacturer's instructions. Briefly, the NEBioCalculator was used to calculate different vectors to insert molar ratios (1:1, 1:2, and 1:3) for the respective DNA sizes. A 20 µl ligation reaction was then set up in the presence of 200-400 U of T4 DNA Ligase (New England 68 BioLabs) and a ligase buffer system. The ligation reaction was incubated at 16°C overnight followed by heat inactivation at 65°C for 10 minutes and transformed into competent NEB® 5-alpha *E. coli* calcium-competent cells as explained above.

Table 4: Ligation components used in this study per 20µl reaction

COMPONENTS	**20 ul REACTION**
T4 DNA Ligase Reaction Buffer (10x)	2µl
T4 Ligase Enzyme	1µl
Vector	50 ng

Insert	Differs for each ratio
Deionized Water	Topped up to 20µl

3.1.2.5. Mini preparation of recombinant plasmid DNA

Clones for downstream applications were prepared using Miniprep (as per Zippy Miniprep SOP). Briefly, several colonies were picked from each ligated plates and was grown in 2 ml LB supplemented with kanamycin and was grown overnight at 37^0 C on a shaking incubator. On the following day, 600 µl of bacterial cultures grown were added to 1.5 ml microcentrifuge tubes and was centrifuged for 30 seconds at maximum speed. The supernatant was then discarded, the process was repeated until all required pellets were obtained. After that, 600 µl of water was added for pellet resuspension. Then, 350 µl of cold neutralization buffer was added and mixed thoroughly. It was then centrifuged at 11, 000 xg for 2-4 minutes. The supernatant was then carefully transferred into Zymo-Spin IIN column. The column was placed on the collection tube and centrifuged for 15 seconds. The flowthroughs were discarded and 200 µl of Endo-Wash Buffer was added to the column and centrifuged for 30 seconds. Zippy Wash Buffer (400 µl) was then added to the to the column and centrifuged for 1 minute. Columns containing different clones were then placed into new 1.5 microcentrifuge tubes and 30 µl of nuclease free water was added and centrifuged for 30 seconds to elute the plasmids DNA.

3.1.2.6. Restriction Mapping of Recombinant DNA

Restriction mapping was used to identify the clones harbouring plasmids to be prepared for sequencing. Briefly, the agarose gel simulation was done using SnapGene software to find the unique cutters that can show a properly difference between the pMT-ETA that

was used as backbone and the newly ligated inserts. The unique cutters that were used for this experiment are shown in the table below.

Table 5: Shows different cutters and the quantity that was used for restriction mapping.

COMPONENT	**QUANTITY**
Plasmid DNA	1µg
Cut Smart Buffer®	5µl
MauBI	1µl
PstI	1µl
Nuclease free water	Topped up to 20µl

After confirming the clones, the DNA sequencing was used to confirm and characterise the presence of both the scFv and the plasmid composition. Primers were designed and procured from Inqaba Biotechnical Industries (Pretoria, South Africa), and sequencing was conducted at the Central Analytical Facilities (Stellenbosch University, South Africa). To align the sequencing results to the in silico ORF reference files SnapGene® software was used. Following successful cloning validation from sequencing and restriction mapping, bacterial expression was conducted.

3.2. Expression of recombinant proteins

3.2.1. Compatible-solute-supported Periplasmic expression in E. Coli under osmotic stress condition

A major disadvantage accustomed to traditional methods of expressing recombinant proteins such as immunotoxins (RITs) in *E. coli* is the low yield of active proteins recovered from inclusion bodies. To enhance folding, solubility and yield, the recombinant immunotoxins were expressed in BL21(DE) cells (NEB) using the periplasmic stress expression protocol described by Barth *et al.,* [99].

Briefly, a freshly transformed single bacterial colony was used to inoculate 50 ml of TB media and cultivated overnight at 26 °C (225 rpm). 5 ml of this overnight culture was transferred into fresh 250 ml TB medium until an OD600 of 1.6 was reached (5 hours, 26 °C, and 180 rpm). Stress was induced by the addition of 0.5 M Sorbitol, 4 % NaCl, 10 mM Glycine-Betain, and 100 ml TB/ZnCl2 media. After incubation for 30 minutes at 26°C, expression of recombinant protein was induced by the addition of 2 mM IPTG. Induction was continued for 16 h at 26 °C while shaking (225 rpm). Afterward, the IPTG-induced cells were harvested by centrifugation (4000 × g, 10 min, 4°C) and stored at -80°C. For purification, the frozen pellet was resuspended in ice-cold preparation buffer (pH 8.0) containing; 75 mM Tris/HCl, 300 mM NaCl, 5 mM DTT, 10 mM EDTA, 10% (v/v) glycerol, and complete protease inhibitor (1 Tab / 50 ml, Sigma Aldrich). To release the periplasmic content, the 69 samples were sonicated six times (60 s at 200 W), and cell debris was removed by centrifugation (24,000 × g, 20 min, 4°C). DTT, EDTA, and diverse metabolic chemicals were removed by dialysis against phosphate-buffered saline (PBS) plus 0.4 M

NaCl (pH 7.4) at 4°C overnight. To prevent unspecific binding during protein purification by IMAC, the bacterial lysate was supplemented with 5 mM imidazole.

3.3. Immobilized metal ion affinity chromatography (IMAC)

IMAC is a widely used technique to purify or rapidly enrich Poly histidine tagged proteins. To purify bacteria-expressed fusion proteins, an Äkta Avant purifier system (GE Healthcare) loaded with pre-packed His Trap Excel (GE Healthcare) was used.

3.3.1. Purification of bacterial lysate

3.3.1.1. 1st IMAC Purification

All the bacterial lysates (soluble fractions) were cleared by passing them through a 0.45 µm filter (Millipore) before loading them onto a ready-to-use His-Trap column at a flow rate of 5 ml/minute. Afterwards, the column was washed with a wash buffer containing 20 mM imidazole until the baseline was reached. Finally, bound proteins were eluted using an elution buffer containing 500 mM imidazole at a flow rate of 5 ml/minute. The eluted protein fractions were subsequently screened by Sodium dodecyl sulphate polyacrylamide gel electrophoresis before concentrating fractions (using the Amicon® ultrafiltration device 10K) with the protein of interest.

3.3.1.2. 2nd IMAC Purification

The concentrated protein fractions were then further purified using the 2nd IMAC protocol. Briefly, the concentrated proteins were applied to 1 ml His-Trap HP column using a loading buffer containing 10 mM imidazole. The proteins were then washed to remove all the contaminants that might have bound to our protein of interest using the buffer containing 30 mM imidazole. It was then eluted using the elution buffer containing 250 mM imidazole. It was then concentrated using a 30 kD size Amicon tube.

3.4. Protein analysis

3.4.1. Sodium dodecyl sulphate polyacrylamide gel electrophoresis (SDS-PAGE)

To analyse protein samples, a 10 % SDS-PAGE was used to separate proteins based on their specific molecular weight. Briefly, protein samples were denatured by mixing with 4x Laemmli buffer (3:1) and heating for 5 minutes at 95°C. Thereafter, 25 µl of denatured protein samples and 3 µl of prestained protein molecular weight marker (Thermofisher) were loaded onto a polyacrylamide gel. The proteins were separated by running the gel at 100 Volts for 90 minutes in a Mini-PROTEANII chamber (Bio-Rad) in 1x running buffer. Thereafter, protein bands were visualized and analysed by staining the gel with Aqua-stain for 15- 30 minutes.

3.4.2. Western blotting

Western blot (also called protein immunoblot) is a widely used technique that allows the specific detection of protein separated by gel electrophoresis. Briefly, proteins separated by SDS-PAGE were transferred from the polyacrylamide gel onto a Whatman® nitrocellulose membrane (Sigma) using an Xcell II Blot Module (Bio-Rad) for electro-tank blotting at 100 Volts for 90 minutes in transfer buffer. This allows the movement of negatively charged proteins from the gel toward the positively charged anode of the blotting chamber. Afterward, unspecific binding of the detection antibody to the nitrocellulose membrane was prevented by blocking it with 5% non-fat dry milk for 1 hour at RT. The membrane was washed three times with 1x PBST and incubated with an anti-His-tag primary antibody at 4 °C overnight on a rocker. Thereafter, unbound antibodies were removed by washing the membrane in TBS-Tween (4 times) and incubating it with horseradish peroxidase-conjugated anti-rabbit-IgG secondary 72 antibodies (1:5,000;

Sigma) for 1 hr at RT. A second set of washes was performed in TBS-Tween (4 times) before staining with the chemiluminescent substrate. For detection, the nitrocellulose membrane was covered evenly with the enhanced chemiluminescence (ECL) mixture for 1 minute and the luminesce signal was captured by a Gel Doc.

3.5. Analysis of RITs binding to cell lines

The uptake of receptor-bound scFv fusion proteins and RITs was performed and monitored using confocal microscopy on adherent cells only (such as TNBC cells).

The primary cell line of interest used is MCF-7 (positive cell lines, due to the overexpression of LIV-1 and TROP2), and SiHa and HERK293 (as negative cell lines, and have not been recorded to overexpress LIV-1 and TROP2). On 6-chambered cell plates, the cells will be seeded in a complete medium dependent on cell line type and left to grow overnight at 5% CO2, 37°C. The cells will then be washed for 1 hour using PBS and stained with Alexa 488/647 and Phycoerythrin (PE)-conjugated anti-His tag antibody, containing the labelled recombinant immunotoxin. The cells will be washed again with PBS (pH 7.4) and counterstained using nuclear stain DAPI. Following staining, the cells will then be fixed with 2%paraformaldehyde, and images of the result will be captured using a confocal microscope with the help of Professor Dirk Lang in the core facility.

3.6. Cell viability assay

Measurement of cell viability was done by using the XTT cell proliferation Kit II (Sigma Aldrich). This assay is based on the ability of mitochondria enzymes in metabolic active cells to reduce the tetrazolium salt XTT (sodium 2,3, -bis(2-methoxy-4-nitro-5-sulfophenyl)-5- [(phenylamino)-carbonyl]-2H-tetrazolium) to a water-soluble orange

formazan dye. Briefly, 5x 10^3 cells were seeded per well into a 96-well plate and incubated at standard cell culture conditions (37°C and 5% CO_2). After 24 hours, serial concentrations of recombinant fusion proteins were added, and the cells were incubated for an additional 72 hours. The readout was conducted after incubation of the cells for 4 hours with freshly prepared XTT labelling reagent and electron coupling reagent mixture (50:1) at 37°C and 5% CO_2. The absorbance of the reduced XTT was measured at 450 nm with a reference of 655 nm using a spectrophotometer (Bio-Rad). The concentration of recombinant fusion protein required to kill 50 % of cells (IC_{50}) was calculated by normalizing data to untreated control and zeocin control using the GraphPad Prism v8.0 software. All experiments were carried out in triplicate.

Chapter 4: Results

In this study four novel RITs were generated (anti-hliv22(scFv)-ETA', anti-trop2(scFv)-ETA', anti-hliv22(scFv)- (R456C+R90A)-dETA' and anti-trop2(scFv)- (R456C+R490A)-dETA') to evaluate their potential in selectively targeting antigen positive TNBC cells and delivering therapeutic probes. The RITs were successfully expressed in the periplasmic space of BL21 (DE3) *E. coli* cells using the osmotic stress protocol. The expressed rITs were purified using IMAC, characterized using SDS and western blot techniques. The binding of the rITs was assessed using confocal microscopy, followed by XTT assays for cytotoxicity studies. Therefore, this section of the study reports on the findings of the study, describing the design and development of these RITs, their functional characterization, and *in vitro* assessments.

4.1. In Silico Plasmid Design

The in-silico plasmid design was conducted as explained in **subsection 3.1.1**. The pMT hliv22 (scFv)-ETA' and trop2 (scFv)-ETA' plasmid vector sequences were already optimized by removing rare and repetitive codons to reduce immunogenicity, stabilize and reduce nuclease degradation in our lab, as well as the sequences of including the desired different point of mutations were already available in the lab. The SnapGene® software was used for the in-silico design of the pMT-hLIV22(scFv)-dETA' and trop2 (scFv)-dETA' having the desired point of mutations (**R456C+R490A**) vector map. Briefly, the optimized sequences of different point mutations were inserted using Not1 and BIP1 restriction sites into the pMT hliv22(scFv) and pMT trop2 (scFv) ETA' backbones that are shown in **figure 14**. The ETA' vectors were created to incorporate all essential features necessary for the later experiments. This design helped the efficient expressions of

functional RITs. The rIT was specifically crafted to be able to show and bind to the LIV- 1 and trop2 target antigens, thereby effectively delivering the dETA' toxin payload.

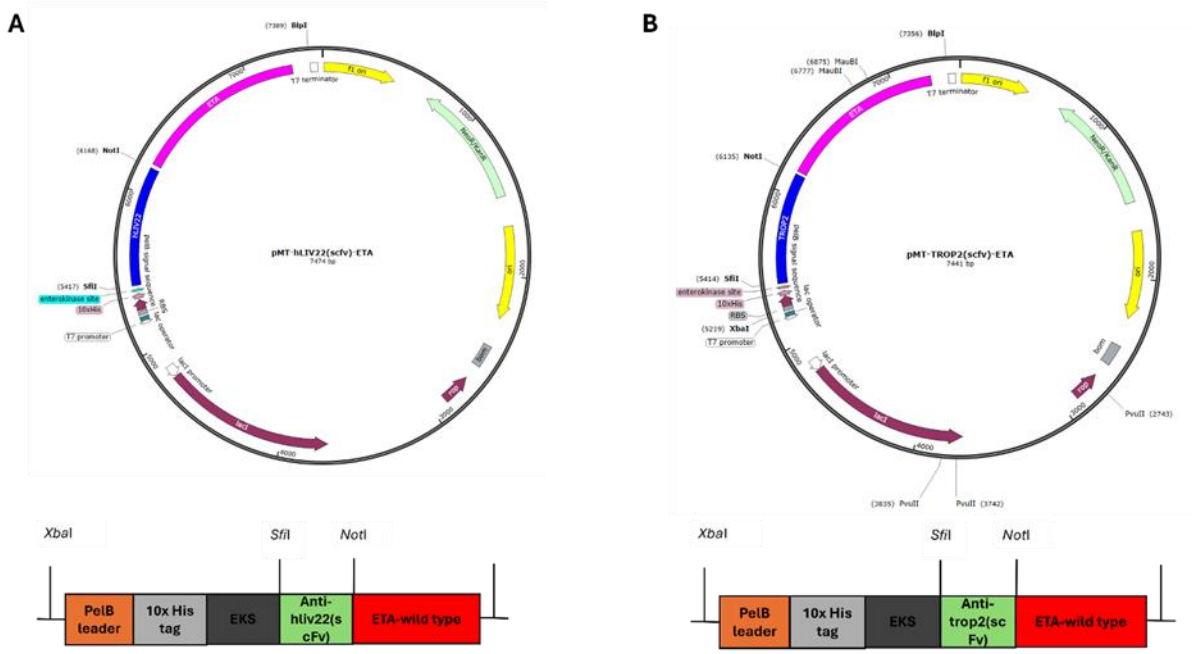

Figure 13: ***Shows (A)pMT anti-hliv22(scFv) and (B) pMT anti-trop2 (scFv) ETA' backbone vector and their open reading frames that were used to insert new mutation by replacing ETA'.***

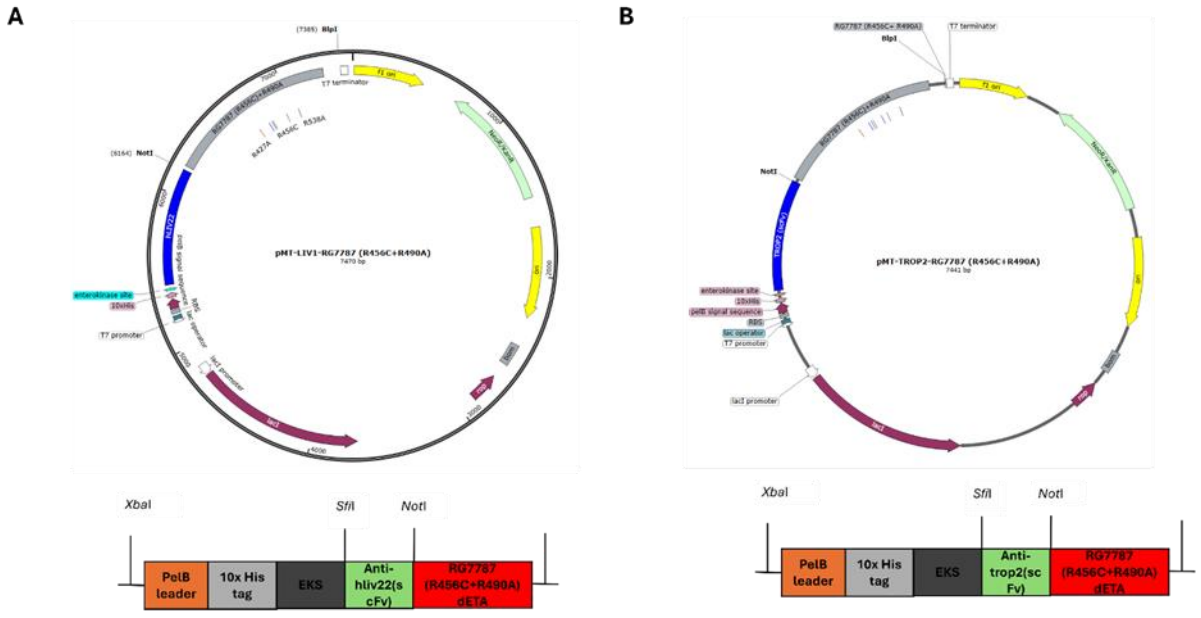

Figure 14: ***The restriction sites (BlPI and NotI) that made it easier to introduce the (A) hLIV22(scFv) sequence into the pMT hliv22-ETA' and (B) trop2-ETA' plasmids are highlighted by the ORF.*** *From cloning to functionality testing, the most important components of the pMT hliv22-ETA' and pMT trop2-ETA' backbone were ETA/dETA' (deliverance of cytotoxic payload into cells); EKS, enterokinase cleavage site (downstream removal of N-terminal elements i.e. His-Tag); pelB, pectate lyase of Erwinia carotovora (transportation of rIT into periplasmic space); 10x His-Tag, poly (10X) histidine tag (for rIT purification, characterisation, and functionality testing); KanR, kanamycin resistance gene*

(selective screening The SnapGene® software was used to acquire the images. created using the Microsoft PowerPoint program.

4.2. Molecular cloning

Once the designed ORFs were synthesized, the sequences of the desired protein were sent for DNA synthesis at (**Genescript Company, Netherlands**). The DNA came in a pUC vector franked with Not1 and BLP1 enzymes for easily cutting off the main inserts (dETA', R456C+R490A) as shown in a supplementary (**Figure 34**). The DNA was subjected to 20 ul of water and was transformed into NEB® 5-alpha *E. coli* calcium-competent cells as described **in subsection 3.1.2.1** and plated on LB agar containing ampicillin. The grown colonies DNA was extracted using a Neocleobond Plasmid extraction kit then digested from the pUC vector using Noti and BLPI restriction enzymes.

4.3. Ligation and Transformation

As explained in **subsection 3.1.2.4**, the required digested fragments were removed from the gel and the DNA was extracted using a gel extraction kit. The extracted DNA fragments were ligated using T4 ligase enzyme overnight at 16^0 C to our available pMT vector containing trop2 and hliv22 (scFv) respectively as shown in **figure 13**. On the following day, the ligated DNA was transformed into NEB® 5-alpha *E. coli* calcium-competent cells, plated on agar plates, and incubated overnight at 37^0 C. To increase the chance of the insert being taken up by the vector, each construct ligated has three controls shown by **figure15&16**, 0:1, 1:1 & 3:1. On the 1:0 plate for hliv22 (R456C+R490A) dETA', there were less than 15 colonies, whereas the 1:1 and 1:3 agar plates both had >100 colonies and on the 1:0 plate for trop2 (R456C+R490A) dETA', there was only 1 colony observed in an agar plate, 15 colonies on 1:1 agar plate and >100 colonies on 1:3 agar plate. The 1:3 ratio plates had four colonies selected and cultured in 3mL of LB broth supplemented

with kanamycin (50mg/mL). The plasmids were isolated using a zippy plasmid miniprep explained in **subsection 3.1.2.5**.

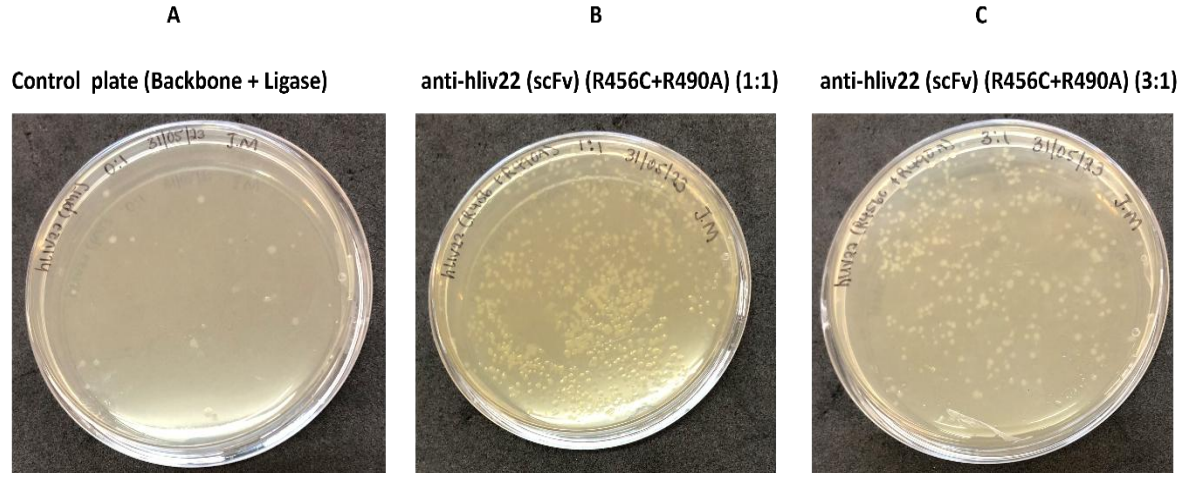

Figure 15: The agar plates for anti-hliv22 (scFv) (R456C+R490A) dETA'. Fewer colonies were grown on the negative control plate A, more colonies were grown on 1:1 plate B as expected, and many colonies were observed in 3:1 plate C as expected. Two colonies were picked in each plate and were placed and grown in LB media at 37^{0} C in the shaking incubator overnight.

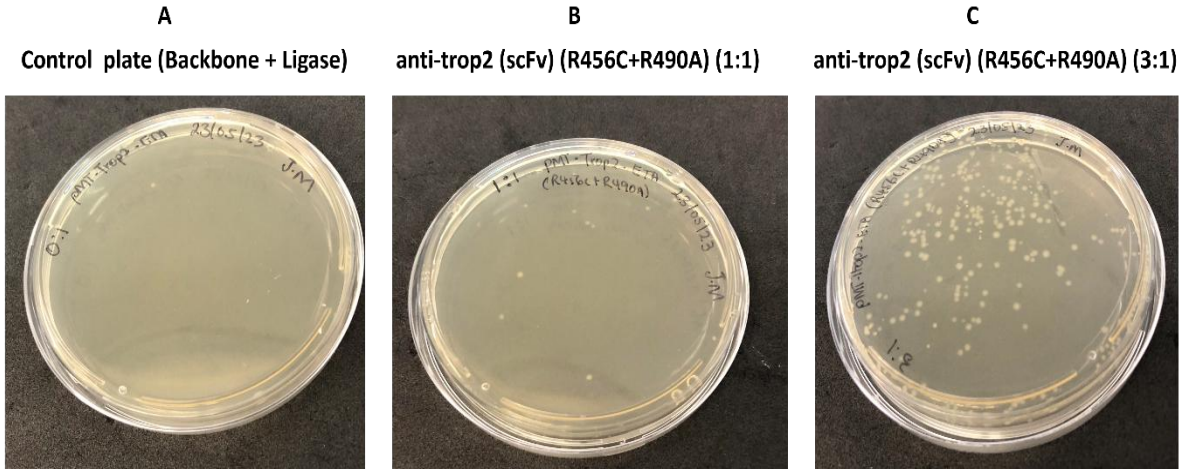

Figure 16: The agar plates for anti-trop2 (scFv)-(R456C+R490A) dETA'. Very few colonies were grown on the negative control plate A, few colonies were grown on 1:1 plate B as expected, and many colonies were observed in 3:1 plate C as expected. Two colonies were picked in each plate and were placed and grown in LB media at 37^{0} C in the shaking incubator overnight.

4.4. Restriction Mapping

Although restriction enzymes are site-specific, ligases are sometimes not, therefore there is a chance of self-ligation (auto-ligation) even though the vector is double-digested. To confirm if that did not happen, a restriction mapping is used to check whether the insert has been taken up by the vector. Agarose gel simulation is done computational using SnapGene software. Different unique cutters are used to check the difference between the new ligated plasmid and the plasmid used to extract the vector. For all the plasmids PstI and MauBI restriction enzymes showed a distinct difference between the pMT used to extract the vector and the new desired plasmids.

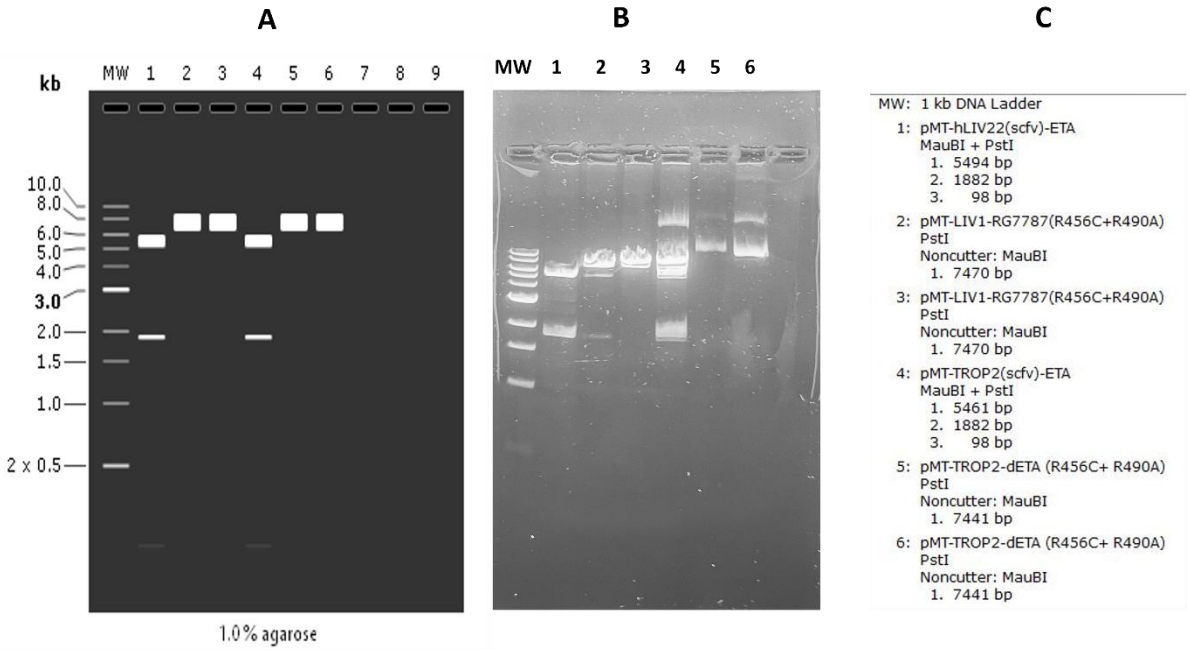

Figure 17: ***Restriction mapping of selected colonies potentially containing pMT-hLIV22(scFv)(R456C+R490A) & pMT-trop2(scFv)(R456C+R490A). (A)*** *In silico designed simulation devised to map the expected band sizes resulting from digestion with PstI and MauBI. Images were obtained from the SnapGene® software.* ***(B)*** *1.2% agarose gel of the digested pMT- hLIV22(scFv)-ETA', 2 colonies of pMT-hliv22(scFv)-dETA', pMT-trop2(scFv)-ETA' and 2 colonies of pMT-trop2(scFv)-dETA' plasmids extracted from the selected bacterial colonies. Following digestion for one hour at 37˚C with PstI and MauBI, the gel was run for 60 minutes at 120V.* ***(C)*** *Bands expected sizes when using MauBI and PstI restriction cutters.*

Isolated DNA clones showing proper endonuclease restriction profiles were sent to Inqaba Biotech company (**Pretoria, South Africa**) for Sanger sequencing, to confirm successful molecular cloning. The positive ligation products were transformed into BL21 *E. coli* cells for protein expression.

4.5. Expression of rITs fusion proteins

Successfully ligated plasmids confirmed by Sanger sequencing were transformed as explained in **subsection 3.2.1** and were expressed in *E. coli* BL21(DE) cells using the periplasmic stress expression protocol readily available in Barth Lab. From a total of 2L cultures that were expressed, hliv22(scFv)-ETA' produced a total pellet of 70g, while its dETA' version produced 68g of a pellet. For trop2(scFv)-ETA' produced 59.6g of a pellet while its dETA' version produced 54g of a pellet.

4.6. Purification of rITs

The recombinant immunotoxins were purified as described in **subsection 3.3.1** using the Reinhard Rosinke purification protocol. Briefly, the protein purification was prepared by resuspension of the frozen pellets in ice-cold preparation buffer (lysis buffer) (pH 8.0) and complete protease inhibitor (1 Tablet / 50 ml). To release the periplasmic content, the samples were sonicated for 2 min 30s, and cell debris was removed by centrifugation (24,000 × g, 20 minutes, 4°C) after a clear supernatant was carefully removed from the pellet and was filtered to avoid any clogging in the AKTA-AVANT machine while loading.

4.7. 1st IMAC Purification

The purification method used for 1st IMAC purification was similar for all four RITs fusion proteins. A 5 ml His Trap HP purification column was used as explained in the method

(**subsection 3.3.1**). The AKTA-AVANT system, purification column was equilibrated before loading the clear lysates. Thereafter, the samples were loaded at a 5ml/min flow rate using a loading buffer and were eluted with a 5ml/min flow rate using an elution buffer.

4.7.1. Elution Profiles for All RITs Constructs

Figure (18-21) shows the chromatograms of immobilized metal affinity chromatography (1ST IMAC) following hLIV22(scFv)-ETA' and dETA' as well as trop2(scFv) ETA' and dETA' rIT purification. X-axis shows the absorbance profile (UV 280nm) of eluate from IMACI purification of bacterially expressed in these rITs while Y-axis shows the Akta flow-through which includes, equilibration of the column step, sample application to the column step, followed by washing of the column to remove all the contaminants and lastly the elution step.

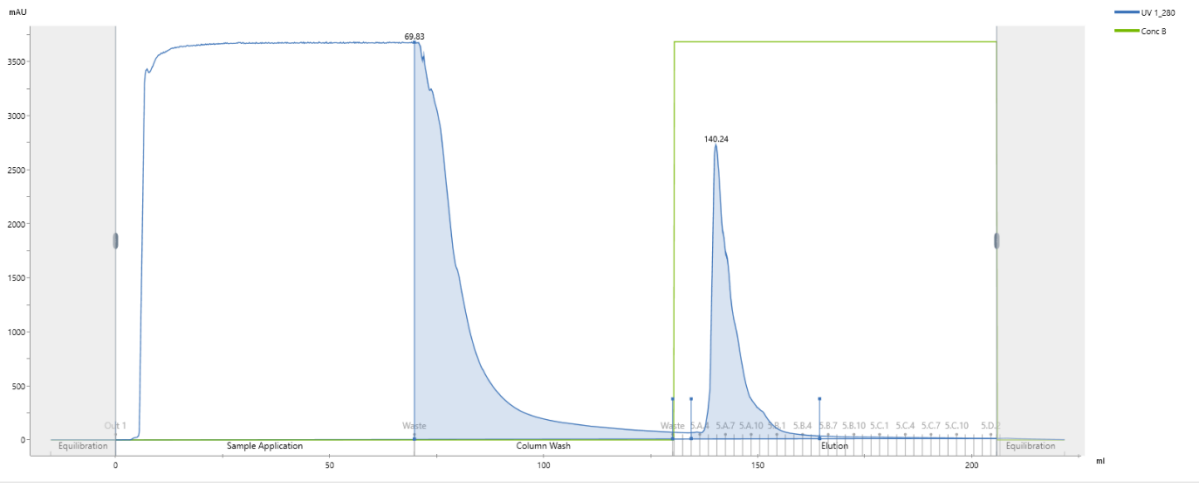

Figure 18: ***Affinity chromatography chromatogram showing purification of target protein for pMT-hliv22 (scFV) ETA' wild type.*** *The graph represents the UV absorbance at 280 nm (blue trace) and the buffer concentration gradient (green line) over the course of the protein purification process. After equilibration, the sample was applied, with unbound proteins eluting around* ***60 mL*** *during the wash phase. The target protein eluted sharply at approximately* ***140 mL*** *during*

the elution phase, as indicated by the major peak. The column was then re-equilibrated to prepare for the next run. The gradient corresponds to the introduction of an elution buffer to dissociate the bound protein from the affinity resin.

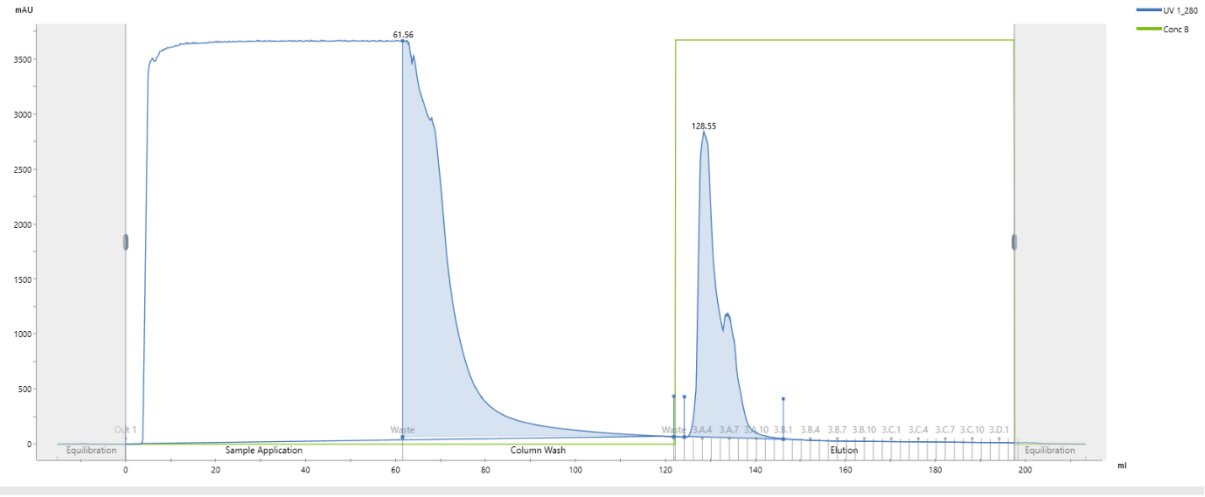

Figure 19: ***Representative chromatogram of protein purification using affinity chromatography pMT-hliv22 (scFv) (R456C+R490A).*** *The UV absorbance at 280 nm (blue line) indicates protein presence throughout the purification process. The chromatogram shows distinct phases: column equilibration, sample application, column wash, and elution. The primary protein peak was eluted at approximately* ***128 mL****, indicating the target protein fraction. The initial large peak during the sample application (~61 mL) corresponds to non-specifically bound or unretained proteins, which were discarded as waste. The elution phase was triggered with a concentration gradient (green line), allowing specific elution of the bound protein. This elution peak represents the purified protein, collected for further analysis.*

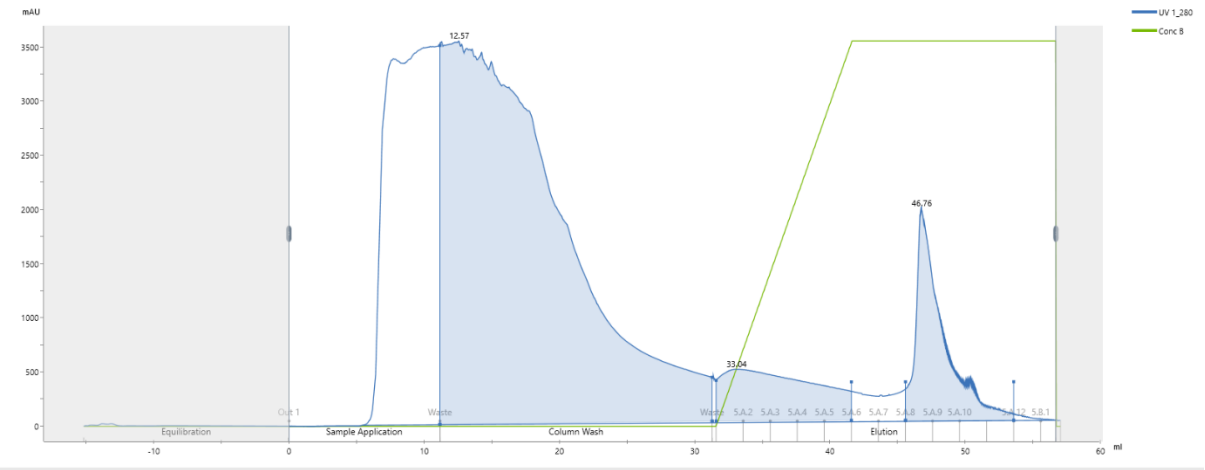

Figure 20: ***Affinity chromatography profile depicting purification of target protein under gradient elution conditions for pMT-trop2(scFv) ETA'.*** *The UV absorbance at 280 nm (blue line) reflects protein elution across the purification stages. After equilibration, the sample was applied, resulting in a broad peak with a maximum at* ***12 mL****,*

indicating non-specifically bound or unretained proteins washed off during the column wash. A gradual concentration gradient (green line) was applied, leading to a sharp elution peak at ***46 mL****, corresponding to the target protein fraction. Subsequent smaller peaks may represent protein isoforms or minor contaminants. The column was re-equilibrated following the elution step to restore initial conditions.*

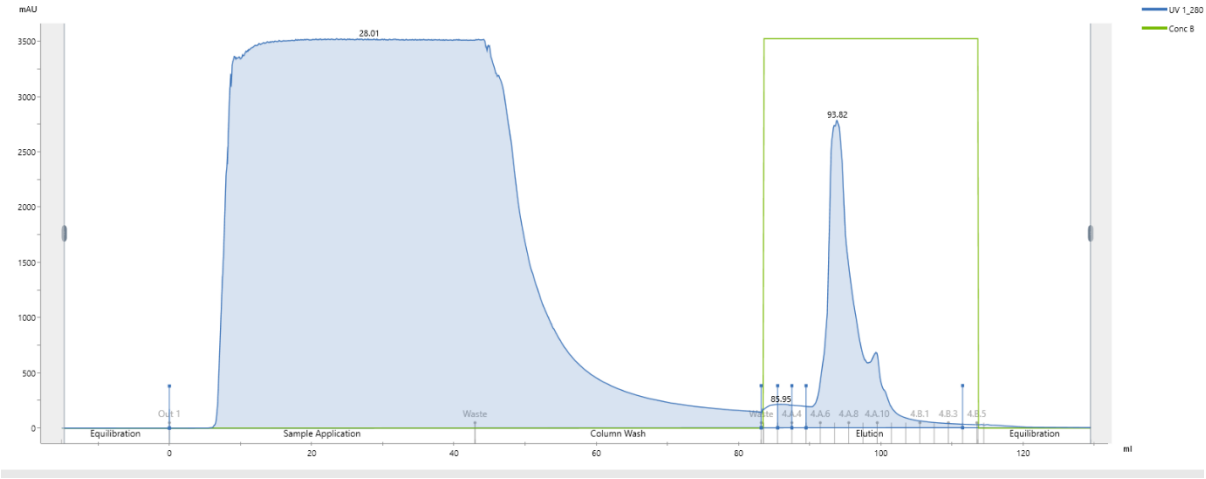

Figure 21: ***Affinity chromatography profile depicting purification of target protein under gradient elution conditions for pMT-trop2 (scFv)(456C+R490A).*** *The UV absorbance at 280 nm (blue line) reflects protein elution across the purification stages. After equilibration, the sample was applied, resulting in a broad peak with a maximum at* ***9 mL****, indicating non-specifically bound or unretained proteins washed off during the column wash. A gradual concentration gradient (green line) was applied, leading to a sharp elution peak at* ***95 mL****, corresponding to the target protein fraction. Subsequent smaller peaks may represent protein isoforms or minor contaminants. The column was re-equilibrated following the elution step to restore initial conditions.*

4.8. 2nd IMAC Purification

After the 1st IMAC purification, all the eluted fractions on the elution peak were pooled and screened on SDS-PAGE, the most concentrated fractions were concentrated for further purification. In this study, the purification method setting used for the 2nd IMAC purification was similar for all the RITs fusion proteins. One ml His Trap HP purification column was used as explained in the method (**section 3.3.2)**. The AKTA-AVANT system, purification column was equilibrated before loading the clear lysates. Thereafter, the

sample was loaded at a 1ml/min flow rate using a loading buffer and was eluted with a 1ml/min flow rate using an elution buffer.

4.8.1. 2nd IMAC Elution Profiles for rITs Fusion Proteins

Figure (22-25) shows the chromatograms of immobilized metal affinity chromatography (2nd IMAC) following hLIV22(scFv)-ETA' and dETA' as well as trop2(scFv) ETA' and dETA' rIT purification. X-axis shows the absorbance profile (UV 280nm) of eluate from IMACI purification of bacterially expressed in these rITs while Y-axis shows the Akta flow-through which includes the column equilibration step, sample application to the column step, followed by washing of the column to remove all the contaminants and lastly the elution step.

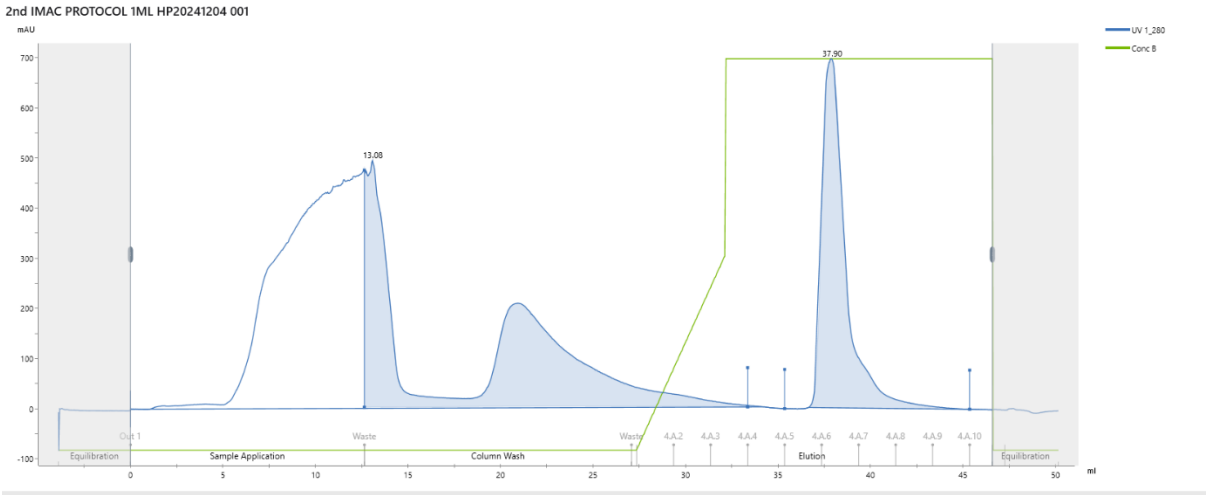

Figure 22: ***IMAC II Purification Chromatogram (Protocol IML HP) for pMT-hliv222 (scFv) ETA'-wild type.*** *The chromatogram shows protein elution profile monitored by UV absorbance at 280 nm (blue line) during immobilized metal affinity chromatography (IMAC). Two major protein peaks are observed: the first at approximately 12.5 mL during sample application/wash phase, likely representing unbound proteins, and a second, sharper peak around 37 mL during the elution phase, representing the target protein of interest. The green line indicates the concentration gradient of buffer used for elution. The x-axis represents the elution volume in milliliters, while the y-axis shows the absorbance in mAU. The chromatogram includes various phases of the purification process including equilibration, sample application, column wash, and final elution of the bound protein.*

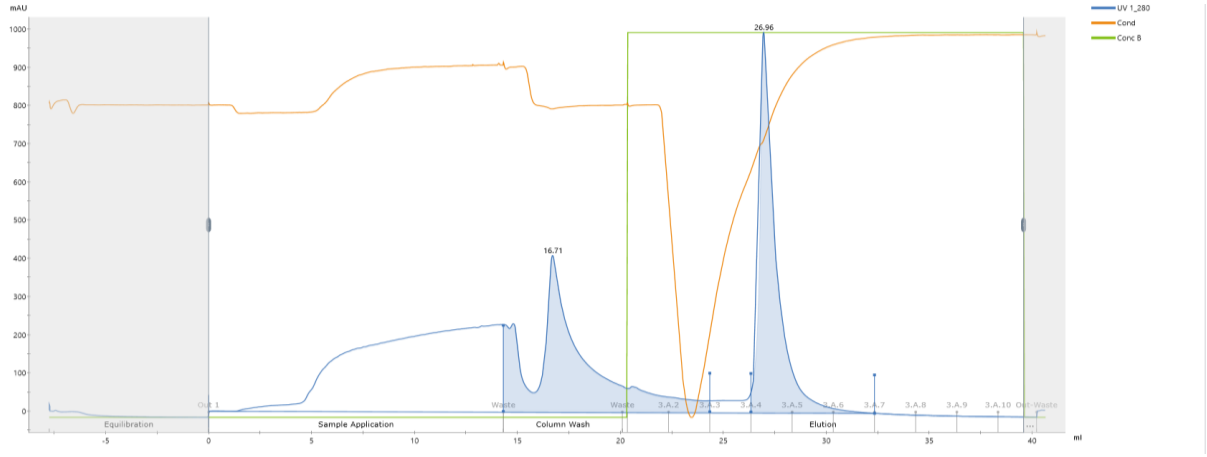

Figure 23: ***IMAC II Purification Chromatogram (Protocol IML HP) for pMT-hliv222 (scFv)(456C+R490A).*** *The chromatogram shows protein elution profile monitored by UV absorbance at 280 nm (blue line) during immobilized metal affinity chromatography (IMAC). Two major protein peaks are observed: the first at approximately 15 mL during column wash phase, likely representing unbound proteins, and a second, sharper peak around 28 mL during the elution phase, representing the target protein of interest. The green line indicates the concentration gradient of buffer used for elution. The x-axis represents the elution volume in millilitres, while the y-axis shows the absorbance in mAU. The chromatogram includes various phases of the purification process including equilibration, sample application, column wash, and final elution of the bound protein.*

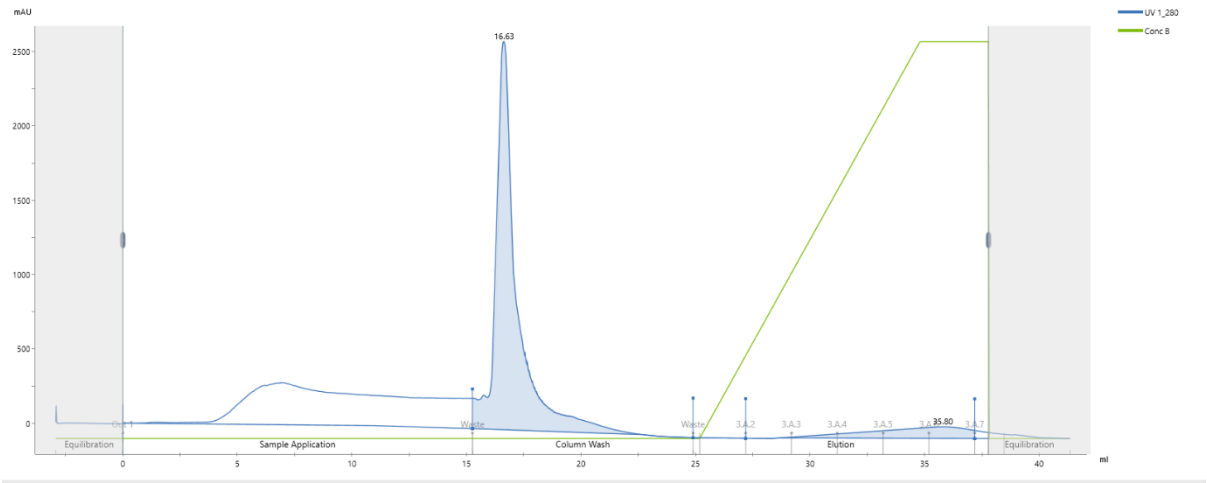

Figure 24: ***IMAC II Purification Chromatogram (Protocol IML HP) for pMT-trop2 (scFv) ETA'-wild type.*** *The chromatogram shows protein elution profile monitored by UV absorbance at 280 nm (blue line) during immobilized metal affinity chromatography (IMAC). Two major protein peaks are observed: the first at approximately 15 mL during column wash phase, likely representing unbound proteins, and a second peak around 33 mL during the elution phase, representing the target protein of interest. The green line indicates the concentration gradient of buffer used for elution. The x-axis represents the elution volume in millilitres, while the y-axis shows the absorbance in mAU. The*

chromatogram includes various phases of the purification process including equilibration, sample application, column wash, and final elution of the bound protein.

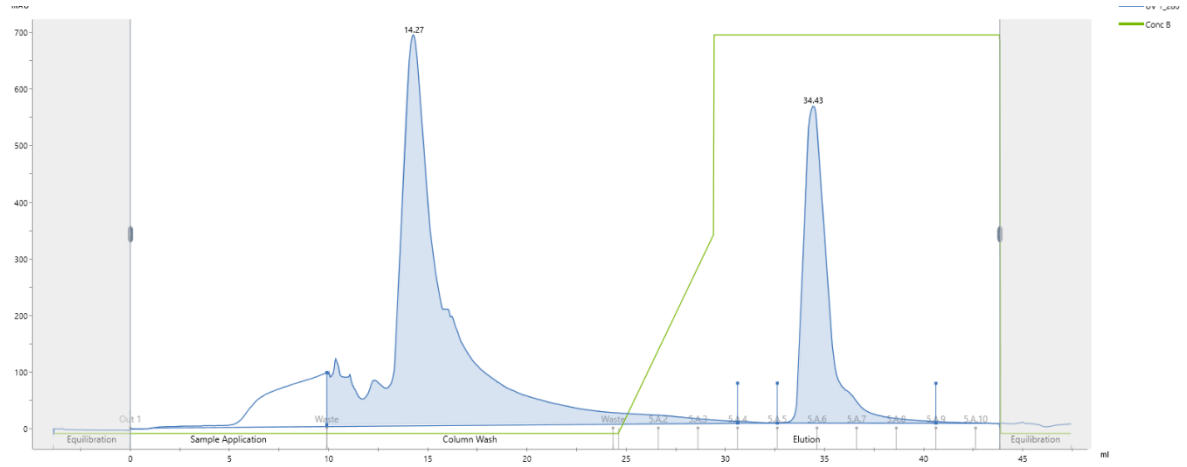

Figure 25: ***IMAC II Purification Chromatogram (Protocol IML HP) for pMT-trop2 (scFv)(456C+R490A).*** *The chromatogram shows protein elution profile monitored by UV absorbance at 280 nm (blue line) during immobilized metal affinity chromatography (IMAC). Two major protein peaks are observed: the first at approximately 10 mL during column wash phase, likely representing unbound proteins, and a second sharp peak around 33 mL during the elution phase, representing the target protein of interest. The green line indicates the concentration gradient of buffer used for elution. The x-axis represents the elution volume in millilitres, while the y-axis shows the absorbance in mAU. The chromatogram includes various phases of the purification process including equilibration, sample application, column wash, and final elution of the bound protein.*

4.9. Protein Characterization and Quantification

From the second IMAC purification, the eluted fractions of the rITs proteins were concentrated down to 500 ul using a 30 kD Amicon filter for each construct. The recombinant immunotoxin fusion proteins were quantified using densitometry and characterized using SDS-PAGE and Western Blot. All the recombinant immunotoxin fusion proteins were expected to show at 72 kD band size.

4.9.1. SDS-PAGE and Western Blot

After calculating the yield of full-length recombinant immunotoxin fusion proteins (FPs) in concentrated samples, it was crucial to confirm protein integrity and functionality at both the N- and C-terminals. Immunoblot analysis was performed using an anti-His antibody to bind to the His tag on the N-terminal of the FPs. This method also identifies His-tagged proteins that may contain truncated or degraded functional proteins. The samples were prepared by adding 5 µl of loading dye to 5µg/µl of the protein. Samples were incubated at 95 ^{0}C for 10 minutes. After incubation was over, they were then loaded into the SDS gel and transferred to the membrane for Western Blot analysis.

Comparing the WB to the accompanying SDS-PAGE gel confirmed the hLIV22-ETA & dETA' (R456C+R490A) as well as trop-ETA' & dETA'(R456C+R490A) RITs at ~72 kDa. The bands seen in this Western blot were expected to reflect His-tagged proteins. As a result, this blot had the added advantage of detecting not only the rIT of interest but also the presence of other His-tagged proteins. Furthermore, it permitted the detection of probable degradation products, which were indicated by the presence of extra or shortened bands. Protein degradation was detected at approximately 34 kDa.

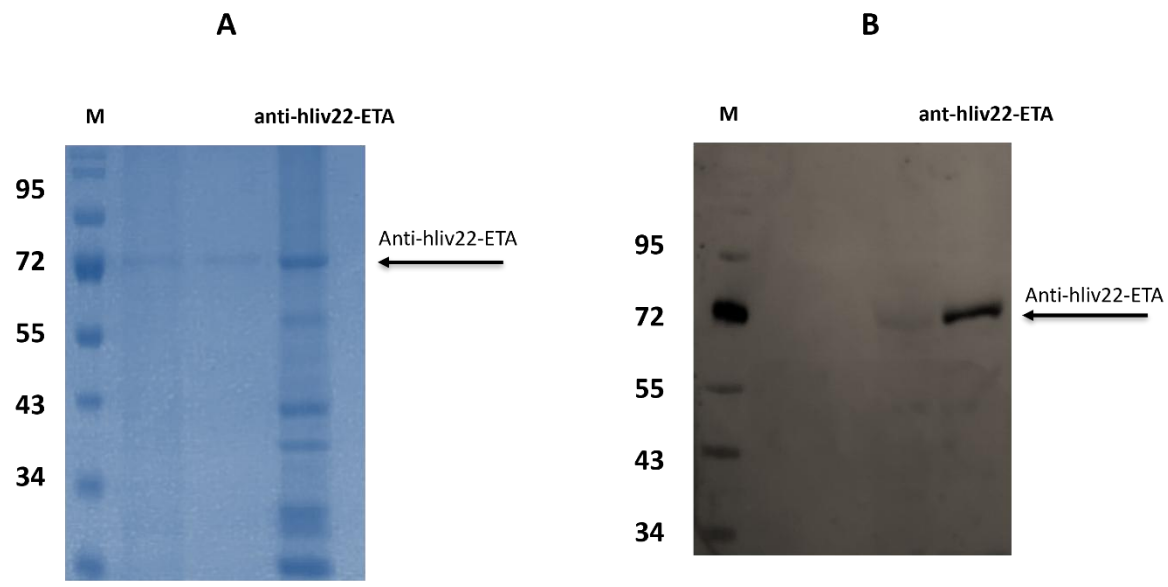

*Figure 26**: SDS and Western blot (WB) analysis of HLIV22(scFv)-ETA wild type rIT** (A) 10% SDS-PAGE gel stained with Aquastain solution and (B) WB analysis of concentrated a trop2 (scFv)-R456C+R490A dETA' (~72 kDa). Two identical SDS-PAGE gels were run at 120V for 2 hours, each containing 5 µg/u.*

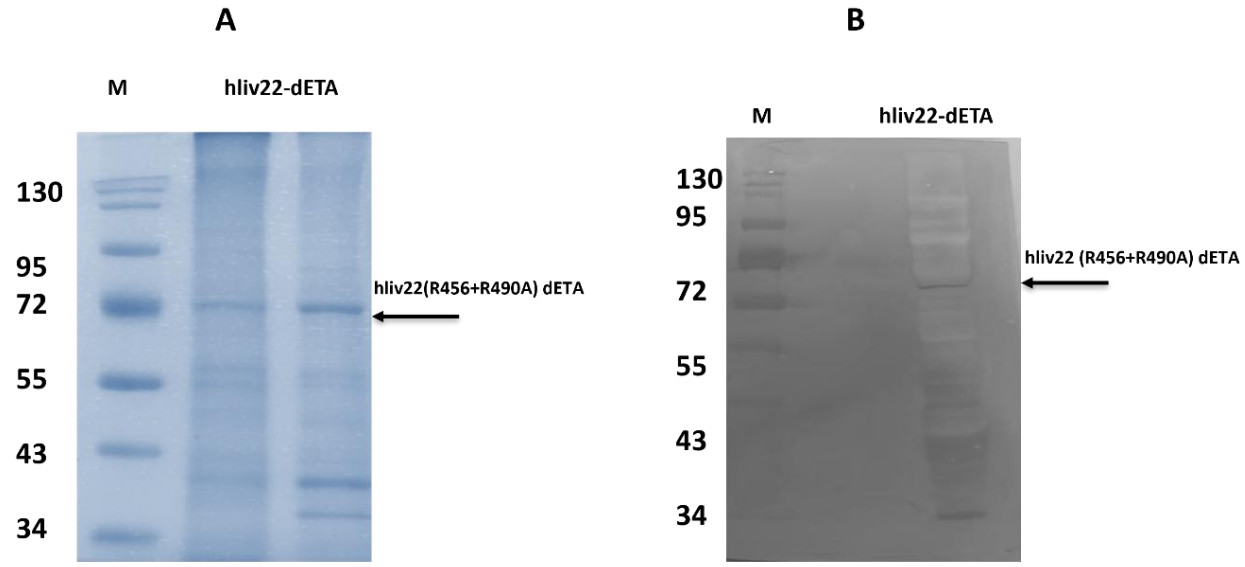

*Figure 27: **SDS and Western blot (WB) analysis of HLIV22(scFv)-R456C+R490A rIT** (A) 10% SDS-PAGE gel stained with Aquastain solution and (B) WB analysis of concentrated a trop2 (scFv)-R456C+R490A dETA' (~72 kDa). Two identical SDS-PAGE gels were run at 120V for 2 hours, each containing 5 µg/u.*

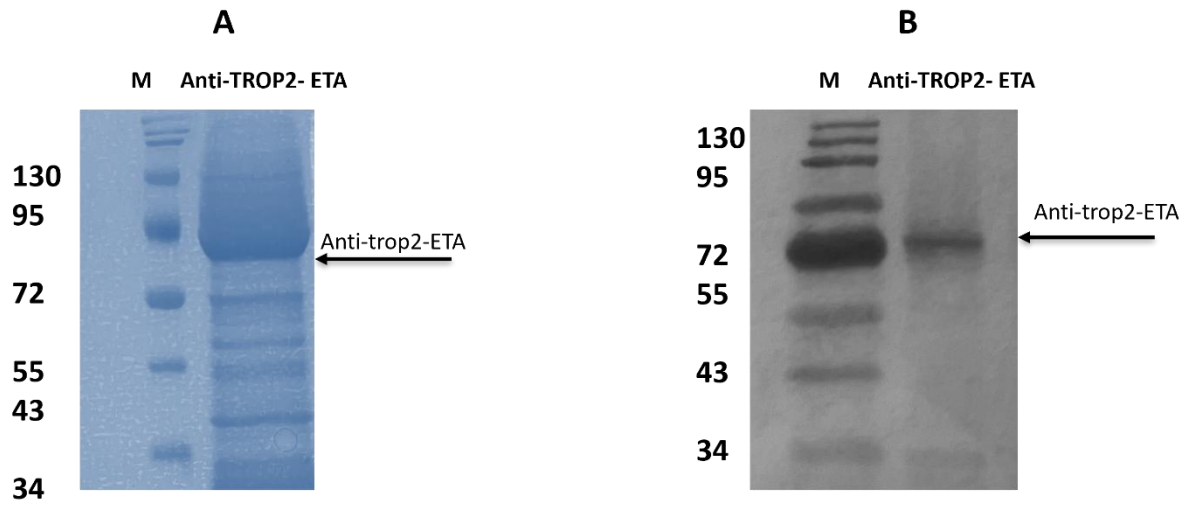

Figure 28: ***SDS and Western blot (WB) analysis of trop2(scFv)-ETA rIT*** *(A) 10% SDS-PAGE gel stained with Aquastain solution and (B) WB analysis of concentrated a trop2 (scFv)-ETA' (~72 kDa). Two identical SDS-PAGE gels were run at 120V for 2 hours, each containing 5 µg/u.*

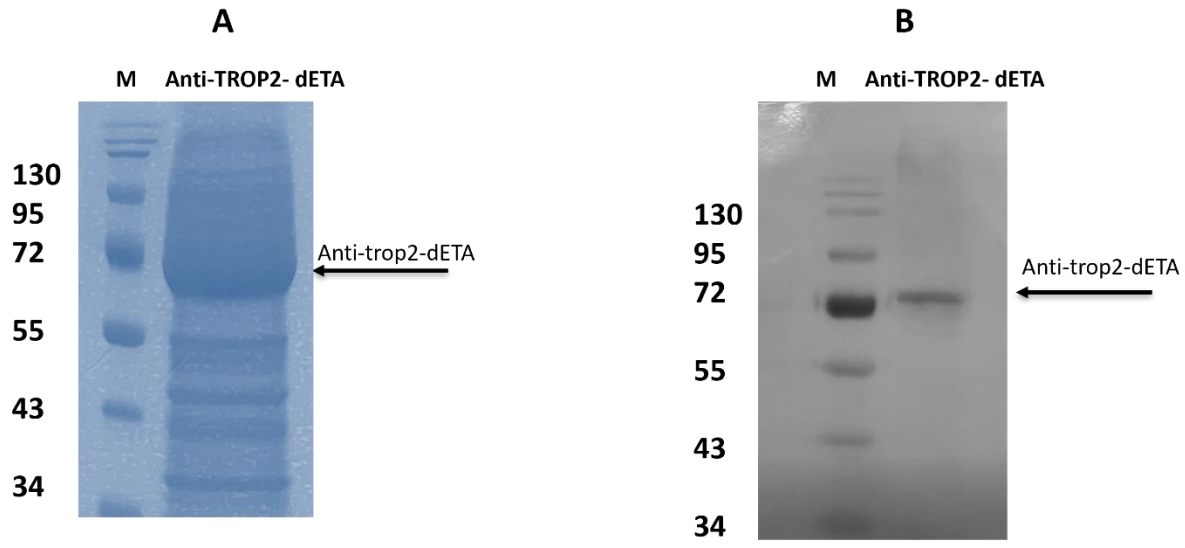

Figure 29: ***SDS and Western blot (WB) analysis of trop2(scFv)-R456C+R490A rIT (A)*** *10% SDS-PAGE gel stained with Aquastain solution and (B) WB analysis of concentrated a trop2 (scFv)-R456C+R490A dETA'' (~72 kDa). Two identical SDS-PAGE gels were run at 120V for 2 hours, each containing 5 µg/u.*

4.9.2. Protein Quantification

Densitometry was utilised to determine the yield, purity, and absolute quantity of full-length protein in the protein elution sample from the IMACs. On an SDS-Page gel, serial dilutions of BSA standards were performed in parallel with each rIT and the actual rIT concentrations determined are listed in **Table 8**.

Table 6: Protein quantification and purity assessment of bacterially expressed rITs

rIT	Concentration determined using densitometry (µg/µl)	Absolute protein yield (µg)
Hliv22(scFv)-ETA'	0.42	218.2
Hliv22(scFv)-dETA'	0.511	255.6
Trop2(scFv)-ETA'	0.58	290.1
Trop2(scFv)-dETA'	0.44	268.8

The low protein yield amount, purity and low concentration necessitated a repetition of time-consuming experiments such as protein expression to produce more protein and two-step of protein purification. With that challenge being accounted, these rITs downstream experiments (binding and toxicity) studies were only performed in one positive breast cancer cell line each and one negative cell line.

4.10. Binding analysis on fixed cells using confocal microscopy.

Confocal microscopy was used to assess the cell surface binding and internalization capabilities of hLIV22(scFv)-R456C+R490A-dETA', hlv22(scFv)-ETA', trop2(scFv)-R456C+R490A)-dETA' and trop2(scFv)-ETA'. This evaluation was conducted using relevant LIV-1 & trop-2-overexpressing cell line, MCF-7 due to LIV-1 and trop-2 overexpression. SiHa and HERK293 were used as an antigen negative cell line that did not overexpress LIV-1 and trop2 respectively. The antigen negative cell lines should not demonstrate cell surface binding.

The binding analysis principle uses the His-Tag at the rIT's N-terminal as an attachment site for the anti-His PE fluorophore. The 6X His Alexa Flour 647/488 PE tagged rITs were incubated with the target cell lines, fixed, and studied using confocal microscopy, and surface binding and internalization signals were observed in MCF-7 cells. Blue fluorescence indicated nuclear DNA staining. Green/Red fluorescence emission along the cell perimeter was interpreted as surface binding, whereas green or red fluorescence within the cell's cytoplasm suggested internalization. Furthermore, the negative control (SiHa and HERK293T cells) showed no significant fluorescence, indicating that it was successful.

A. Anti-hliv22(scFv)-ETA' (MCF-7) (+)

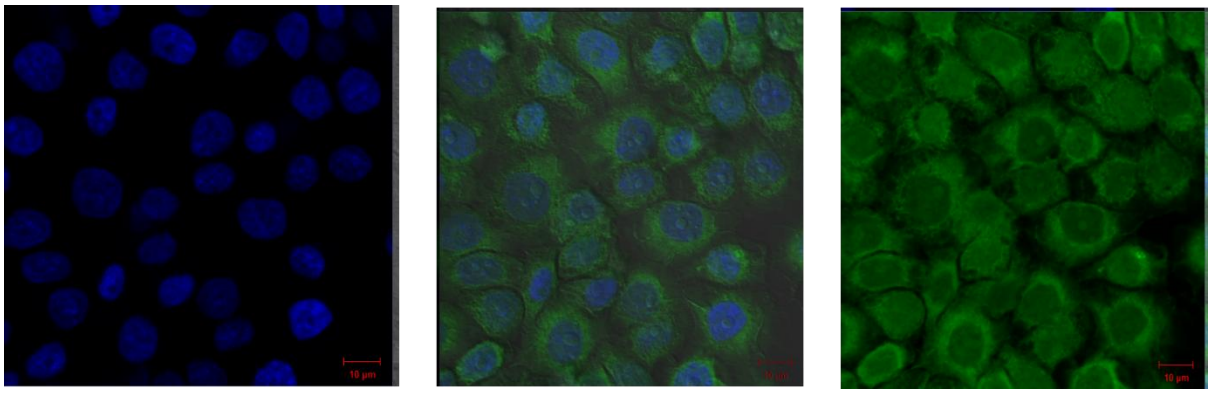

B. Anti-hliv22(scFv)-dETA' (MCF-7) (+)

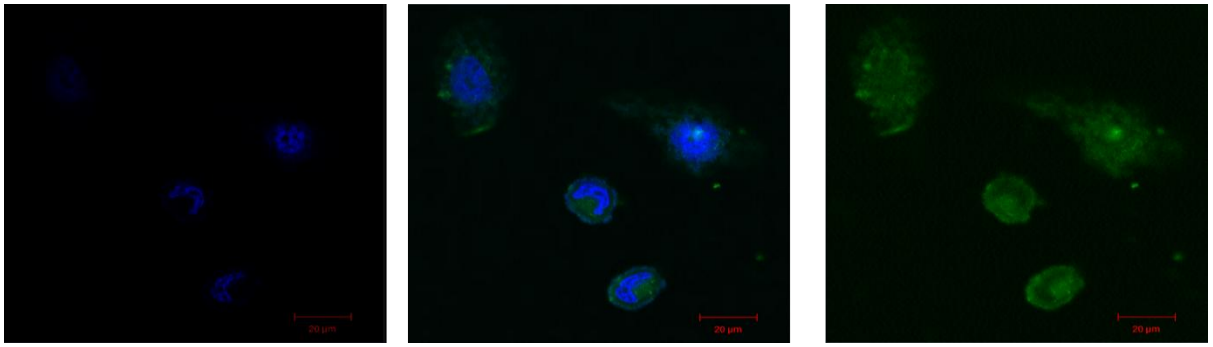

C. Anti-hliv22-ETA' (SiHa) (-)

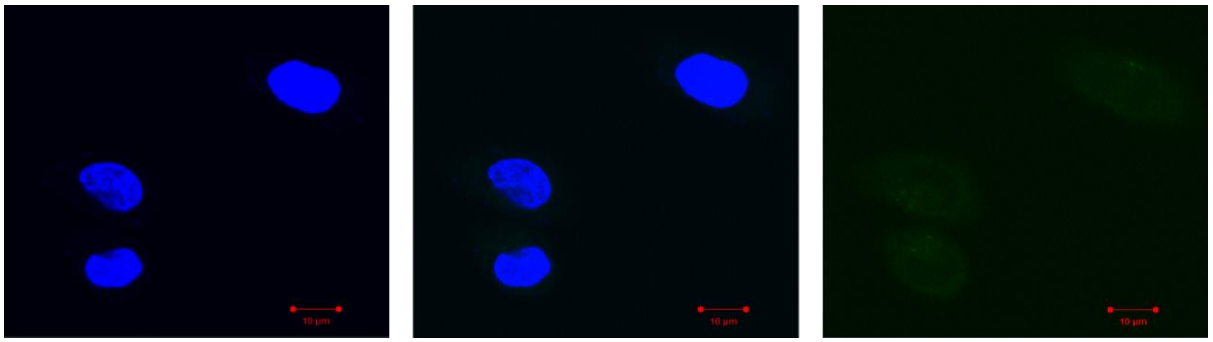

Figure 30: ***Fixed cell confocal imaging for assessment of the binding and internalization capabilities of hLIV22(scFv)-ETA' wild type and (R456C+R490A)-dETA on MCF-7 BC cell line. (A&B) MCF-7 breast cancer cell line, antigen-positive test, (C)*** *SiHa cervical cancer cell line, antigen-negative control. For 10-20 minutes at 37°C, the cell lines were incubated with 15 µM of conjugated protein mix. The cell nuclei (represented by the blue signal) were stained with Hoechst (diluted in a 1:5000 ratio to cell culture media). The cells were fixed with 4% paraformaldehyde (PFA), and thoroughly washed with 1X PBS before the coverslips were mounted onto a microscope slide. Images were obtained*

from a Zeiss confocal scanner microscope (LSM880) equipped with an Airy scan. All represented images were subjected to minor image processing, for more clarity in the visualization of binding/internalization events (represented by the green signal). The first panel indicates the Hoechst stain signal only, the middle panel indicates the combination of the Hoechst and Alexa 488 signal, and the last panel shows the Alexa 488 stain signal only.

A. Anti-trop-2(scFv)-ETA' (MCF-7) (+)

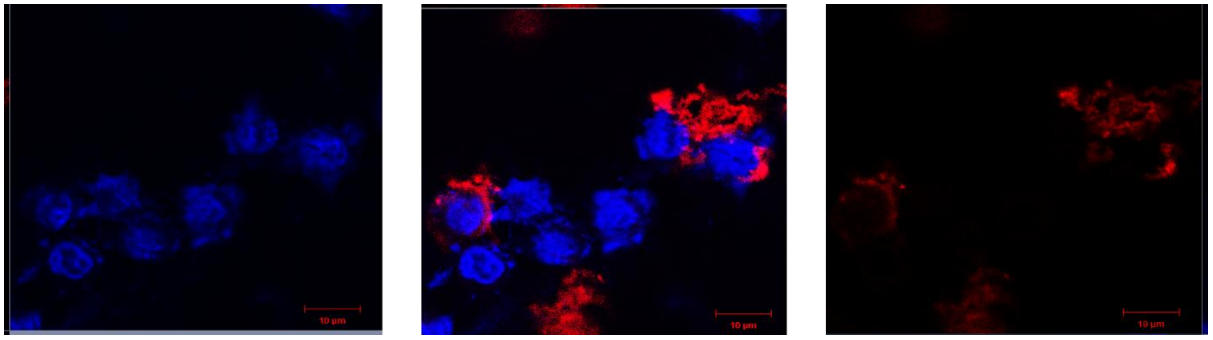

B. Anti-trop-2(scFv)-dETA' (MCF-7) (+)

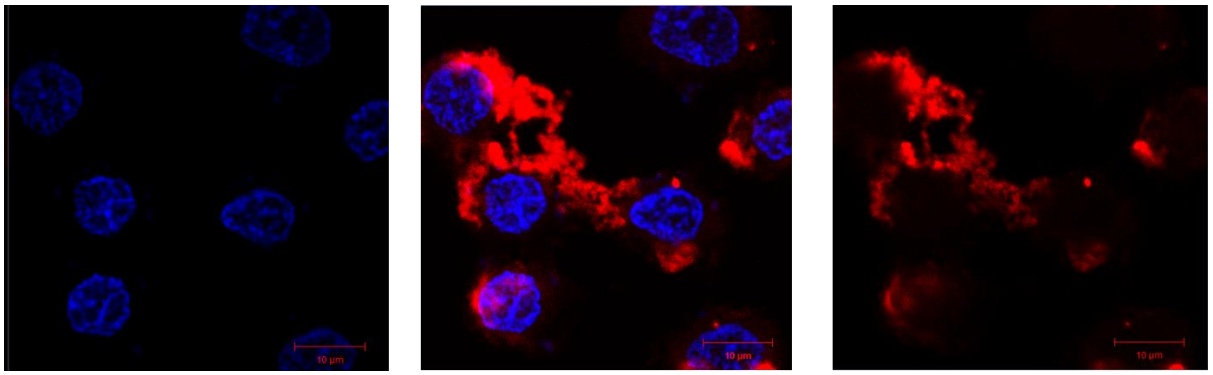

C. Anti-trop-2(scFv)-ETA' (HERK293T) (-)

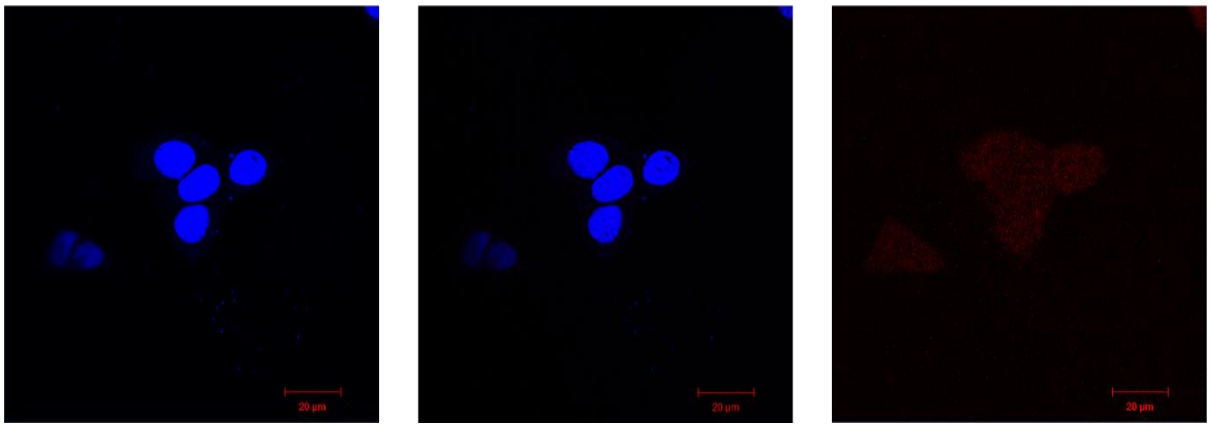

Figure 31: ***Fixed cell confocal imaging for assessment of the binding and internalization capabilities of trop2(scFv) ETA' (WT) and (R456C+R90A)-dETA on cancer cell lines. (A&B) MCF-7 BC cell line, antigen-positive test, (B)*** *HERK293T cell line, antigen-negative control. For 10-20 minutes at 37°C, the cell lines were incubated with 15 μM of conjugated protein mix. The cell nuclei (represented by the blue signal) were stained with Hoechst (diluted in a 1:5000 ratio to cell culture media). The cells were fixed with 4% paraformaldehyde (PFA), and thoroughly washed with 1X PBS before the coverslips were mounted onto a microscope slide. Images were obtained from a Zeiss confocal scanner microscope (LSM880) equipped with an Airy scan. All represented images were subjected to minor image processing, for more clarity in the visualization of binding/internalization events (represented by the red signal). The first panel indicates the Hoechst stain signal only, the middle panel indicates the combination of the Hoechst and Alexa 647 signal, and the last panel shows the Alexa 647 stain signal only.*

4.11. Cytotoxicity Assay

After showing that the rITs binding exclusively to breast cancer MCF-7 antigen-positive cancer cells, the cell viability assay was performed to examine the potential for tumor cell death. The cancer cell lines were treated with each of the rIT in an increasing concentration, and XTT cell viability tests were used to assess cytotoxicity in comparison to the untreated (100%) and 0% cell viability controls. Fit curve and interpolated IC_{50} values were also calculated using GraphPad prism program. Using serially diluted rITs, we observed a dose-dependent reduction in MCF-7 cell viability, allowing us to calculate the IC_{50} values displayed in (**Figure 32**). Each experiment was repeated twice with three replicates in each experiment.

The hliv22 (scFv)-ETA' wild type construct demonstrates a high efficacy with an IC_{50} of 2.297 nM compared to its mutant counterpart hliv22 (scFv) (R456C+R490A)-dETA' shows reduced potency (IC_{50} of 40.61 nM), representing an approximately 18-fold decrease in effectiveness. The TROP-2-targeting constructs demonstrate moderate potency, with TROP-2 (scFv)-ETA' showing an IC_{50} of 32.70 nM and TROP-2 (scFv)-dETA' exhibiting a slightly higher IC_{50} of 46.58 nM. These findings indicate that modifications to the exotoxin portion, whether through truncation (dETA') or specific mutations (R456C+R490A), generally reduce cytotoxic effectiveness. All immunotoxins successfully reduce cell viability to near-zero at higher concentrations, though the wild-type HER2-targeting construct clearly emerges as the most potent option among all tested immunotoxins for targeting MCF-7 breast cancer cells.

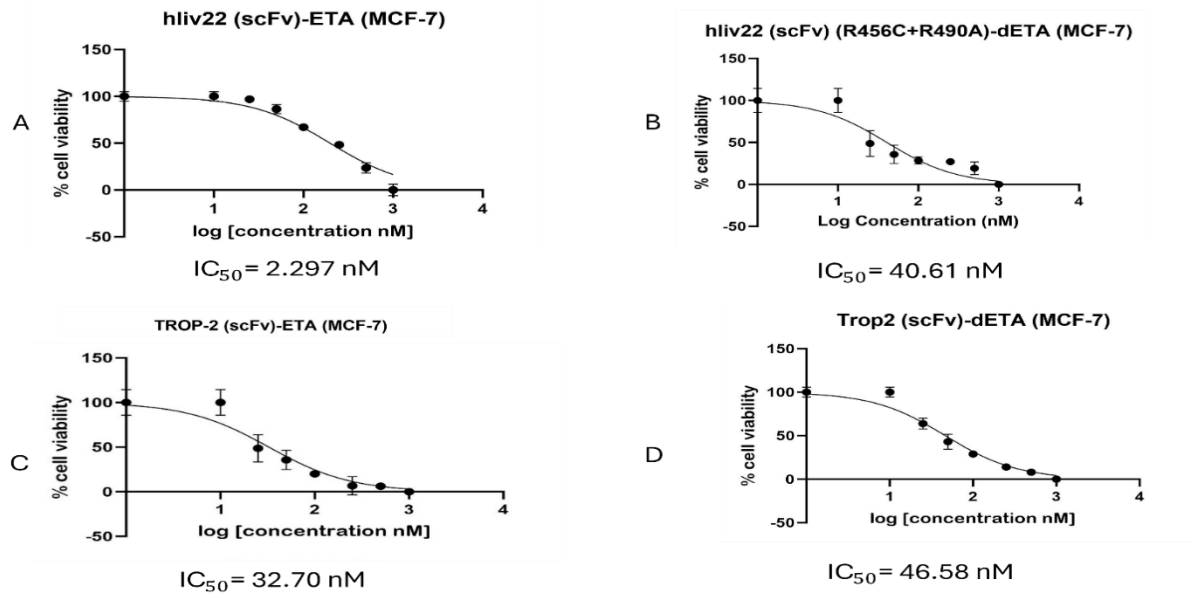

Figure 32: (A-D) ***Shows the cytotoxicity evaluation of ETA' and dETA'-based rITs****. The cytotoxicity activity was assessed using an XTT cell viability assay. The cells treated with serially diluted concentrations of rITs followed by performing a XTT cell viability assay. Controls were untreated (negative control) and cells treated with zeocin(100µg/ml) (positive control). MCF-7 cell line was served as positive control for both hliv22 rITs and trop-2 rITs.*

For the antigen-negative controls, the cell viability of the SiHa and HERK293T cells were not affected by the anti-hliv22(scFv)- ETA' and anti-trop2(scFv)-ETA' rITs respectively, indicating that the rITs do not kill non-specifically. The same was observed with the anti-hliv22(scFv)-dETA' as the cell viability of the SiHa and HERK293T cells were not affected by anti-trop2-dETA'.

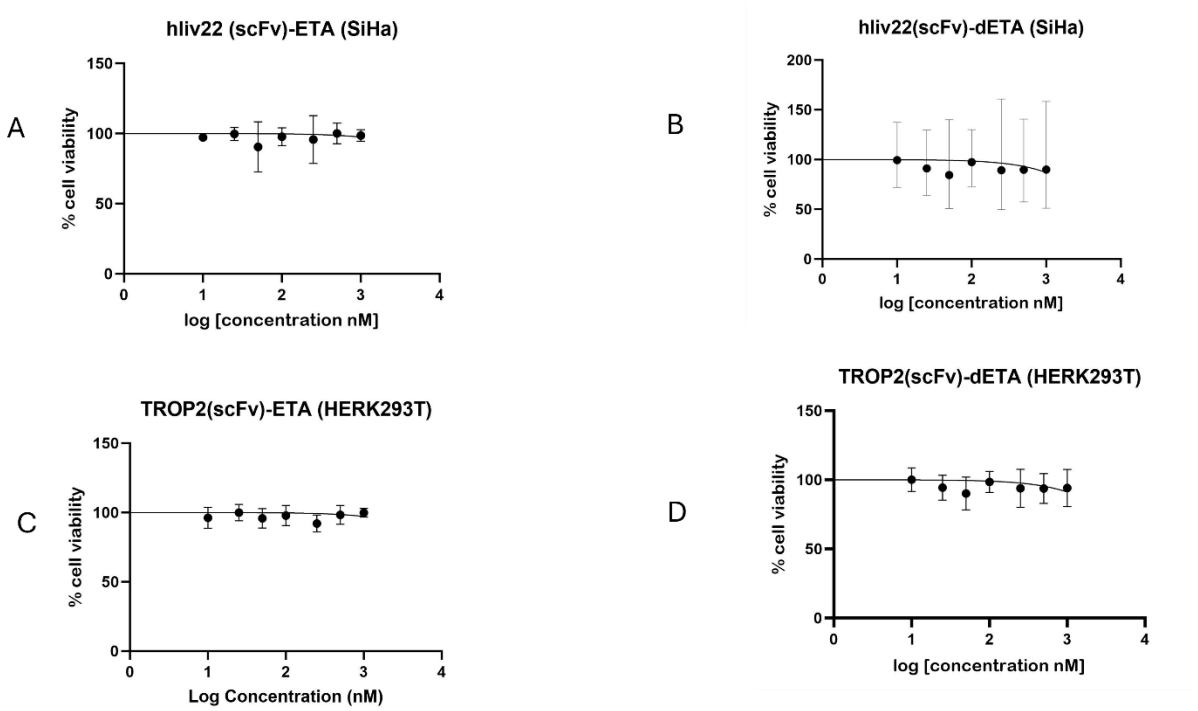

Figure 33: ***(A-D) shows the cytotoxicity evaluation of ETA'' and dETA-based rITs****. The cytotoxicity activity was assessed using an XTT cell viability assay. The cells treated with serially diluted concentrations of rITs followed by performing a XTT cell viability assay. Controls were untreated (negative control) and cells treated with zeocin(100µg/ml) (positive control). The HERK293T cell lines served as an antigen negative control for trop-2 rITs. The SiHa cell line served as an antigen negative control for the anti-hliv22 rITs.*

Chapter 5: Discussion

5.1. A precision medicine approach to triple-negative breast cancer

An aggressiveness and lack of oestrogen receptor alpha (ER−), progesterone receptor (PR−), and human epidermal growth factor receptor two loci (HER2−) markers in the TBNC subtype, make it challenging to treat patients that present this breast cancer type, as the current treatment used for breast cancer treatment targets this absence biomarkers. TNBC accounts for 11-20% of all breast cancers [100] and usually affects premenopausal women, particularly African women, and has a greater death and recurrence rate than other kinds of breast cancer, particularly within the first five years. Due to a lack of targeted medicines that are specific and have fewer side effects, TNBC patients continue to have a poor prognosis, prompting a significant effort to identify molecular targets for treatment [101], [102].

Fortunately, clinicians now have greater access to personalized treatments for managing solid tumors. TNBC is now at the forefront of targeted therapy due to advancements in tumor characterization. As TNBC is characterized by unique molecular changes; individualized and successful treatment is crucial for this population due to the significant risk of distant recurrence and mortality. Historically, cytotoxic chemotherapy has been the primary treatment for TNBC, although it can lead to off-target tissue damage and drug resistance. Neoadjuvant chemotherapy is widely utilized because it enables close monitoring of the early treatment response and provides useful prognostic information. Patients who obtain a complete pathological response after neoadjuvant chemotherapy are expected to have much better long-term results. Poor responders, on the other hand, are more likely to experience relapse and mortality. Therefore, identifying

those subgroups that are more likely to benefit from advancements in the tailored approach is difficult nowadays, when multiple targeted medicines are accessible [102], [103].

Our laboratory employs protein engineering to develop recombinant immunotoxins; cancer-targeted therapies that use a cytotoxic bacterial toxin payload to destroy cancer cells. Their development for application in solid tumor malignancies was slowed due to immunological concerns and a narrow therapeutic window. However, recent research has revived the topic. Our literature mentioned that SS1P recombinant immunotoxin had limited clinical activity due to patients about 90% developing antibodies to SS1P after just three doses and could not be retreated [83], [77].

To address this challenge, Ira Pastan's collaboration with Roche Diagnostic GmbH developed RG7787 (Ro6927005) recombinant immunotoxin. This rIT has a molecular weight of 72 kDa and contains a humanized anti-mesothelin Fab that is fused to the mutated toxin. RG7787 is currently undergoing Phase 1 clinical testing in patients with mesothelin-positive cancer including (mesothelioma, ovarian, pancreatic, gastric, and triple-negative breast cancers) [102], [104]. However, in their study findings when they were evaluating the efficacy of this RIT against mesothelin-positive cancer cell lines three of the four gastric cancer cell lines were more sensitive to SSIP than RG7787 as shown by (**Table 7**) [102].

Table 7: Sensitivity of gastric cell lines to RITs. The results from the table were captured from the study: Efficacy of RG7787, a next-generation mesothelin-targeted immunotoxin, against triple-negative breast and gastric cancers [104]**.**

Sample	Sites/cell ($x10^3$)	IC_{50} (ng/mL)		IC_{50} (pM)	
		SS1P	RG7787	SS1P	RG7787
MKN7	5.6	2.3	>100	37.1	>1200
MKN28	16.1	0.34	5.6	5.5	75.6
MKN45	9.9	2.3	0.5	37.1	6.8
MKN74	4.2	2.3	12	37.1	162.0

Therefore, to try and recover the enzymatic activity of such recombinant de-immunized immunotoxins, this study has developed a new version of RG7787 rITs with an inserted cysteine in position R456.

5.2. Production of RG7787 rITs fusion proteins

Immunotherapy has revolutionized modern medicine, especially in the treatment of cancer and auto-immune diseases. Its selective delivery of catalytically active protein toxins to the ability to overcome several drawbacks mainly associated with off-target effects and minimal residual disease associated with conventional treatments. However, the ability to produce enough active protein for preclinical and clinical use remains a challenge. The standard method of producing recombinant proteins such as immunotoxins in large quantities is to transform Gram-negative bacteria and subsequently recover the desired protein from inclusion bodies by intensive de- and renaturing procedures. One major disadvantage of this technique is the low yield of

protein recovery. So, in this study an alternative strategy established by Barth *et al.* exploiting the expression of recombinant immunotoxin in the periplasmic space with the presence of compatible solutes was applied [99].

5.3. Recombinant Immunotoxin fusion proteins yield, stability, and functionality

In this study, all recombinant immunotoxins generated were expressed in a bacterial host expression system (*E. coli* BL21 (DE3)). Various elements should be considered when selecting a bacterial host expression system for recombinant protein production. *E. coli* BL21 (DE3) is an extremely useful host for expression of recombinant proteins. The rapid doubling times, low cost, easy manipulation, and convenience of expressing recombinant fusion proteins make this organism the first-choice tool for life science applications [105]. Extensive genetic research over several decades has offered crucial information and tools for altering and engineering bacterial strains, making it an appealing alternative for recombinant protein expression [106].

5.3.1. Implementation of the periplasmic expression methodology

This method of protein expression was designed to allow the synthesis of difficult-to-produce recombinant proteins, including immunotoxins, within the periplasmic space of *E. coli* BL21 (DE3) bacteria. Protein of interest was obtained by subjecting the *E. coli* BL21 (DE3) cells to osmotic stress conditions in the presence of compatible solutes. These compatible solutes function by using a stress response to induce the production of heat shock proteins by creating a stabilizing periplasmic microenvironment at high salt concentrations. Adding compatible solutes to shaking cultures enables bacterial growth within the described osmotic stress conditions as used in this study.

E. coli strain BL21 (DE3) has unique genetic changes in the Lon protease and OmpT protease genes, which cause enzyme deficiencies. The expression system includes the Lac operon, which consists of a Lac promoter before an operon and the LacI repressor encoded by a particular gene. The presence of IPTG activates the lac operon by binding to the active LacI repressor, causing its dissociation from the operator site. Furthermore, this strain harbours a DE3 lysogen that contains the T7 RNA polymerase gene under the control of a LacUV5 promoter [107], [108], [109]. The PelB signal sequence is used for sending the recombinant protein to *E. coli's* BL21 (DE3) periplasmic region. A lower induction temperature is generally better for recombinant protein production, hence a temperature of 26°C was used in this study. This is because it causes an energy conservation response, which slows central carbon metabolism and results in a reduced growth rate. The production of recombinant proteins places a metabolic cost on the host, resulting in the buildup of target proteins in insoluble clumps known as inclusion bodies. Because hydrophobic interactions between amino acids are temperature sensitive, aggregation reactions are favoured at higher temperatures. Protein aggregation can be reduced by lowering the induction temperature. The optical density of the culture is also a significant consideration, as high cell densities may not be optimal for protein production. Metabolic activity reduces at high cell densities due to a variety of variables, including food restrictions, acetate generation, lower availability of dissolved oxygen, and increasing carbon dioxide levels, all of which hamper recombinant gene expression. Furthermore, high temperatures can increase the likelihood of plasmid loss due to their rapid growth rates [110], [111], [112], [113], [114].

The duration of the induction is also important, as extended incubation might lead to protein aggregation. Many studies have used a conventional induction time of 16 hours.

However, for some proteins, a longer induction period at a low temperature may be advantageous. In 2000, Barth *et al.,* discovered that by prolonging the induction period, they were able to accumulate 95% functional proteins, as opposed to conventional circumstances, which yielded less than 10% functional protein [99]. In contrast, Mukherjee *et al.,* in 2004 demonstrated that *E. coli* BL21 (DE3). cells can express 90% of a recombinant single-chain antibody fragment (scFv) linked to a PelB signal sequence. SDS-PAGE analysis indicated that their study contained a high degree of recombinant protein expression [109]. Although, the periplasmic region of *E. coli* BL21 (DE3) was an ideal technique for recombinant protein production, the shaking of cultures technique which was used in this study does not produce enough protein for all the downstream experiments.

5.4. Purification of rITs fusion proteins

To achieve the largest yield and quality of target protein, optimal purification requires balancing multiple purification parameters such as speed, recovery rate, capacity, and resolution. Immobilized Metal Affinity Chromatography (IMAC) was utilized in this study due to its efficiency and specificity for purifying recombinant proteins with affinity tags, making it ideal for demonstrating proof of concept. However, IMAC has limitations, particularly when applied to large-scale, as it often co-purifies contaminants and may not meet the uncompromising purity requirements for therapeutic applications. While IMAC is effective as a first-step purification method, additional processes like ion-exchange or size-exclusion chromatography are typically required to achieve higher purity. The choice of IMAC alone in this study reflects practical constraints, including the cost of consumables and the scalability challenges faced in resource-limited academic environments.

The decision to rely solely on IMAC was guided by the need to maximize resource allocation under the SARChI Chair funding, enabling support for multiple student projects. By prioritizing proof of concept, this approach demonstrates feasibility while setting the stage for future research aimed at achieving higher technological readiness levels. Once positive results are obtained, further funding can be sought to optimize purification protocols, scale up production, and explore more advanced or alternative methods. This practical strategy balances the need for impactful research outcomes with the constraints of limited resources, ensuring meaningful contributions to scientific progress.

IMAC which is based on the interaction between a transition metal ion (Co^{2+}, Ni^{2+}, Cu^{2+}, or Zn^{2+}) immobilized on a matrix and a particular amino acid side chain [115], [116]. Specific amino acids can bind to the target DNA of the protein, resulting in the production of a "tag" on the protein. Several affinity tags are available, including the Histidine tag (His-tag), Arg-tag, GST tag, and Strep-tag II. In our study, the target protein was purified using a His-tag. This affinity tag was used because of its advantages over others such as ease of incorporation into the desired protein. The poly-His tag is often attached to the target protein's N or C terminus during genetic modification [116]. Histidine has the strongest contact with immobilized metal matrices due to electron donor groups on the imidazole ring that easily coordinate with the transition metal. In addition, a poly-His tag can be eluted from the IMAC resin under mild circumstances, allowing the target protein to maintain its biological activity. As previously mentioned, although the His-tag affinity tag has numerous advantages over other affinity tags, it does have certain drawbacks, including nonspecific protein binding to the IMAC column which resulted in a reduction of our protein yield throughout the purification process [117].

Studies have also shown that using the poly-His-tag affinity tag for purification can lead to contamination of the final product due to cellular proteins with multiple adjacent histidine residues that bind to the IMAC matrix and may coelute with the target protein, resulting in contamination of the finished product. In attempt to resolve this issue, another study proposed the use of 10mM 2-mercaptoethanol in the loading, washing, or elution buffer could potentially resolve these difficulties [115]. Additionally, this study suggested that nonspecific hydrophobic interactions with the IMAC matrix may contribute to nonspecific protein coelution. To overcome this, low amounts of non-ionic detergents such as Triton X-100 or Tween 20 in the buffers may minimize nonspecific protein interactions without compromising target protein binding to the IMAC matrix. Adding salt (500mM NaCl), glycerol (20%), or low ethanol (20%) can minimize nonspecific hydrophobic protein interactions with the IMAC matrix [117]. In our study, a binding buffer containing 300mM NaCl, 10% Glycerol, 100 Tris-HCl, and 150 Imidazole, provided better purity. Due to the huge number of contaminating proteins found, the imidazole concentration in the binding buffer is substantially greater than that advised by previous studies. As a result, adding 150 mM imidazole to the binding buffer significantly reduced nonspecific protein during purification.

Nickel resin was used to recharge the columns used for purification in this study due to its different advantages such as giving the highest yield of the recombinant fusion proteins [118]. Our recombinant protein vector plasmid contains a 6xHis tag which has a high affinity for nickel. Nonspecific binding caused by electrostatic attraction to the nickel beads was minimized by the addition of NaCl to our loading buffer. After the application of the sample, a wash buffer containing a low concentration of imidazole was used to elute any proteins that were weakly bound to the nickel column. For the elution

of our recombinant fusion protein from a Ni column, an elution buffer containing a high concentration of imidazole was used. Other elution methods used include lowering the pH of our buffers from 8.0 to 7.4 so that the histidine becomes protonated and no longer has affinity for the nickel resin or using strong chelating agents such as EDTA and EGTA. The use of a strong chelating agent results in the nickel being stripped from the column and the elution of protein-nickel complexes. Another advantage of using an IMAC column for recombinant protein purification is that the nickel-histidine reaction is not dependent on the secondary structure. Therefore, a nickel column can be used for the purification of denatured protein. A further potential benefit of using a nickel column is that a protein can be renatured while still bound to the nickel resin. An elution buffer containing imidazole was used to retain the renatured state. Further, an intense and complete desalting buffer exchange technique was implemented to enhance the process. This procedure was crucial for removing imidazole from IMACI elution and enhancing protein binding to the column. With all these parameters adjusted, and followed, the purity of our fusion proteins remained poor as shown by SDS results.

5.5. Addressing Protein Impurities & Degradation

The stability of the RIT fusion is more important to obtain accurate results, mainly in sensitive experiments such as XTT assays. A degraded protein can interfere with the functionality of the rITs which can result in faulty results during cytotoxicity studies. Protein stability can be defined as the persistence of molecular integrity or biological function despite adverse influences or conditions, such as heat or other deleterious conditions. Our RIT fusion proteins are stored at 4 ^{0}C after purification for short-term storage or -20 ^{0}C for long-term storage as suggested by study PIERCE company [119].

However, protein degradation was still observed as shown by SDS in (**figure 26A ,27A, 28A & 29A**) regardless of these storage conditions. There are many environmental factors that we speculate might lead to the observed degradation. One the reason could be the effect of the change in temperature during the purification procedure, from filtering the supernatant containing our RIT fusion proteins to running them for both 1st and 2nd IMAC purification on the AKTA machine with columns and buffers that are stored at room temperature. Also, when running the post-purification experiments, these rITs are taken in and out of their optimal storage condition which can also further lead to more proteolytic degradation. For future purpose, storing the purification machine in the optimal storage for proteins (4 ^{0}C) can be employed to avoid proteolytic degradation caused by the change in temperature.

Another key deleterious condition during protein chromatography is the presence of proteolytic enzymes, referred to as proteases [120]. Protein levels within cells are regulated by both synthesis and breakdown rates. Protein half-lives within cells range from minutes to several days, and varied rates of protein breakdown play a crucial role in cell control. Many rapidly degraded proteins serve as regulatory molecules, such as transcription factors. These proteins must have a high turnover rate for their levels to respond swiftly to environmental stimuli. Other proteins degrade rapidly in response to certain signals, offering another mechanism for controlling intracellular enzyme activity.

In eukaryotic cells, two major pathways (ubiquitin-proteasome pathway and lysosomal proteolysis mediate protein degradation. In eukaryotic cells, ubiquitin serves as a marker for cytosolic and nuclear proteins, allowing for fast proteolysis. The covalent binding of several ubiquitin molecules marks proteins for fast breakdown. The enzyme E1 is

responsible for initial ubiquitin activation. The activated ubiquitin is subsequently transported to one of several distinct ubiquitin-conjugating enzymes (E2). In most situations, the ubiquitin is then transported to a ubiquitin ligase (E3) and finally to a specific target protein. Multiple ubiquitins are then introduced, and the polyubiquitinated proteins are destroyed by a protease complex (the proteasome). The other major pathway of protein degradation in eukaryotic cells involves the uptake of proteins by lysosomes. Lysosomes are membrane-enclosed organelles that contain an array of digestive enzymes, including several proteases. Lysosomes contain a variety of digesting enzymes, including proteases. Its mechanism of action involves the absorption of lysosomes cellular proteins through fusion with autophagosomes, which are created by enclosing regions of cytoplasm or organelles (such as mitochondrion) in endoplasmic reticulum fragments. This fusion produces a phagolysosome, which digests the contents of the autophagosome [121].

Proteases can degrade target proteins during protein purification therefore selecting the right source organism/tissue and using protease inhibitors can help limit degradation effects. Our lab utilizes protease inhibitors to avoid degradation, they prevent protein degradation and extraction by blocking or inactivating the enzymes released by the subcellular compartment during cell lysis. This helps to prevent the proteins' structural and functional integrity from being compromised. In this study, protease inhibitors in tablet form were added to the lysis buffer to protect our fusion proteins during bacterial cell extraction and protein purification. However, the amount of degradation observed emphasizes the importance to implement or improve the current used method.

5.6. Binding, internalization, and intracellular routing of rIT fusion proteins

To develop effective RITs, different factors need to be considered. These include the specificity and affinity of the antibody, the internalization and processing of the rITs as well and the intracellular release of the toxin-component [122], [123]. It is, therefore, important to understand and optimize these parameters when considering the application of the RITs.

5.6.1. Selection of cancer cell lines

Understanding a cell line's origin and general characteristics is critical because it determines its utility in your research. In this study, MCF-7 (ATCC: HTB-22) was used as a BC positive cell line. MCF-7 is a breast cancer cell line that expresses both LIV-1 and trop2 antigens. MCF-7 cells are valuable for in *vitro* breast investigations because they preserve certain perfect properties of the mammary epithelium, such as the processing of oestrogen (oestradiol) via oestrogen receptors (ER) in the cell cytoplasm. When produced *in vitro*, the cells can form domes, while epithelial-like cells grow in monolayers [124]. MCF-7 has been previously wildly used to masses the impact of liv-1 and trop2 antigens expression on the cancer cell growth to identify the potential mechanisms underlying this discovery in breast cancer [125], [126], [127], [128], [129], [130], [131].

After confirmation of full-length protein preparation of hliv22(scFv)-ETA', hliv22(scFv)-dETA', anti-trop2(scFv)-ETA' and trop2(scFv)-dETA' by SDS-PAGE and Western blot, *in vitro* functionality of these rITs was tested on MCF-7 cell line.

The results observed during the cell surface binding studies showed hliv22(scFv)-ETA' and trop2(scFv)-ETA'-specific cell surface binding when tested using MCF-7 BC cell line. This was reflected by the emission of green or red fluorescence depending on the antibody used situated at the cell perimeter was taken as an indication of surface binding and green fluorescence within the cytoplasm of the cell.

5.6.2. Cytotoxicity of rITs

After confirming the selective binding of each of the rITs, XTT assays were performed to evaluate the rITs ability to kill the target cells. MCF-7 cells were treated with increasing concentrations of rITs and the IC_{50} value of the rITs was calculated using GraphPad prism software.

5.6.2.1. Efficacy of the new version of RG7787

In comparison to previously developed recombinant immunotoxins (rITs), RG7787 exhibits improved features for clinical application, including reduced nonspecific toxicity, lower immunogenicity, and enhanced resistance to degradation by lysosomal proteases. When tested *in vitro* against triple-negative breast cancer (TNBC) cell lines such as HCC70 and SUM149, RG7787 demonstrated >95% cell killing, with IC_{50} values below 100 pM, indicating strong cytotoxic activity. However, its performance against gastric cancer cell lines was more variable. As shown in the data in **Table 7** for MKN7, MKN28, MKN45, and MKN74, three of the four cell lines (MKN7, MKN28, and MKN74) were more sensitive to SS1P than to RG7787, with IC_{50} values for RG7787 being 4- to >13-fold higher in some cases. This suggests that while RG7787's immunogenic profile is improved through epitope depletion, these modifications resulting in a decrease of enzymatic potency compared to its wild type.

In this study, two ETA'-based recombinant immunotoxins targeting LIV-1 and TROP2 (hliv22(scFv)-ETA' and TROP2(scFv)-ETA) were evaluated for their cytotoxicity against the MCF-7 breast cancer cell line. Both constructs demonstrated strong and specific cytotoxic activity, with IC_{50} values in the low nanomolar range (~35–40 pM), while their deimmunized versions (dETA variants) showed moderately reduced activity (IC_{50} ~100–120 pM). Importantly, the new RG7787-derived constructs with a Cysteine mutation at position R456 (replacing the original Alanine) showed only a 1.4-fold reduction in activity when fused to TROP2, suggesting partial restoration of enzymatic activity. This is a marked improvement over the 4- to >13-fold activity reduction observed with RG7787 in gastric cancer lines, as previously reported by Alewine *et al.,* and reflects a significant advancement in rIT design.

When comparing these finding to the results of previous MSc studies, the fold differences in activity observed in this study align with similar trends reported in earlier research where (Marc Henry and Takunda Ngwenya) within our research unit developed a different version of RG7787 dETA' containing a thymine (T) mutation at position R456 in place of the arginine (A) mutation, without the R490A modification. Marc research demonstrated a recovery of enzymatic activity for the mutants tested against cervical cancer cell lines, as compared to the reduced activity of the original RG7787. Specifically, the best-performing ETA' rIT, anti-LGR5(scFv)-ETA', exhibited an IC_{50} of 12.79 nM, while the highest IC_{50} observed for the dETA' variant, anti-CD90(scFv)-dETA', was 22.34 nM. This represents an approximately 1.8-fold difference in IC_{50} values, indicating a substantial improvement in enzymatic activity for the new version of RG7787 (dETA') construct targeting CD90.

Takunda's findings focused on the efficacy of ETA'- and dETA'-based rITs targeting CD90, LGR5, and EpCAM against triple-negative breast cancer (TNBC) cells (MDA-MB-468). In his study, ETA'-based rITs targeting LGR5 and EpCAM demonstrated significantly stronger targeted cytotoxic effects when compared to their dETA' counterparts. Conversely, the dETA' form of the anti-CD90(scFv)-dETA' rIT exhibited greater cytotoxicity than the corresponding wild-type ETA' construct. His work showed that the published RG7787 variants were approximately two-fold less effective than wild-type for mesothelin-targeting constructs, and a significant 27-fold difference was observed between the LGR5 and EpCAM-targeting rITs.

These findings not only validates the experimental approach but also strengthens the overall conclusions drawn from this study. By demonstrating a significant improvement in the enzymatic activity of the rITs and highlighting their strong cytotoxic effects, this work contributes to advancing the development of recombinant immunotoxins for targeted cancer therapy.

These findings require further validation using recombinant proteins of higher purity to ensure the consistency and reliability of the observed cytotoxic activities. In addition, pre-clinical studies should be conducted to evaluate the cytotoxic efficacy of the dETA'-based rITs across a broader range of triple-negative breast cancer (TNBC) cell lines, to determine whether these constructs exhibit similar or enhanced activity compared to their ETA'-based counterparts. Furthermore, *in vivo* studies are essential for assessing the immunogenicity of these rITs. The enzymatic and biological activity data generated for both the anti-hliv22, and anti-trop2 immunotoxin variants underscore their significant potential as immunotherapeutic agents. These findings are particularly relevant for

targeting diseases like TNBC, which are characterized by elevated levels of LIV-1 and TROP2, highlighting the therapeutic promise of rITs in addressing cancers associated with these biomarkers.

5.7. Application of rIT fusion proteins

Immunogenicity has been a major obstacle to the development of therapeutically effective immunotoxins for solid tumors, although immunogenicity has proven successful in treating certain haematologic cancers where the immune system is inhibited [132]. As a result, there has been little success in creating these compounds for solid tumors. However, studies have recently shown significant malignant regressions in mesothelioma patients receiving immunotoxin and immune suppression treatment [102]. In this study, we have successfully developed novel recombinant immunotoxins designed to exhibit enhanced therapeutic activity while minimizing immunogenicity. These innovations hold significant promise, as clinical trials have demonstrated that reducing the human anti-drug immune response is critical for enabling repeated dosing of immunotoxins, thus improving their long-term efficacy. Such advancements could lead to substantial tumor responses in certain patients following treatment, marking an exciting progression for the field of targeted cancer therapies. These findings lay a strong foundation for future research, and larger-scale clinical trials will be essential in validating the full therapeutic potential of immunotoxins and realizing their initial promise as a viable treatment option in TNBC.

Chapter 6: Conclusion & Future Perspective

The identification of new tumor markers and antigens has consistently driven the development of novel recombinant immunotoxins (rITs) with lower immunogenicity, reduced toxicity, minimal resistance, and enhanced efficacy. Ongoing structural modifications of PE-ITs are crucial to reduce their immunogenicity while preserving their therapeutic effectiveness. The potential of combination therapies, including chemotherapeutic agents and small molecule inhibitors, should be explored through in vivo animal studies and clinical trials to verify their synergistic effects. Additionally, combining immunotoxins with radiotherapy should be considered for clinical trials, as it has shown promising results in preclinical studies, leading to improved outcomes.

In the future, new PE-based immunotoxins (PE-ITs) targeting additional solid cancers should be explored in clinical trials. To improve their efficacy and reduce immunogenicity, further truncations of the PE toxin should be considered, potentially through amino acid deletions, insertions, or conjugation with other toxin components. Moreover, PE-ETA should not be limited to cancer treatment but expanded to other areas of immunotherapy, such as the treatment of other diseases like organ fibrosis, Ebola, and HIV viral infections.

The preliminary data generated from this study, together with the work produced by previous MSc students in our laboratory, provides compelling evidence that computer simulation can be a valuable tool in predicting the effects of mutations on the enzymatic activity of recombinant immunotoxins (rITs), particularly RG7787 variants. By using such computational methods, we can model how specific changes in the amino acid sequences of rITs influence their structural and functional properties. This predictive

capability is essential for designing rITs with enhanced or recovered enzymatic activity, thus increasing the optimization process for therapeutic applications.

In the future, to maximize the potential of recombinant immunotoxins (rITs) for therapeutic applications, it is critical to optimize protein production at a larger scale. In this study, the expression systems used were effective in generating the desired immunotoxins; however, to meet the demands of pre-clinical and clinical development, higher protein yields are required. One promising approach to address this challenge is the use of high-density fermentation techniques, which can significantly enhance the expression levels of recombinant proteins.

High-density fermentation, as opposed to traditional batch cultivation methods, allows for the cultivation of bacterial cells at much higher cell densities, leading to a substantial increase in protein output. By employing high-density expression systems, it is possible to improve not only the yield of recombinant immunotoxins but also the consistency and quality of the expressed protein, which is crucial for downstream experiments and therapeutic efficacy.

Future work would include exploring the effect of other mutations that were introduced is still needed to compare their enzymatic activities. This will includes developing, assessing and comparing this rIT with only R456C without the presence of R490A, the mutation that was found to restore enzymatic activity in RG7787 [102] and compare this rIT enzymatic activity with other mutations that were introduced i.e. R456T in the presence of R490A mutation.

In conclusion, the introduction of novel mutations into the RG7787 immunotoxin has led to a significant recovery of enzymatic activity compared to the original RG7787 described

by Alewine *et al,*. These improvements in enzymatic activity demonstrate the potential of targeted protein engineering to optimize rITs for therapeutic purposes. However, these findings need further confirmation through the use of highly purified protein preparations, as purity is crucial to ensure the accuracy and reliability of the results. Following this, pre-clinical studies are required to assess the *in vivo* efficacy, and immunogenicity of the modified RG7787 constructs to determine their therapeutic potential for clinical applications. The advancements achieved in this study are already influencing ongoing patent applications from organizations such as the National Institutes of Health (NIH) and Roche. The mutation introduced in RG7787 could shape the future development of rITs, positioning them as a competitive and potentially transformative therapeutic option in the field of immunotherapy [102], [104].

Chapter 7: References

[1] S. Dawood *et al.*, 'Defining breast cancer prognosis based on molecular phenotypes: Results from a large cohort study', *Breast Cancer Res Treat*, vol. 126, no. 1, pp. 185–192, Feb. 2011, doi: 10.1007/s10549-010-1113-7.

[2] A. Society of Clinical Oncology, 'Breast Cancer Trusted Information to Help Manage Your Care from the American Society of Clinical Oncology'. [Online]. Available: www.Cancer.Net,

[3] M. C. U. Cheang *et al.*, 'Defining Breast Cancer Intrinsic Subtypes by Quantitative Receptor Expression', *Oncologist*, vol. 20, no. 5, pp. 474–482, May 2015, doi: 10.1634/theoncologist.2014-0372.

[4] Y. Feng *et al.*, 'Breast cancer development and progression: Risk factors, cancer stem cells, signaling pathways, genomics, and molecular pathogenesis', Jun. 01, 2018, *Chongqing University*. doi: 10.1016/j.gendis.2018.05.001.

[5] 'R e v i e w A R t i c l e', doi: 10.3978/j.issn.2072-1439.2013.05.24.

[6] S. Attalla, T. Taifour, T. Bui, and W. Muller, 'Insights from transgenic mouse models of PyMT-induced breast cancer: recapitulating human breast cancer progression in vivo', Jan. 21, 2021, *Springer Nature*. doi: 10.1038/s41388-020-01560-0.

[7] Y. Feng *et al.*, 'Breast cancer development and progression: Risk factors, cancer stem cells, signaling pathways, genomics, and molecular pathogenesis', Jun. 01, 2018, *Chongqing University*. doi: 10.1016/j.gendis.2018.05.001.

[8] S. Łukasiewicz, M. Czeczelewski, A. Forma, J. Baj, R. Sitarz, and A. Stanisławek, 'Breast cancer—epidemiology, risk factors, classification, prognostic markers, and

current treatment strategies—An updated review', Sep. 01, 2021, *MDPI*. doi: 10.3390/cancers13174287.

[9] A. Bhushan, A. Gonsalves, and J. U. Menon, 'Current state of breast cancer diagnosis, treatment, and theranostics', May 01, 2021, *MDPI*. doi: 10.3390/pharmaceutics13050723.

[10] D. Barba *et al.*, 'Breast cancer, screening and diagnostic tools: All you need to know', *Crit Rev Oncol Hematol*, vol. 157, p. 103174, Jan. 2021, doi: 10.1016/J.CRITREVONC.2020.103174.

[11] D. Barba *et al.*, 'Breast cancer, screening and diagnostic tools: All you need to know', Jan. 01, 2021, *Elsevier Ireland Ltd*. doi: 10.1016/j.critrevonc.2020.103174.

[12] S. Lei *et al.*, 'Global patterns of breast cancer incidence and mortality: A population-based cancer registry data analysis from 2000 to 2020', *Cancer Commun*, vol. 41, no. 11, pp. 1183–1194, Nov. 2021, doi: 10.1002/cac2.12207.

[13] L. Liao, 'Inequality in breast cancer: Global statistics from 2022 to 2050', *The Breast*, vol. 79, p. 103851, Feb. 2025, doi: 10.1016/j.breast.2024.103851.

[14] O. Amato, V. Guarneri, and F. Girardi, 'Epidemiology trends and progress in breast cancer survival: earlier diagnosis, new therapeutics', Nov. 01, 2023, *Lippincott Williams and Wilkins*. doi: 10.1097/CCO.0000000000000991.

[15] F. Mckenzie *et al.*, 'African Breast Cancer-Disparities in Outcomes (ABC-DO): protocol of a multicountry mobile health prospective study of breast cancer survival in sub-Saharan Africa', doi: 10.1136/bmjopen-2016.

[16] J. Moodley, L. Cairncross, T. Naiker, and M. Momberg, 'Understanding pathways to breast cancer diagnosis among women in the Western Cape Province, South Africa: A qualitative study', *BMJ Open*, vol. 6, no. 1, 2016, doi: 10.1136/bmjopen-2015-009905.

[17] J. Moodley, L. Cairncross, T. Naiker, and M. Momberg, 'Understanding pathways to breast cancer diagnosis among women in the Western Cape Province, South Africa: A qualitative study', *BMJ Open*, vol. 6, no. 1, 2016, doi: 10.1136/bmjopen-2015-009905.

[18] C. Nel, A. Mannel, and D. Kruger, 'Triple-negative breast cancer – a retrospective audit of 151 cases seen at the Charlotte Maxeke Johannesburg Academic Hospital Breast Unit', *South African Journal of Surgery*, vol. 60, no. 2, pp. 115–118, Jun. 2022, doi: 10.17159/2078-5151/SAJS3675.

[19] D. Barba *et al.*, 'Breast cancer, screening and diagnostic tools: All you need to know', *Crit Rev Oncol Hematol*, p. 157, 2021, doi: 10.1016/j.critrevonc.2020.103174ï.

[20] L. Yin, J. J. Duan, X. W. Bian, and S. C. Yu, 'Triple-negative breast cancer molecular subtyping and treatment progress', Jun. 09, 2020, *BioMed Central Ltd*. doi: 10.1186/s13058-020-01296-5.

[21] F. M. Howard and O. I. Olopade, 'Epidemiology of Triple-Negative Breast Cancer A Review', 2021. [Online]. Available: www.journalppo.com

[22] B. D. Lehmann *et al.*, 'Identification of human triple-negative breast cancer subtypes and preclinical models for selection of targeted therapies', *Journal of*

Clinical Investigation, vol. 121, no. 7, pp. 2750–2767, Jul. 2011, doi: 10.1172/JCI45014.

[23] B. D. Lehmann, J. A. Pietenpol, and A. R. Tan, 'Triple-Negative Breast Cancer: Molecular Subtypes and New Targets for Therapy', 2015.

[24] B. D. Lehmann *et al.*, 'Identification of human triple-negative breast cancer subtypes and preclinical models for selection of targeted therapies', *Journal of Clinical Investigation*, vol. 121, no. 7, pp. 2750–2767, Jul. 2011, doi: 10.1172/JCI45014.

[25] B. D. Lehmann and J. A. Pietenpol, 'Identification and use of biomarkers in treatment strategies for triple-negative breast cancer subtypes', Jan. 2014. doi: 10.1002/path.4280.

[26] B. Weigelt *et al.*, 'Metastatic breast carcinomas display genomic and transcriptomic heterogeneity', *Modern Pathology*, vol. 28, no. 3, pp. 340–351, Mar. 2015, doi: 10.1038/modpathol.2014.142.

[27] A. Prat *et al.*, 'Phenotypic and molecular characterization of the claudin-low intrinsic subtype of breast cancer', 2010. [Online]. Available: http://breast-cancer-research.com/content/12/5/R68

[28] M. De Laurentiis *et al.*, 'Treatment of triple negative breast cancer (TNBC): current options and future perspectives', *Cancer Treat Rev*, vol. 36, no. SUPPL. 3, pp. S80–S86, Nov. 2010, doi: 10.1016/S0305-7372(10)70025-6.

[29] P. Zagami and L. A. Carey, 'Triple negative breast cancer: Pitfalls and progress', Dec. 01, 2022, *Nature Research*. doi: 10.1038/s41523-022-00468-0.

[30] M. De Laurentiis *et al.*, 'Treatment of triple negative breast cancer (TNBC): current options and future perspectives', 2010.

[31] R. Dent, W. M. Hanna, M. Trudeau, E. Rawlinson, P. Sun, and S. A. Narod, 'Pattern of metastatic spread in triple-negative breast cancer', *Breast Cancer Res Treat*, vol. 115, no. 2, pp. 423–428, May 2009, doi: 10.1007/s10549-008-0086-2.

[32] J. Collignon, L. Lousberg, H. Schroeder, and G. Jerusalem, 'Triple-negative breast cancer: Treatment challenges and solutions', May 20, 2016, *Dove Medical Press Ltd*. doi: 10.2147/BCTT.S69488.

[33] J. O. Armitage, M. B. Kastan, J. H. Doroshow, and J. E. Tepper, 'Abeloff's Clinical Oncology E-Book', 2020.

[34] P. Jabbarzadeh Kaboli, S. Shabani, and M. Partovi Nasr, 'Shedding light on triple-negative breast cancer with Trop2-targeted antibody-drug conjugates'. [Online]. Available: https://www.researchgate.net/publication/360033746

[35] R. Saravanan *et al.*, 'Zinc transporter LIV1: A promising cell surface target for triple negative breast cancer', Nov. 01, 2022, *John Wiley and Sons Inc*. doi: 10.1002/jcp.30880.

[36] T. Takatani-Nakase, C. Matsui, and K. Takahashi, 'Role of the LIV-1 subfamily of zinc transporters in the development and progression of breast cancers: A mini review', *Biomed Res Clin Pract*, vol. 1, no. 3, 2016, doi: 10.15761/brcp.1000114.

[37] K. M. Taylor *et al.*, 'The emerging role of the LIV-1 subfamily of zinc transporters in breast cancer', in *Molecular Medicine*, Jul. 2007, pp. 396–406. doi: 10.2119/2007-00040.Taylor.

[38] M. Chakraborty and M. Hershfinkel, ‘Zinc signaling in the mammary gland: For better and for worse’, Sep. 01, 2021, *MDPI*. doi: 10.3390/biomedicines9091204.

[39] Y. Liu *et al.*, ‘Advances in immunotherapy for triple-negative breast cancer’, Dec. 01, 2023, *BioMed Central Ltd*. doi: 10.1186/s12943-023-01850-7.

[40] G. A. Valencia *et al.*, ‘Immunotherapy in triple-negative breast cancer: A literature review and new advances’, *World J Clin Oncol*, vol. 13, no. 3, pp. 219–236, Mar. 2022, doi: 10.5306/wjco.v13.i3.219.

[41] S. Sriramulu, S. Thoidingjam, C. Speers, and S. Nyati, ‘Present and Future of Immunotherapy for Triple-Negative Breast Cancer’, Oct. 01, 2024, *Multidisciplinary Digital Publishing Institute (MDPI)*. doi: 10.3390/cancers16193250.

[42] L. Cerchia, L. Li, F. Zhang, Z. Liu, and Z. Fan, ‘Immunotherapy for Triple-Negative Breast Cancer: Combination Strategies to Improve Outcome’, 2023, doi: 10.3390/cancers.

[43] M. Vanneman and G. Dranoff, ‘Combining immunotherapy and targeted therapies in cancer treatment’, Apr. 2012. doi: 10.1038/nrc3237.

[44] K. P. Fabian, B. Wolfson, and J. W. Hodge, ‘From Immunogenic Cell Death to Immunogenic Modulation: Select Chemotherapy Regimens Induce a Spectrum of Immune-Enhancing Activities in the Tumor Microenvironment’, Aug. 23, 2021, *Frontiers Media S.A*. doi: 10.3389/fonc.2021.728018.

[45] R. B. Mokhtari *et al.*, ‘Combination therapy in combating cancer SYSTEMATIC REVIEW: COMBINATION THERAPY IN COMBATING CANCER BACKGROUND’, 2017. [Online]. Available: www.impactjournals.com/oncotarget

[46] K. M. Jungles *et al.*, 'Updates in combined approaches of radiotherapy and immune checkpoint inhibitors for the treatment of breast cancer', Oct. 26, 2022, *Frontiers Media S.A*. doi: 10.3389/fonc.2022.1022542.

[47] O. Obidiro, G. Battogtokh, and E. O. Akala, 'Triple Negative Breast Cancer Treatment Options and Limitations: Future Outlook', Jul. 01, 2023, *Multidisciplinary Digital Publishing Institute (MDPI)*. doi: 10.3390/pharmaceutics15071796.

[48] K. Tsuchikama, Y. Anami, S. Y. Y. Ha, and C. M. Yamazaki, 'Exploring the next generation of antibody–drug conjugates', Mar. 01, 2024, *Springer Nature*. doi: 10.1038/s41571-023-00850-2.

[49] M. S. Kang, T. W. S. Kong, J. Y. X. Khoo, and T. P. Loh, 'Recent developments in chemical conjugation strategies targeting native amino acids in proteins and their applications in antibody-drug conjugates', Nov. 07, 2021, *Royal Society of Chemistry*. doi: 10.1039/d1sc02973h.

[50] J. Yu, Y. Song, and W. Tian, 'How to select IgG subclasses in developing anti-tumor therapeutic antibodies', May 05, 2020, *BioMed Central Ltd*. doi: 10.1186/s13045-020-00876-4.

[51] S. Baah, M. Laws, and K. M. Rahman, 'Antibody–drug conjugates—a tutorial review', May 01, 2021, *MDPI AG*. doi: 10.3390/molecules26102943.

[52] A. H. Staudacher and M. P. Brown, 'Antibody drug conjugates and bystander killing: is antigen-dependent internalisation required', 2017, *Nature Publishing Group*. doi: 10.1038/bjc.2017.367.

[53] K. Tsuchikama and Z. An, ‘Antibody-drug conjugates: recent advances in conjugation and linker chemistries’, Jan. 01, 2018, *Higher Education Press*. doi: 10.1007/s13238-016-0323-0.

[54] W. D. Janthur, N. Cantoni, and C. Mamot, ‘Drug conjugates such as antibody drug conjugates (ADCs), immunotoxins and immunoliposomes challenge daily clinical practice’, Dec. 2012. doi: 10.3390/ijms131216020.

[55] J. R. McCombs and S. C. Owen, ‘Antibody Drug Conjugates: Design and Selection of Linker, Payload and Conjugation Chemistry’, *AAPS Journal*, vol. 17, no. 2, pp. 339–351, Mar. 2015, doi: 10.1208/s12248-014-9710-8.

[56] M. Abdollahpour-Alitappeh *et al.*, ‘Antibody–drug conjugates (ADCs) for cancer therapy: Strategies, challenges, and successes’, May 01, 2019, *Wiley-Liss Inc.* doi: 10.1002/jcp.27419.

[57] A. Nagayama, N. Vidula, L. Ellisen, and A. Bardia, ‘Novel antibody–drug conjugates for triple negative breast cancer’, 2020, *SAGE Publications Inc.* doi: 10.1177/1758835920915980.

[58] N. Becker and I. Benhar, ‘Antibody-based immunotoxins for the treatment of cancer’, *Antibodies*, vol. 1, no. 1, pp. 39–69, Jun. 2012, doi: 10.3390/antib1010039.

[59] R. Mazor, M. Onda, and I. Pastan, ‘Immunogenicity of therapeutic recombinant immunotoxins’, Mar. 01, 2016, *Blackwell Publishing Ltd*. doi: 10.1111/imr.12390.

[60] S. Srivastava and S. Luqman, ‘Immune-O-Toxins as the magic bullet for therapeutic purposes’, *Biomedical Research and Therapy*, vol. 2, no. 1, Jan. 2015, doi: 10.7603/s40730-015-0002-4.

[61] C. Alewine, R. Hassan, and I. Pastan, ‘Advances in Anticancer Immunotoxin Therapy’, *Oncologist*, vol. 20, no. 2, pp. 176–185, Feb. 2015, doi: 10.1634/theoncologist.2014-0358.

[62] K. Hollevoet, E. Mason-Osann, X. F. Liu, S. Imhof-Jung, G. Niederfellner, and I. Pastan, ‘In vitro and in vivo activity of the low-immunogenic antimesothelin immunotoxin RG7787 in pancreatic cancer’, *Mol Cancer Ther*, vol. 13, no. 8, pp. 2040–2049, 2014, doi: 10.1158/1535-7163.MCT-14-0089-T.

[63] M. Onda, R. Beers, L. Xiang, S. Nagata, Q.-C. Wang, and I. Pastan, ‘An immunotoxin with greatly reduced immunogenicity by identification and removal of B cell epitopes’. [Online]. Available: www.pnas.orgcgidoi10.1073pnas.0804851105

[64] W. Liu *et al.*, ‘Recombinant immunotoxin engineered for low immunogenicity and antigenicity by identifying and silencing human B-cell epitopes’, *Proc Natl Acad Sci U S A*, vol. 109, no. 29, pp. 11782–11787, Jul. 2012, doi: 10.1073/pnas.1209292109.

[65] P. V Liu, ‘IDENTIFICATION OF PATHOGENIC PSEUDOMONADS BY EXTRACELLULAR ANTIGENS’’. [Online]. Available: https://journals.asm.org/journal/jb

[66] R. N. Morgan, S. E. Saleh, H. A. Farrag, and K. M. Aboshanab, ‘New insights on Pseudomonas aeruginosa exotoxin A-based immunotoxins in targeted cancer therapeutic delivery’, Jan. 01, 2023, *Newlands Press Ltd*. doi: 10.4155/tde-2022-0055.

[67] J. E. Weldon *et al.*, ‘A recombinant immunotoxin against the tumor-associated antigen mesothelin reengineered for high activity, low off-target toxicity, and

reduced antigenicity', *Mol Cancer Ther*, vol. 12, no. 1, pp. 48–57, Jan. 2013, doi: 10.1158/1535-7163.MCT-12-0336.

[68] R. J. Kreitman *et al.*, 'Phase I trial of anti-CD22 recombinant immunotoxin moxetumomab pasudotox (CAT-8015 or HA22) in patients with hairy cell leukemia', *Journal of Clinical Oncology*, vol. 30, no. 15, pp. 1822–1828, May 2012, doi: 10.1200/JCO.2011.38.1756.

[69] A. S. Wayne *et al.*, 'A Novel Anti-CD22 Immunotoxin, Moxetumomab Pasudotox: Phase I Study in Pediatric Acute Lymphoblastic Leukemia (ALL)', *Blood*, vol. 118, no. 21, p. 248, Nov. 2011, doi: 10.1182/BLOOD.V118.21.248.248.

[70] R. N. Morgan, S. E. Saleh, K. M. Aboshanab, and H. A. Farrag, 'ADP-ribosyl transferase activity and gamma radiation cytotoxicity of Pseudomonas aeruginosa exotoxin A', *AMB Express*, vol. 11, no. 1, Dec. 2021, doi: 10.1186/s13568-021-01332-3.

[71] V. S. Allured, R. J. Colliert, S. F. Carrollt, and D. B. Mckay, 'Structure of exotoxin A of Pseudomonas aeruginosa at 3.0-Angstrom resolution', 1986. [Online]. Available: https://www.pnas.org

[72] J. E. Wedekind *et al.*, 'Refined crystallographic structure of Pseudomonas aeruginosa exotoxin A and its implications for the molecular mechanism of toxicity', *J Mol Biol*, vol. 314, no. 4, pp. 823–837, Dec. 2001, doi: 10.1006/JMBI.2001.5195.

[73] R. Mazor, E. M. King, and I. Pastan, ‘Strategies to Reduce the Immunogenicity of Recombinant Immunotoxins’, *Am J Pathol*, vol. 188, no. 8, pp. 1736–1743, Aug. 2018, doi: 10.1016/J.AJPATH.2018.04.016.

[74] V. K. Chaudhary, Y. Jinno, D. Fitzgerald, and I. Pastan, ‘Pseudomonas exotoxin contains a specific sequence at the carboxyl terminus that is required for cytotoxicity (endocytosis/toxin/translocation/endoplasmic reticulum/signal sequence)’, 1990. [Online]. Available: https://www.pnas.org

[75] M. I. Li, F. Dyda, I. Benhart, I. Pastant, and D. R. Davies, ‘The crystal structure of Pseudomonas aeruginosa exotoxin domain III with nicotinamide and AMP: Conformational differences with the intact exotoxin’, 1995. [Online]. Available: https://www.pnas.org

[76] R. J. Kreitman, R. Hassan, D. J. FitzGerald, and I. Pastan, ‘Phase I trial of continuous infusion anti-mesothelin recombinant immunotoxin SS1P’, *Clinical Cancer Research*, vol. 15, no. 16, pp. 5274–5279, Aug. 2009, doi: 10.1158/1078-0432.CCR-09-0062.

[77] I. Pastan, R. Hassan, D. J. FitzGerald, and R. J. Kreitman, ‘Immunotoxin treatment of cancer’, 2007. doi: 10.1146/annurev.med.58.070605.115320.

[78] R. Hassan *et al.*, ‘Phase 1 study of the antimesothelin immunotoxin SS1P in combination with pemetrexed and cisplatin for front-line therapy of pleural mesothelioma and correlation of tumor response with serum mesothelin, megakaryocyte potentiating factor, and cancer antigen 125’, *Cancer*, vol. 120, no. 21, pp. 3311–3319, Nov. 2014, doi: 10.1002/cncr.28875.

[79] W. Liu *et al.*, ‘Recombinant immunotoxin engineered for low immunogenicity and antigenicity by identifying and silencing human B-cell epitopes’, *Proc Natl Acad Sci U S A*, vol. 109, no. 29, pp. 11782–11787, Jul. 2012, doi: 10.1073/pnas.1209292109.

[80] M. Onda, R. Beers, L. Xiang, S. Nagata, Q.-C. Wang, and I. Pastan, ‘An immunotoxin with greatly reduced immunogenicity by identification and removal of B cell epitopes’. [Online]. Available: www.pnas.orgcgidoi10.1073pnas.0804851105

[81] R. Mazor, M. Onda, and I. Pastan, ‘Immunogenicity of therapeutic recombinant immunotoxins’, Mar. 01, 2016, *Blackwell Publishing Ltd*. doi: 10.1111/imr.12390.

[82] O. Alex Akinrinmade, ‘GENERATION AND EVALUATION OF NOVEL CD64-SPECIFIC IMMUNOTHERAPEUTIC AGENTS TO SELECTIVELY TARGET DYSREGULATED MACROPHAGES’, 2020.

[83] R. Mazor, E. M. King, and I. Pastan, ‘Strategies to Reduce the Immunogenicity of Recombinant Immunotoxins’, *Am J Pathol*, vol. 188, no. 8, pp. 1736–1743, Aug. 2018, doi: 10.1016/J.AJPATH.2018.04.016.

[84] W. Liu *et al.*, ‘Recombinant immunotoxin engineered for low immunogenicity and antigenicity by identifying and silencing human B-cell epitopes’, *Proc Natl Acad Sci U S A*, vol. 109, no. 29, pp. 11782–11787, Jul. 2012, doi: 10.1073/pnas.1209292109.

[85] R. Mazor *et al.*, ‘Recombinant immunotoxin for cancer treatment with low immunogenicity by identification and silencing of human T-cell epitopes’, *Proc Natl Acad Sci U S A*, vol. 111, no. 23, pp. 8571–8576, Jun. 2014, doi: 10.1073/pnas.1405153111.

[86] R. Mazor and I. Pastan, ‘Immunogenicity of Immunotoxins Containing Pseudomonas Exotoxin A: Causes, Consequences, and Mitigation’, Jun. 26, 2020, *Frontiers Media S.A*. doi: 10.3389/fimmu.2020.01261.

[87] R. Mazor, M. Onda, and I. Pastan, ‘Immunogenicity of therapeutic recombinant immunotoxins’, Mar. 01, 2016, *Blackwell Publishing Ltd*. doi: 10.1111/imr.12390.

[88] J. E. Weldon and I. Pastan, ‘A guide to taming a toxin - Recombinant immunotoxins constructed from Pseudomonas exotoxin A for the treatment of cancer’, Dec. 2011. doi: 10.1111/j.1742-4658.2011.08182.x.

[89] M. Onda *et al.*, ‘Characterization of the B Cell Epitopes Associated with a Truncated Form of Pseudomonas Exotoxin (PE38) Used to Make Immunotoxins for the Treatment of Cancer Patients 1’, 2006. [Online]. Available: http://journals.aai.org/jimmunol/article-pdf/177/12/8822/1220393/zim02406008822.pdf

[90] M. Onda, R. Beers, L. Xiang, S. Nagata, Q.-C. Wang, and I. Pastan, ‘An immunotoxin with greatly reduced immunogenicity by identification and removal of B cell epitopes’, 2008. [Online]. Available: www.pnas.orgcgidoi10.1073pnas.0804851105

[91] D. M. Roscoe, L. H. Pai, and I. Pastan, ‘Identification of epitopes on a mutant form of Pseudomonas exotoxin using serum from humans treated with Pseudomonas exotoxin containing immunotoxins’, *Eur J Immunol*, vol. 27, no. 6, pp. 1459–1468, Jun. 1997, doi: 10.1002/eji.1830270624.

[92] C. Oseroff *et al.*, 'Molecular Determinants of T Cell Epitope Recognition to the Common Timothy Grass Allergen', *The Journal of Immunology*, vol. 185, no. 2, pp. 943–955, Jul. 2010, doi: 10.4049/jimmunol.1000405.

[93] C. Oseroff *et al.*, 'Molecular Determinants of T Cell Epitope Recognition to the Common Timothy Grass Allergen', *The Journal of Immunology*, vol. 185, no. 2, pp. 943–955, Jul. 2010, doi: 10.4049/jimmunol.1000405.

[94] J. Tassignon *et al.*, 'Monitoring of cellular responses after vaccination against tetanus toxoid: Comparison of the measurement of IFN-γ production by ELISA, ELISPOT, flow cytometry and real-time PCR', *J Immunol Methods*, vol. 305, no. 2, pp. 188–198, Oct. 2005, doi: 10.1016/J.JIM.2005.07.014.

[95] R. Mazor *et al.*, 'Identification and elimination of an immunodominant T-cell epitope in recombinant immunotoxins based on Pseudomonas exotoxin A', *Proc Natl Acad Sci U S A*, vol. 109, no. 51, Dec. 2012, doi: 10.1073/pnas.1218138109.

[96] R. J. Kreitman, R. Hassan, D. J. FitzGerald, and I. Pastan, 'Phase I trial of continuous infusion anti-mesothelin recombinant immunotoxin SS1P', *Clinical Cancer Research*, vol. 15, no. 16, pp. 5274–5279, Aug. 2009, doi: 10.1158/1078-0432.CCR-09-0062.

[97] C. Nel, A. Mannel, and D. Kruger, 'Triple-negative breast cancer – a retrospective audit of 151 cases seen at the Charlotte Maxeke Johannesburg Academic Hospital Breast Unit', *South African Journal of Surgery*, vol. 60, no. 2, pp. 115–118, Jun. 2022, doi: 10.17159/2078-5151/SAJS3675.

[98] J. G. Brown, J. Entwistle, N. Glover, and G. C. Macdonald, ‘Preclinical Safety Evaluation of Immunotoxins’, 2008.

[99] S. Barth, M. Huhn, B. Matthey, A. Klimka, E. A. Galinski, and A. A. Engert, ‘Compatible-Solute-Supported Periplasmic Expression of Functional Recombinant Proteins under Stress Conditions’, 2000.

[100] G. Bianchini, J. M. Balko, I. A. Mayer, M. E. Sanders, and L. Gianni, ‘Triple-negative breast cancer: Challenges and opportunities of a heterogeneous disease’, Nov. 01, 2016, *Nature Publishing Group*. doi: 10.1038/nrclinonc.2016.66.

[101] K. A. Akshata Desai, ‘Triple Negative Breast Cancer – An Overview’, *Hereditary Genetics*, 2012, doi: 10.4172/2161-1041.s2-001.

[102] R. Hassan, C. Alewine, and I. Pastan, ‘New life for immunotoxin cancer therapy’, Mar. 01, 2016, *American Association for Cancer Research Inc.* doi: 10.1158/1078-0432.CCR-15-1623.

[103] K. Pinilla, L. M. Drewett, R. Lucey, and J. E. Abraham, ‘Precision Breast Cancer Medicine: Early Stage Triple Negative Breast Cancer—A Review of Molecular Characterisation, Therapeutic Targets and Future Trends’, Aug. 08, 2022, *Frontiers Media S.A*. doi: 10.3389/fonc.2022.866889.

[104] C. Alewine, L. Xiang, T. Yamori, G. Niederfellner, K. Bosslet, and I. Pastan, ‘Efficacy of RG7787, a next-generation mesothelin-targeted immunotoxin, against triple-negative breast and gastric cancers’, *Mol Cancer Ther*, vol. 13, no. 11, pp. 2653–2661, Nov. 2014, doi: 10.1158/1535-7163.MCT-14-0132.

[105] Q. Li, C. A. Richard, M. Moudjou, and J. Vidic, 'Purification and refolding to amyloid fibrils of (His)6-tagged recombinant shadoo protein expressed as inclusion bodies in E.coli', *Journal of Visualized Experiments*, vol. 2015, no. 106, Dec. 2015, doi: 10.3791/53432.

[106] J. Kaur, A. Kumar, and J. Kaur, 'Strategies for optimization of heterologous protein expression in E. coli: Roadblocks and reinforcements', Jan. 01, 2018, *Elsevier B.V.* doi: 10.1016/j.ijbiomac.2017.08.080.

[107] L. Briand *et al.*, 'A self-inducible heterologous protein expression system in Escherichia coli', *Sci Rep*, vol. 6, Sep. 2016, doi: 10.1038/srep33037.

[108] J. Ratelade, M. C. Miot, E. Johnson, J. M. Betton, P. Mazodier, and N. Benaroudj, 'Production of recombinant proteins in the lon-deficient BL21(DE3) strain of Escherichia coli in the absence of the DnaK chaperone', *Appl Environ Microbiol*, vol. 75, no. 11, pp. 3803–3807, Jun. 2009, doi: 10.1128/AEM.00255-09.

[109] W. Schumann, L. Carlos, and S. Ferreira, 'Production of recombinant proteins in Escherichia coli'. [Online]. Available: www.sbg.org.br

[110] M. Mühlmann, E. Forsten, S. Noack, and J. Büchs, 'Optimizing recombinant protein expression via automated induction profiling in microtiter plates at different temperatures', *Microb Cell Fact*, vol. 16, no. 1, Nov. 2017, doi: 10.1186/s12934-017-0832-4.

[111] A. Sandomenico, J. P. Sivaccumar, and M. Ruvo, 'Evolution of escherichia coli expression system in producing antibody recombinant fragments', Sep. 01, 2020, *MDPI AG*. doi: 10.3390/ijms21176324.

[112] J. Glazyrina *et al.*, 'Open Access RESEARCH High cell density cultivation and recombinant protein production with Escherichia coli in a rocking-motion-type bioreactor', 2010. [Online]. Available: http://www.microbialcellfactories.com/content/9/1/42http://www.microbialcellfactories.com/content/9/1/42

[113] S. Mojtabavi, N. Samadi, and M. A. Faramarzi, 'Osmolyte-induced folding and stability of proteins: Concepts and characterization', Sep. 01, 2019, *Iranian Journal of Pharmaceutical Research*. doi: 10.22037/ijpr.2020.112621.13857.

[114] B. C. Joseph, S. Pichaimuthu, and S. Srimeenakshi, 'An Overview of the Parameters for Recombinant Protein Expression in Escherichia coli', *J Cell Sci Ther*, vol. 06, no. 05, 2015, doi: 10.4172/2157-7013.1000221.

[115] J. A. Bornhorst and J. J. Falke, '[16] Purification of Proteins Using Polyhistidine Affinity Tags'.

[116] V. Riguero *et al.*, 'Immobilized metal affinity chromatography optimization for poly-histidine tagged proteins', *J Chromatogr A*, vol. 1629, Oct. 2020, doi: 10.1016/j.chroma.2020.461505.

[117] R. R. Burgess, 'A brief practical review of size exclusion chromatography: Rules of thumb, limitations, and troubleshooting', Oct. 01, 2018, *Academic Press Inc.* doi: 10.1016/j.pep.2018.05.007.

[118] 'Ni 2+-IDA Metal Chelate Agarose Resin Technical Datasheet'. [Online]. Available: www.proteinark.com

[119] 'TECHNICAL RESOURCE'. [Online]. Available: www.piercenet.com

[120] A. J. Almeida and E. Souto, ‘Solid lipid nanoparticles as a drug delivery system for peptides and proteins’, Jul. 10, 2007. doi: 10.1016/j.addr.2007.04.007.

[121] Cooper GM, *The Cell: A Molecular Approach*. , 2nd Edition. 2000.

[122] A. Antignani and D. FitzGerald, ‘Immunotoxins: The role of the toxin’, Aug. 2013. doi: 10.3390/toxins5081486.

[123] C. Alewine, R. Hassan, and I. Pastan, ‘Advances in Anticancer Immunotoxin Therapy’, *Oncologist*, vol. 20, no. 2, pp. 176–185, Feb. 2015, doi: 10.1634/theoncologist.2014-0358.

[124] L. Westergard, H. M. Christensen, and D. A. Harris, ‘The cellular prion protein (PrPC): Its physiological function and role in disease’, *Biochim Biophys Acta Mol Basis Dis*, vol. 1772, no. 6, pp. 629–644, Jun. 2007, doi: 10.1016/j.bbadis.2007.02.011.

[125] D. L. Manning, R. J. Daly, P. G. Lord, K. F. Kelly, and C. D. Green, ‘Effects of oestrogen on the expression of a 4.4 kb mRNA in the ZR-75-1 human breast cancer cell line’, *Mol Cell Endocrinol*, vol. 59, no. 3, pp. 205–212, Oct. 1988, doi: 10.1016/0303-7207(88)90105-0.

[126] H. Shen, H. Qin, and J. Guo, ‘Concordant correlation of LIV-1 and E-cadherin expression in human breast cancer cell MCF-7’, *Mol Biol Rep*, vol. 36, no. 4, pp. 653–659, Apr. 2009, doi: 10.1007/s11033-008-9225-4.

[127] E. Guerra *et al.*, ‘The 2EF Antibody Targets a Unique N-Terminal Epitope of Trop-2 and Enhances the In Vivo Activity of the Cancer-Selective 2G10 Antibody’, *Cancers (Basel)*, vol. 15, no. 14, Jul. 2023, doi: 10.3390/cancers15143721.

[128] J. Harper, F. Xiao, G. Venkatraman, I. G. Camarillo, and R. Sundararajan, 'Low voltage nanosecond electroporation for breast cancer treatment: an in vitro study', *Electroporation-Based Therapies for Cancer: From Basics to Clinical Applications*, pp. 185–198, Jan. 2014, doi: 10.1533/9781908818294.185.

[129] L. Westergard, H. M. Christensen, and D. A. Harris, 'The cellular prion protein (PrPC): Its physiological function and role in disease', *Biochimica et Biophysica Acta (BBA) - Molecular Basis of Disease*, vol. 1772, no. 6, pp. 629–644, Jun. 2007, doi: 10.1016/J.BBADIS.2007.02.011.

[130] M. Trerotola *et al.*, 'Upregulation of Trop-2 quantitatively stimulates human cancer growth', *Oncogene*, vol. 32, no. 2, pp. 222–233, Jan. 2013, doi: 10.1038/onc.2012.36.

[131] S. M. Zimmers *et al.*, 'TROP2 methylation and expression in tamoxifen-resistant breast cancer', *Cancer Cell Int*, vol. 18, no. 1, Jul. 2018, doi: 10.1186/s12935-018-0589-9.

[132] U. Brinkman, 'Recombinant immunotoxins: protein engineering for cancer therapy', *Mol Med Today*, vol. 2, no. 10, pp. 439–446, Oct. 1996, doi: 10.1016/1357-4310(96)84848-9.

Appendix

Chemicals and consumables were purchased from various companies, including Beckham Coulter (California, USA), Bio-Rad (California, USA), Genescript (Piscataway, USA), Inqaba Biotechnological Industries (Pretoria, South Africa), New England Biolabs (Massachusetts, USA), Sigma Aldrich (Missouri, USA), Qiagen (Hilden, Germany), and Thermofisher Scientific (Waltham, USA).

Stock solutions and buffers were made with de-ionized water, following conventional laboratory techniques or manufacturer's instructions. Buffers were filtered with 0.45µm filters and degassed. Antibiotics, kanamycin, and Isopropyl β-d-1-thiogalactopyranoside (IPTG) were produced as stock solutions, filtered (0.22 µm), and kept at -20°C. Buffers were titrated using either 1M HCl (acid) or 10M NaOH (alkaline). The recipe for each buffer is summarized below (**Table 9**). Other solutions, such as RPMI 1640 and DMEM medium, were autoclaved for 25 minutes at 121°C. 1% penicillin, 10% fetal bovine serum, and streptomycin were added to RPMI and DMEM medium.

Table A1: Shows the list of buffers and media used to conduct experiments

EXPERIMENT	REAGENT	COMPOSITION	CONCENTRATION
Molecular Cloning	Luria Broth (LB)	Distilled water	
	Luria Broth Agar	Distilled water	
	SOC		

	10X TAE (pH 7.5)	Tris Base Glacial Acetic Acid EDTA Distilled Water	0.4M 1.14% (v/v) 10mM
Bacterial Expression	Terrific Broth (TB)	Glycerol Distilled Water	
Protein Characterization	SDS PAGE gel (10% Separating gel)	Acrylamide Tris-HCL (pH 8.8) SDS TEMED APS	30% 1.5 M 10% 10%
	SDS PAGE gel (4% Stacking gel)	Acrylamide Tris-HCL (pH 6.8) SDS TEMED APS	30% 1.5 M 10% 10%
	10X SDS Running Buffer (pH 8.3)	Tris-Base Glycine	250mM 1.92M

		SDS	1% (w/v)
	10X PBS (pH 7.4)	NaCl KCL Na2HPO4 KH2PO4	1.37M 27Mm 81mM 15mM
	TBST	Tween 20 Tris NaCl	0.1% (w/v) 20mM 150mM

Table A2: Shows the equipment used during laboratory experiments.

USED FOR:	**EQUIPMENT NAME**	**MANUFACTURER (MODEL)**
Molecular Cloning & Protein Expression	Sonicator	Sonica L.L.C (Qsonica)
	Centrifuge	Beckman coulter (Allegra X-30R)
	Spectrophotometer	Denovix (Denovix Ds-11)
	Shaking incubator	Yinder Co Ltd (LM-510RD)
	Gel imager	Bio-Rad (G Box Chemi XL)
	Heating block	Eppendorf (Thermomixer Comfort)
	SpeedVac drier	SP Scientific (miVAC DNA-23050-L00)

	Micro-centrifuge	LMS Co Ltd (MCF-2360)
	Weighing balance	Radwag (P5600.R2)
	Vortex	LMS Co Ltd (VTX-3000L)
	pH meter	Dostmann Electronic (pH50+DHS)
Protein Purification	Protein purification equipment	GE Healthcare (AKTA Avant)
Protein Characterization	Tissue culture incubator	Nuaire (In-VitroCell)
	Western Blot	Bio-Rad (Trans-Blot Cell)
	Electrophoresis	Bio-Rad (PowerPacTM HC)
In-vitro studies	Cell counter	Bio-Rad (TC20)
	BSLII Cabinet	ESCO Life technologies (Airstream AC2-458)
	Microscope	Bio-Rad (Zoe)
	Vortex	LMS Co Ltd (VTX-3000L)

Table A3: Shows the reagents that were used for protein characterization, functionality and cytotoxicity.

REAGENT	**SOURCE**	**CATALOGUE NUMBER**
Aqua stain	Bulldog Bio, UK	AS001000

Color Prestained Protein Standard Broad Range	New England Biolabs, UK	P7719S
PVDF transfer membrane	Roche, CH	03010040001
1-step TMB-Blotting Substrate Solution	Thermo-fisher Scientific, USA	34018
His-Tag primary antibody	Anatech analytical technology, ZA	CST2365S
Goat-anti-rabbit-IgG horadish peroxidase (HRP)	Bio-Rad, USA	1706515
Anti-His PE antibody	R&D systems, USA	IC050P
Mowiol®	Merk, USA	475904
Anti-Fade (Propyl-gallate)	Sigma Alridch, USA	P3130
Cell Proliferation Kit II (XTT)	Roche, CH	52751200

Table A4: Shows the list of cell lines that were used in the study.

CELL LINE NAME	**SOURCE**
HeLa	Cervical carcinoma derived from a 31-year-old patient, American Type Culture Collection (ATCC, USA)

SiHa	Fragments of a primary uterine tissue sample from a 55-year-old, female, Japanese patient with squamous cell carcinoma, American Type Culture Collection (ATCC, USA)
ME-180	Uterus of a 66-year-old, White female patient with epidermoid carcinoma, American Type Culture Collection (ATCC, USA)
MCF-7	MCF-7 is a breast cancer cell line isolated in 1970 from a 69-year-old White woman, American Type Culture Collection (ATCC, USA)

Table A5: Shows the media and their components used to grow and maintain cancer cell lines.

REAGENT	**COMPOSITION**	**CONCENTRATION**	**SOURCE**
RPMI-1640	GlutaMAX Sodium pyruvate Phenol red Fetal Bovine serum Penicillin Streptomycin	2mM 3.7g/L 15.0 mg/L 10% v/v 100 I.U/mL 100µg/mL	Gibco 61870
DMEM	GlutaMAX	2Mm	Gibco 10566

	Sodium bicarbonate	3.7g/L	
	Phenol red	16.0 mg/L	
	Fetal Bovine serum	10% v/v	
	Penicillin	100 I.U/Ml	
	Streptomycin	100µg/Ml	

Supplementary Figures

Restriction digestion of pMT hliv22(scFv)-ETA', trop2(scFv)-ETA' and pUC57 vector containing (RG7787 (R456C+R490A) dETA'

As detailed in (**subsections 2.2.1),** pUC57 vector containing (RG7787 (R456C+R490A)-dETA'), from Genescript and the pMT-Hliv22(scFv)-ETA' and pMT-trop2(scFv)-ETA' backbone vectors (provided by MB&I unit) were amplified and digested using BlpI and NotI enzymes. The expected fragment sizes for both pMTs are (**inserts and backbone) and for pUC (insert, backbone)**. The fragments of interest were isolated using AGE and aligned with the SnapGene® software simulation of the expected bands, as seen in Figure A2. All DNA fragments successfully aligned with the simulations and were thus considered successfully digested. The relevant bands were then excised from the gel in preparation for ligation (**subsections 2.2.).** All digestions consisted of an undigested and single digested (using Not1) controls.

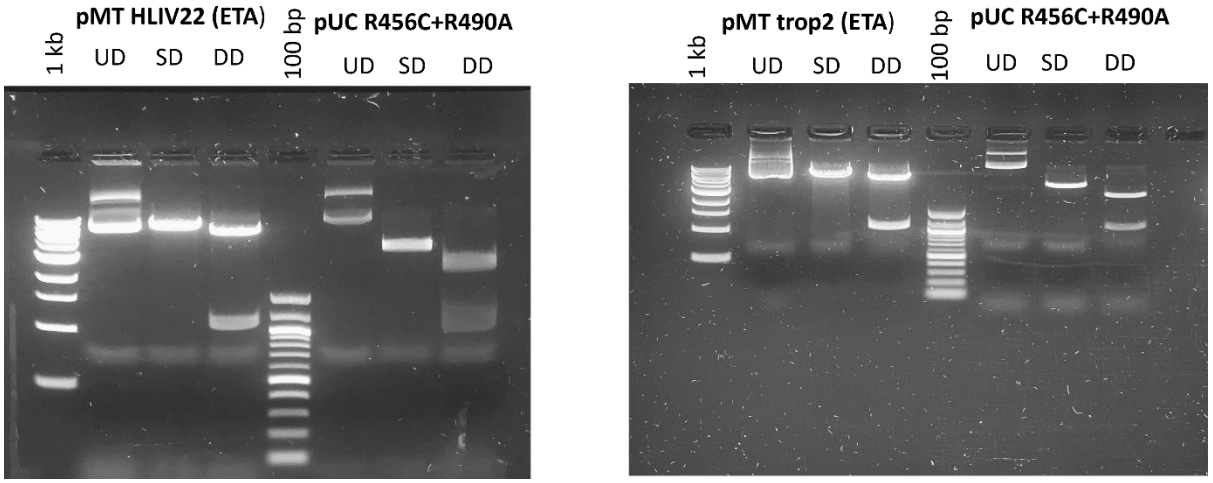

Figure 34: UD-Undigested, SD-Single digested (Not-1) and DD-Double digested (Not1 &BlpI)